

Electronic Supplementary Information (ESI)

Dynamic Covalent Bond Constrained Ureas for Multimode Fluorescence Switching, Thermally Induced Emission, and Chemical Signaling Cascades

Fazli Sattar,^{a,b} Zelin Feng,^a Hanxun Zou,^{*a} Hebo Ye,^a Yi Zhang,^{*c} and Lei You^{*a,b,d}

a. State Key Laboratory of Structural Chemistry, Fujian Institute of Research on the Structure of Matter, Chinese Academy of Sciences, Fuzhou, Fujian 350002, China.

b. University of Chinese Academy of Sciences, Beijing 100049, China.

c. School of Materials Science and Energy Engineering, Foshan University, Foshan, Guangdong 528000, China.

d. Fujian Science & Technology Innovation Laboratory for Optoelectronic Information of China, Fuzhou 350108, China.

Email: lyou@fjirsm.ac.cn, zouhanxun@fjirsm.ac.cn, imzhy@fosu.edu.cn

TABLE OF CONTENTS

| | |
|--|----------------|
| 1. General Methods..... | S3–S4 |
| 2. Synthesis and Characterization..... | S5–S41 |
| 3. Response toward Base, Anion, and Acid..... | S42–S53 |
| 4. Dynamic Covalent Reactions..... | S54–S64 |
| 5. Thermally Activated Fluorescence..... | S65–S68 |
| 6. Chemical Cascade Reactions..... | S69–S78 |
| 7. Solid State Luminescent Materials..... | S79–S84 |
| 8. Computational Data..... | S85–S90 |
| 9. References..... | S91 |

1. General Methods

^1H NMR and ^{13}C NMR spectra were recorded on a 400 MHz Bruker Biospin avance III spectrometer. Deuterated reagents for characterization and *in situ* reactions were purchased from Sigma–Aldrich Chemical Co. and Cambridge Isotope Laboratories, Inc. (purity $\geq 99.9\%$). The chemical shifts (δ) for ^1H NMR spectra, given in ppm, are referenced to the residual proton signal of the deuterated solvent. Mass spectra were recorded on a Bruker IMPACT–II spectrometer. Melting points (MP) were measured on a WRX-4 digital melting point apparatus. Acetonitrile for fluorescence experiments was purchased from Energy Chemical (purity $\geq 99.9\%$). All other reagents were obtained from commercial sources and were used without further purification, unless indicated otherwise.

Dynamic covalent reactions. Dynamic Covalent Reactions (DCRs) were performed *in situ* in $\text{DMSO-}d_6$ or CD_3CN without isolation and purification. To a stirred solution of **1(F)** (~15 mM, 1.0 equiv) in deuterium reagents (0.60 mL), was added a thiol (3.0 equiv). The mixture was stirred and characterized by ^1H NMR and ESI mass spectral analysis. See specific conditions in figure captions of the main text or supporting information if necessary.

Fluorescence experiments in solution. Fluorescence spectra in solution were recorded on a microplate reader (BioTek SYNERGY H4) at a concentration of 50 μM of each probe in acetonitrile. Stock solutions of components were prepared, and titrations were then conducted by mixing **1** with 1,8–diazabicyclo[5.4.0]undec–7–ene (DBU), methanesulfonic acid (MA), or anions. Anions for anionic recognition experiments were added as a stock solution of $\text{Bu}_4\text{N}^+\text{X}^-$ in CH_3CN . For signaling cascade reactions, a stock solutions of **3(F)** was titrated to a solution of fluorescent switch (0.2 mM) in DMSO or CH_3CN . Please see specific conditions in figure captions of the main text or supporting information if necessary.

Absolute quantum yields (ϕ) were determined on a FLS920 fluorescence spectrometer (Edinburgh Instruments).^{S1, S2} A degassed solution of each probe (50 μM in acetonitrile, deaerated by a nitrogen flow) was excited at its maximum wavelength.

The quantum yield was calculated according to equation-S1.

$$\phi = \frac{N_{emission}}{N_{absorption}} = \frac{\int L_{emission}}{\int E_{solvent} - \int E_{sample}} \quad (\text{Equation-S1})$$

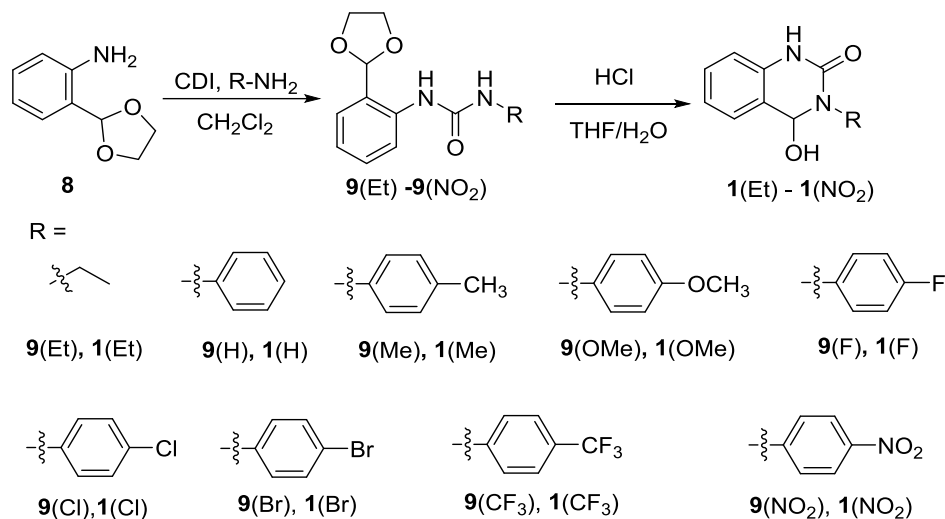
where $N_{emission}$ is the number of photons emitted from a sample, $N_{absorption}$ is the number of photons absorbed by a sample, L_{sample} is the emission intensity of sample, E_{sample} and $E_{solvent}$ are the intensity of the excitation light with and without a sample, respectively.

Thermally activated luminescent materials. The powder of **1(F)** was activated by heating under vacuum for 12 h. For solution studies the samples were heated in an external constant temperature bath. After the desired temperature was reached and the samples were equilibrated for 5 min, the emission intensity of solutions was recorded. The solid state fluorescence was measured on a FLS920 fluorescence spectrometer (Edinburgh Instruments). Probes loaded filter papers for reversible thermally-activated materials were prepared by soaking a square Whatman filter paper (2 cm × 2 cm) into a solution of **1(F)** in CH₃CN (10.0 mM), followed by evaporation to dry. The filter papers were activated by heating for 1 min using a hair drier. The cooling process was conducted by putting the activated filter papers at room temperature for 1 min. The photographs were taken under a 365 nm UV lamp in a dark room.

Vapor-responsive luminescent materials. **1(F)** loaded filter papers for the visualization of volatile vapors were prepared as above mentioned method. Solid samples for the visualization of volatile vapors were prepared by grinding the solid **1(F)** (50 mg) into a powder in quartz crucible. The filter papers or solid powder were activated by HCl vapor (generated from aqueous HCl, 37.5%, w/w), followed by exposure to different vapors generated from liquid amines and methyl mercaptan (5% in 1,3-propanediol, w/w), respectively. For the real sample test, individual florets (~50 g, measuring 2-3 mm long) were cut from each broccoli head (purchased from Bravo YH supermarket), collected, crushed, and immersed into 20 mL of 10 mM phosphate buffer solution (pH 8.0).^{S3} The mixture and a solid sample of **1(F)** (50 mg) activated with HCl vapor were placed in a sealed jar for the detection of vapors generated during broccoli florets spoilage. The photographs were taken under a 365 nm UV lamp in a dark room.

2. Synthesis and Characterization

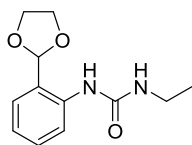
Scheme S1. The Synthesis of Urea Derivatives



General Procedure

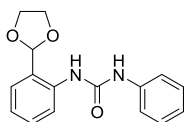
To a stirred solution of *N,N'*-carbonyldiimidazole (CDI) (1.0 equiv) in CH_2Cl_2 was added 2-(1,3-dioxolan-2-yl)aniline **8**^{S4} (1.0 equiv) in CH_2Cl_2 dropwise at room temperature under nitrogen. The mixture was stirred at r.t. for 6 h, and R-NH_2 (1.0 equiv) was added. The resulting mixture was stirred for another 6 h at r.t. and monitored by TLC. The solvent was removed under vacuum, and crude products were purified by silica gel column chromatography to afford intermediates **9(Et) – 9(NO₂)**.^{S5}

To a solution of **9(Et)** (200 mg, 0.85 mmol) in THF (20 mL) was added aqueous HCl (10 mL). The reaction was stirred at room temperature for 16 h. The mixture was extracted with EtOAc (200 mL) and washed with saturated aqueous NaHCO_3 (50 mL). The organic phase was dried over MgSO_4 . The crude product was obtained after removal of solvent under vacuum and recrystallized to afford pure **1(Et)**. Other compounds, including **1(H)**, **1(Me)**, **1(OMe)**, **1(F)**, **1(Cl)**, **1(Br)**, **1(CF₃)**, and **1(NO₂)**, were obtained from the corresponding intermediates according to the similar procedure as **1(Et)**.



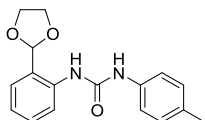
1-(2-(1,3-dioxolan-2-yl)phenyl)-3-ethylurea: Compound **9**(Et) was synthesized from **7** and ethylamine according to the general procedure.

The crude product was purified by silica gel column chromatography using petroleum ether/ethyl acetate (3:1, v/v, containing 2% Et₃N) as an eluent to obtain **9**(Et) as a white solid (91%). MP: 139.8-140.5 °C. ¹H NMR (DMSO-*d*₆): δ 7.87 (d, *J* = 8.4 Hz, 1H), 7.66 (br, 1H), 7.35 (d, *J* = 7.6 Hz, 1H), 7.27 (td, *J* = 8.4, 1.2 Hz, 1H), 6.97 (t, *J* = 7.6 Hz, 1H), 6.90 (t, *J* = 5.2 Hz, 1H), 5.74 (s, 1H), 4.14 – 3.92 (m, 4H), 3.12 – 3.06 (m, 2H), 1.07 – 1.04 (t, *J* = 7.2 Hz, 3H). ¹³C NMR (DMSO-*d*₆): δ 154.9, 138.4, 129.2, 125.4, 121.6, 121.5, 101.1, 64.7, 34.0, 15.4. ESI–HRMS: *m/z* calculated for C₁₂H₁₆N₂O₃Na [M + Na]⁺: 259.1053; found: 259.1053.



1-(2-(1,3-dioxolan-2-yl)phenyl)-3-phenylurea: Compound **9**(H) was synthesized from **7** and aniline according to the general procedure. The

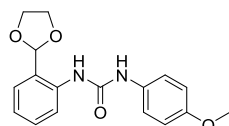
crude product was purified by silica gel column chromatography using petroleum ether/ethyl acetate (4:1, v/v, containing 2% Et₃N) as an eluent to obtain **9**(H) as a white solid (84%). MP: 145.3-146.5 °C. ¹H NMR (CD₃CN): δ 8.13 (m, 1H), 8.06 (d, *J* = 8.0 Hz, 1H), 7.99 – 7.96 (m, 1H), 7.84 (d, *J* = 8.4 Hz, 1H), 7.80 (br, 1H), 7.71 (d, *J* = 7.2 Hz, 1H), 7.61–7.54 (m, 4H), 7.41–7.36 (m, 2H), 7.08 (td, *J* = 7.6, 1.2 Hz, 1H), 5.59 (s, 1H), 3.82–3.65 (m, 4H). ¹³C NMR (CD₃CN): δ 153.7, 140.5, 138.6, 130.4, 129.9, 128.4, 127.5, 123.8, 123.7, 120.4, 103.4, 65.9. ESI–HRMS: *m/z* calculated for C₁₆H₁₅N₂O₃ [M – H][−]: 283.1083; found: 283.1072.



1-(2-(1,3-dioxolan-2-yl)phenyl)-3-(p-tolyl)urea: Compound **9**(Me)

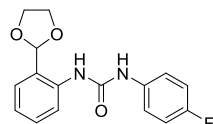
was synthesized from **7** and *p*-toluidine according to the general procedure. The crude product was purified by silica gel column chromatography using petroleum ether/ethyl acetate (4:1, v/v, containing 2% Et₃N) as an eluent to obtain **9**(Me) as a white solid (76%). MP: 138.9-140.1 °C. ¹H NMR (CD₃CN): δ 7.96 (d, *J* = 8.4 Hz, 1H), 7.66 (br, 1H), 7.59 (br, 1H), 7.43 (dd, *J* = 7.6, 1.2 Hz, 1H), 7.40 – 7.32 (m, 3H),

7.15 (d, $J = 8.4$ Hz, 2H), 7.09 (td $J = 7.6, 0.8$ Hz, 1 H), 5.77 (s, 1H), 4.13 – 3.98 (m, 4H), 2.31 (s, 3 H). ^{13}C NMR (DMSO- d_6): δ 152.6, 137.4, 137.2, 130.7, 129.2, 127.0, 126.7, 122.7, 122.4, 118.5, 101.0, 64.7, 20.4. ESI–HRMS: m/z calculated for $\text{C}_{17}\text{H}_{18}\text{N}_2\text{O}_3\text{Na}$ $[\text{M} + \text{Na}]^+$: 321.1215; found: 321.2106.



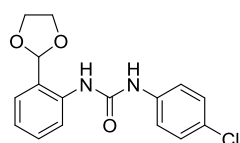
1-(2-(1,3-dioxolan-2-yl)phenyl)-3-(4-methoxyphenyl)urea:

Compound **9**(OMe) was synthesized from **7** and 4-methoxyaniline according to the general procedure. The crude product was purified by silica gel column chromatography using petroleum ether/ethyl acetate (4:1, v/v, containing 2% Et_3N) as an eluent to obtain **9**(OMe) as a white solid (79%). MP: 166.3-166.9 °C. ^1H NMR (CD_3CN): δ 7.97 (d, $J = 8.0$ Hz, 1H), 7.65 (br, 1H), 7.46 (br, 1H), 7.42 (dd, $J = 7.6, 1.2$ Hz, 1H), 7.39 – 7.32 (m, 3H), 7.08 (td, $J = 7.2, 0.8$ Hz, 2H), 6.93 – 6.89 (m, 2H), 5.74 (s, 1H), 4.07 – 3.97 (m, 4H), 3.78 (s, 3H). ^{13}C NMR (DMSO- d_6): δ 154.5, 152.7, 137.5, 132.8, 129.2, 127.0, 126.4, 122.5, 122.3, 120.2, 114.0, 101.1, 64.7, 55.2. ESI–HRMS: m/z calculated for $\text{C}_{17}\text{H}_{18}\text{N}_2\text{O}_4\text{Na}$ $[\text{M} + \text{Na}]^+$: 337.1164; found: 337.1156.



1-(2-(1,3-dioxolan-2-yl)phenyl)-3-(4-fluorophenyl)urea:

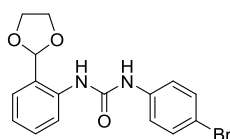
Compound **9**(F) was synthesized from **7** and 4-fluoroaniline according to the general procedure. The crude product was purified by silica gel column chromatography using petroleum ether/ethyl acetate (4:1, v/v, containing 2% Et_3N) as an eluent to obtain **9**(F) as a white solid (87%). MP: 176.8-177.7 °C. ^1H NMR (CD_3CN): δ 7.94 (d, $J = 8.4$ Hz, 2 H), 7.71 (br, 1H), 7.67 (br, 1H), 7.51 – 7.47 (m, 2H), 7.44 (dd, $J = 7.6, 1.2$ Hz, 1 H), 7.38 (td, $J = 8.0, 1.6$ Hz, 1 H), 7.13 – 7.05 (m, 3 H), 5.79(s, 1H), 4.18 – 4.00 (m, 4H). ^{13}C NMR (CD_3CN): δ 160.7, 158.3, 153.9, 153.8, 138.5, 136.7, 130.5, 128.4, 127.6, 123.9, 123.7, 122.3, 122.2, 116.3, 116.1, 103.4, 65.9. ESI–HRMS: m/z calculated for $\text{C}_{16}\text{H}_{14}\text{FN}_2\text{O}_3$ $[\text{M} - \text{H}]^-$: 301.0988; found: 301.0979.



1-(2-(1,3-dioxolan-2-yl)phenyl)-3-(4-chlorophenyl)urea:

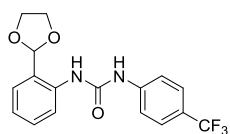
Compound **9**(Cl) was synthesized from **7** and 4-chloroaniline

according to the general procedure. The crude product was purified by silica gel column chromatography using petroleum ether/ethyl acetate (4:1, v/v, containing 2% Et₃N) as an eluent to obtain **9(Cl)** as a white solid (89%). MP: 181.2-182.2 °C. ¹H NMR (CD₃CN): δ 7.92 (d, *J* = 8.0 Hz, 1 H), 7.84 (br, 1 H), 7.70 (1 br, H), 7.52 – 7.48 (m, 2H), 7.45 (dd, *J* = 7.6, 1.2 Hz, 1H), 7.39 (td, *J* = 7.6, 1.6 Hz, 1 H), 7.33 – 7.30 (m, 2H), 7.12 (td, *J* = 8.4, 0.8 Hz, 1H), 5.80(1 H, s), 4.20 – 4.01 (m, 4 H). ¹³C NMR (DMSO-*d*₆): δ 152.4, 138.9, 137.0, 129.2, 128.6, 127.0, 125.3, 123.0, 122.8, 119.7, 101.0, 64.7. ESI–HRMS: *m/z* calculated for C₁₆H₁₄ClN₂O₃ [M – H][–]: 317.0693; found: 317.0682.



1-(2-(1,3-dioxolan-2-yl)phenyl)-3-(4-bromophenyl)urea:

Compound **9(Br)** was synthesized from **7** and 4-bromoaniline according to the general procedure. The crude product was purified by silica gel column chromatography using petroleum ether/ethyl acetate (4:1, v/v, containing 2% Et₃N) as an eluent to obtain **9(Br)** as a white solid (88%). MP: 180.3-181.0 °C. ¹H NMR (CD₃CN): δ 7.92 (d, *J* = 8.0 Hz, 1H), 7.84 (br, 1H), 7.70 (br, 1 H), 7.45 – 7.43 (m, 5H), 7.39 (td, *J* = 8.0, 1.6 Hz, 1H), 7.12 (td, *J* = 7.6, 0.8 Hz, 1H), 5.80 (s, 1H), 4.20 – 4.00 (m, 4 H). ¹³C NMR (CD₃CN): δ 160.7, 158.3, 153.9, 153.8, 138.5, 136.7, 130.5, 128.4, 127.6, 123.9, 123.7, 122.3, 122.2, 116.3, 116.1, 103.4, 65.9. ESI–HRMS: *m/z* calculated for C₁₆H₁₄BrN₂O₃ [M – H][–]: 361.0188; found: 361.0173.

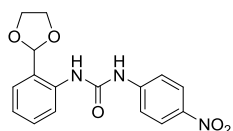


1-(2-(1,3-dioxolan-2-yl)phenyl)-3-(4-

(trifluoromethyl)phenyl)urea: Compound **9(CF₃)** was

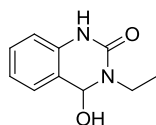
synthesized from **7** and 4-(trifluoromethyl)aniline according to the general procedure. The crude product was purified by silica gel column chromatography using petroleum ether/ethyl acetate (4:1, v/v, containing 2% Et₃N) as an eluent to obtain **9(CF₃)** as a white solid (85%). MP: 211.3-212.1 °C. ¹H NMR (CD₃CN): δ 8.07 (br, 1 H), 7.93 (d, *J* = 8.0 Hz, 1 H), 7.77 (br, 1H), 7.69 (d, *J* = 8.8 Hz, 2H), 7.62 (d, *J* = 8.8 Hz, 2H), 7.47 (dd, *J* = 8.0, 1.6 Hz, 1 H), 7.40 (td, *J* = 8.0, 1.6 Hz, 1H), 7.14 (td, *J* = 7.6, 0.8 Hz, 1H), 5.82 (s, 1H), 4.22 – 4.02 (m, 4H). ¹³C NMR (CD₃CN): δ 153.3, 144.4, 138.1, 130.5, 128.4, 127.9, 127.1, 127.0, 124.4, 124.2, 124.0, 119.3,

103.3, 65.9. ESI–HRMS: m/z calculated for $C_{17}H_{14}F_3N_3O_3$ $[M - H]^-$: 351.0957; found: 351.0945.



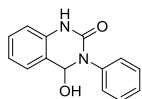
1-(2-(1,3-dioxolan-2-yl)phenyl)-3-(4-nitrophenyl)urea:

Compound **9**(NO₂) was synthesized from **7** and 4-nitroaniline according to the general procedure. The crude product was purified by silica gel column chromatography using petroleum ether/ethyl acetate (4:1, v/v, containing 2% Et₃N) as an eluent to obtain **8**(NO₂) as a white solid (82%). MP: 217.5-218.2 °C. ¹H NMR (CD₃CN): δ 8.33 (br, 1H), 8.21 – 8.17 (m, 2H), 7.94 (d, $J = 8.4$ Hz, 1H), 7.85 (br, 1H), 7.74 – 7.70 (m, 2H), 7.47 (dd, $J = 7.6, 1.2$ Hz, 1H), 7.41 (td, $J = 9.6, 1.6$ Hz, 1H), 7.16 (td, $J = 7.6, 1.2$ Hz, 1H), 5.83 (s, 1 H), 4.23 – 4.03 (m, 4H). ¹³C NMR (CD₃CN): δ 153.0, 147.2, 143.1, 137.8, 130.5, 128.4, 128.1, 126.0, 124.5, 124.1, 103.3, 66.0. ESI–HRMS: m/z calculated for $C_{16}H_{14}N_3O_5$ $[M - H]^-$: 328.0939; found: 328.0933.



3-ethyl-4-hydroxy-3,4-dihydroquinazolin-2(1H)-one: Compound **1**(Et) was synthesized from **9**(Et) and aqueous HCl according to the general procedure. The crude product was recrystallized from dichloromethane

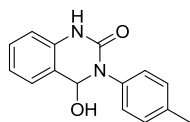
to obtain **1**(Et) as a white solid (69%). MP: 225.1-226.0 °C. ¹H NMR (DMSO-*d*₆) δ 9.56 (s, 1H), 7.23 – 7.18, 6.92 (td, $J = 7.6, 1.2$ Hz, 1H), 6.82 (d, $J = 8.0$ Hz, 1H), 6.22 (d, $J = 7.6$ Hz, 1H), 5.76 (d, $J = 8.0$ Hz, 1H), 3.66 – 3.57 (m, 1H), 3.36 – 3.28 (m, 1H), 1.13 (t, $J = 7.2$ Hz, 1H). ¹³C NMR (DMSO-*d*₆): δ 152.2, 136.8, 129.2, 127.7, 121.2, 121.1, 113.8, 79.0, 14.3. ESI–HRMS: m/z calculated for $C_{10}H_{12}N_2O_2Na$ $[M + Na]^+$ 215.0791; found: 215.0791.



4-hydroxy-3-phenyl-3,4-dihydroquinazolin-2(1H)-one: Compound **1**(H)

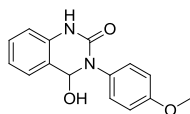
was synthesized from **9**(H) and aqueous HCl according to the general procedure. The crude product was recrystallized from ethyl acetate to obtain **1**(H) as a white solid (91%). MP: 201.3-202.1 °C. ¹H NMR (DMSO-*d*₆): δ 9.96 (s, 1H), 7.45 – 7.37 (m, 4H), 7.28 – 7.24 (m, 3H), 6.97 (d, $J = 7.6$ Hz, 1H), 6.93 (d, $J = 8.0$ Hz, 1H),

6.54 (d, $J = 8.0$ Hz, 1H), 5.92 (d, $J = 8.0$ Hz, 1H). ^{13}C NMR (DMSO- d_6): δ 151.5, 141.7, 136.1, 128.9, 128.4, 127.2, 126.9, 125.9, 121.4, 121.1, 113.7, 81.4. ESI-HRMS: m/z calculated for $\text{C}_{14}\text{H}_{12}\text{N}_2\text{O}_2\text{Na}$ $[\text{M} + \text{Na}]^+$ 263.0791; found: 263.0790.



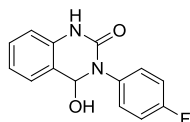
4-hydroxy-3-(p-tolyl)-3,4-dihydroquinazolin-2(1H)-one:

Compound **1**(Me) was synthesized from **9**(Me) and aqueous HCl according to the general procedure. The crude product was recrystallized from petroleum ether/ethyl acetate to obtain **1**(Me) as a white solid (81%). MP: 228.1-228.9 °C. ^1H NMR (DMSO- d_6): δ 9.92 (s, 1H), 7.33 – 7.25 (m, 4 H), 7.18 (d, $J = 8.4$ Hz, 2H), 6.97 (d, $J = 7.2$ Hz, 1H), 6.92 (d, $J = 8.0$ Hz, 1H), 6.49 (d, $J = 8.0$ Hz, 1H), 5.876 (d, $J = 8.0$ Hz, 1H), 2.32 (s, 3H). ^{13}C NMR (CD_3CN): δ 152.7, 140.0, 137.7, 137.1, 130.4, 130.2, 128.8, 128.1, 122.8, 122.0, 114.7, 83.2, 21.1. ESI-HRMS: m/z calculated for $\text{C}_{15}\text{H}_{14}\text{N}_2\text{O}_2\text{Na}$ $[\text{M} + \text{Na}]^+$ 277.0947; found: 277.0948.



4-hydroxy-3-(4-methoxyphenyl)-3,4-dihydroquinazolin-2(1H) - one:

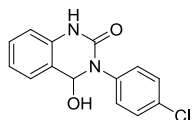
Compound **1**(OMe) was synthesized from **9**(OMe) and aqueous HCl according to the general procedure. The crude product was recrystallized from petroleum ether/ethyl acetate to obtain **1**(OMe) as a white solid (83%). MP: 210.3-211.4 °C. ^1H NMR (DMSO- d_6): δ 9.56 (s, 1 H), 7.23 – 7.18 (m, 2H), 6.91 (td, $J = 7.6, 1.2$ Hz, 1H), 6.22 (d, $J = 7.6$ Hz, 1H), 5.76 (d, $J = 8.0$ Hz, 1H), 3.66 – 3.57 (m, 1H), 3.63 – 3.28 (m, 1H), 1.13 (t, $J = 7.2$, 3H). ^{13}C NMR (DMSO- d_6): δ 157.5, 151.7, 136.2, 134.5, 128.9, 127.0, 121.4, 121.0, 113.6, 81.6, 55.3. ESI-HRMS: m/z calculated for $\text{C}_{15}\text{H}_{14}\text{N}_2\text{O}_3\text{Na}$ $[\text{M} + \text{Na}]^+$ 293.0897; found: 293.0897.



3-(4-fluorophenyl)-4-hydroxy-3,4-dihydroquinazolin-2(1H)-one:

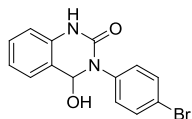
Compound **1**(F) was synthesized from **9**(F) and aqueous HCl according to the general procedure. The crude product was recrystallized from petroleum ether/ethyl acetate to obtain **1**(F) as a white solid (79%). MP: 214.1-214.9 °C. ^1H NMR (DMSO- d_6): δ 9.98 (s, 1H), 7.48 – 7.42 (m, 2H), 7.29 –

7.19 (m, 4 H), 6.98 (td, $J = 7.6, 0.8$ Hz, 1H), 6.93 (d, $J = 8.0$ Hz, 1H), 6.57 (d, $J = 8.4$ Hz, 1H), 5.90 (d, $J = 8.0$ Hz, 1H). ^{13}C NMR (DMSO- d_6): δ 161.4, 159.0, 151.5, 137.9, 136.0, 129.6, 129.5, 129.0, 127.0, 121.3, 121.2, 115.2, 115.0, 113.7, 81.4. ESI-HRMS: m/z calculated for $\text{C}_{14}\text{H}_{11}\text{FN}_2\text{O}_2\text{Na}$ [$\text{M} + \text{Na}$] $^+$ 281.0697; found: 281.0698.



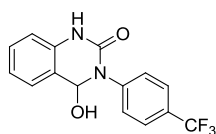
3-(4-chlorophenyl)-4-hydroxy-3,4-dihydroquinazolin-2(1H)-one:

Compound **1(Cl)** was synthesized from **9(Cl)** and aqueous HCl according to the general procedure. The crude product was recrystallized from petroleum ether/ethyl acetate to obtain **1(Cl)** as a white solid (92%). MP: 239.8-240.6 °C. ^1H NMR (DMSO- d_6): δ 10.04 (s, 1H), 7.48 – 7.43 (m, 4H), 7.29 – 7.25 (m, 4H), 6.98 (td, $J = 7.6, 0.08$ Hz, 1H), 6.94 (t, 1 H, m), 6.61 (d, $J = 8.0$ Hz, 1H), 5.94 (d, $J = 8.4$ Hz, 1H). ^{13}C NMR (DMSO- d_6): δ 151.9, 141.1, 137.9, 136.5, 130.7, 129.5, 129.4, 129.4, 128.9, 128.7, 127.5, 125.9, 121.8, 114.3, 81.7. ESI-HRMS: m/z calculated for $\text{C}_{14}\text{H}_{11}\text{ClN}_2\text{O}_2\text{Na}$ [$\text{M} + \text{Na}$] $^+$ 297.0401; found: 297.0397.



3-(4-bromophenyl)-4-hydroxy-3,4-dihydroquinazolin-2(1H)-one:

Compound **1(Br)** was synthesized from **9(Br)** and aqueous HCl according to the general procedure. The crude product was recrystallized from dichloromethane to obtain **1(Br)** as a white solid (90%). MP: 240.9-241.8 °C. ^1H NMR (DMSO- d_6): δ 10.04 (s, 1H), 7.60–7.56 (m, 2H), 7.43 – 7.39 (m, 2 H), 7.29 – 7.26 (m, 2H), 6.98 (t, $J = 7.6$ Hz, 1H), 6.93 (m, 1H), 6.61 (d, $J = 8.4$ Hz, 1H), 5.94 (d, $J = 8.0$ Hz, 1H). ^{13}C NMR (DMSO- d_6): δ 151.3, 141.0, 135.9, 131.3, 129.2, 129.0, 127.0, 121.3, 118.5, 113.8, 81.2. ESI-HRMS: m/z calculated for $\text{C}_{14}\text{H}_{11}\text{BrN}_2\text{O}_2\text{Na}$ [$\text{M} + \text{Na}$] $^+$ 340.9896; found: 340.9896.



4-hydroxy-3-(4-(trifluoromethyl)phenyl)-3,4-

dihydroquinazolin-2(1H)-one: Compound **1(CF₃)** was synthesized from **9(CF₃)** and aqueous HCl according to the general procedure.

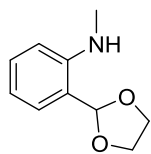
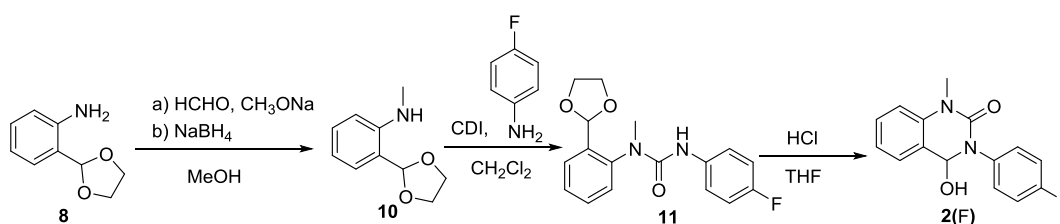
The crude product was recrystallized from ethyl acetate to obtain **1(CF₃)** as a white

solid (97%). MP: 282.6-283.3 °C. ¹H NMR (DMSO-*d*₆): δ 10.16 (s, 1H), 7.76 (d, *J* = 8.8 Hz, 2H), 7.70 (d, *J* = 8.8 Hz, 2H), 7.31 – 7.28 (m, 2H), 7.00 (td, *J* = 8.0, 0.8 Hz, 1H), 6.96 (d, *J* = 8.0 Hz, 1H), 6.72 (d, *J* = 8.0 Hz, 1H), 6.04 (d, *J* = 8.0 Hz, 1H). ¹³C NMR (DMSO-*d*₆): δ 151.2, 145.4, 135.7, 129.1, 127.0, 126.9, 126.9, 125.7, 125.5, 125.4, 123.0, 121.5, 121.3, 113.9, 81.0. ESI-HRMS: *m/z* calculated for C₁₅H₁₁F₃N₂O₂Na [M + Na]⁺ 331.0665; found: 331.0666.



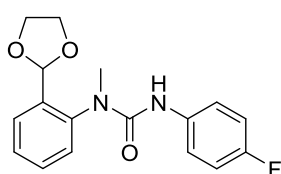
4-hydroxy-3-(4-nitrophenyl)-3,4-dihydroquinazolin-2(1H)-one: Compound **1**(NO₂) was synthesized from **9**(NO₂) and aqueous HCl according to the general procedure. The crude product was recrystallized from petroleum ether/ethyl acetate to obtain **1**(NO₂) as a pale yellow solid (70%). MP: 276.8-277.6 °C. ¹H NMR (DMSO-*d*₆): δ 10.30 (s, 1H), 8.28 – 8.24 (m, 2H), 7.79 – 7.50 (m, 2H), 7.34 – 7.29 (m, 2H), 7.02 (td, *J* = 7.6, 0.8 Hz, 1 H), 6.97 (d, *J* = 8.0 Hz, 1H), 6.85 (d, *J* = 8.0 Hz, 1H), 6.12 (d, *J* = 8.4 Hz, 1 H). ¹³C NMR (CD₃CN): δ 152.1, 148.6, 146.3, 136.5, 130.7, 128.0, 127.6, 124.9, 123.3, 121.9, 115.0, 82.6. ESI-HRMS: *m/z* calculated for C₁₄H₁₁N₃O₄Na [M + Na]⁺ 308.0642; found: 308.0641.

Scheme S2. The Synthesis of Compound **2**(F)



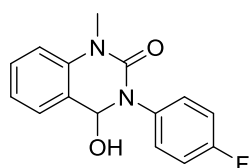
2-(1,3-dioxolan-2-yl)-N-methylaniline: To a mixture of 2-(1,3-dioxolan-2-yl)aniline **8** (400 mg, 2.42 mmol) and sodium methoxide (196 mg, 3.63 mmol) in MeOH (10 mL), was added paraformaldehyde (200 mg). The reaction was stirred at 40 °C for 16 h. Sodium borohydride (137 mg, 3.36 mmol) was then added to the mixture, and the reaction was stirred at 40 °C for another

3 h. The reaction was quenched with 20 mL of saturated aqueous NaHCO₃ and subsequently extracted with Et₂O. The organic phase was washed with brine three times and dried over Na₂SO₄. The crude product was purified via alkaline aluminum oxide column chromatography to afford compound **10** as a light yellow oil (351 mg, 81%). ¹H NMR (DMSO-*d*₆): δ 7.21-7.17 (m, 2H), 6.61 – 6.53 (m, 2H), 5.68 (s, 1H), 5.19 – 5.17 (m, 1H), 4.09 – 3.90 (m, 4H), 2.72 (d, *J* = 4.8 Hz, 3H). ¹³C NMR (DMSO-*d*₆): δ 148.0, 130.5, 127.5, 120.6, 115.4, 110.2, 102.26, 64.8, 30.4. ESI-HRMS: *m/z* calculated for C₁₀H₁₄NO₂Na [M + Na]⁺ 202.0838; found: 202.0838.



3-(4-fluorophenyl)-4-hydroxy-1-methyl-3,4-dihydroquinazolin-2(1H)-one: Compound **11** was synthesized from **10** and 4-fluoroaniline according to the general procedure. The crude product was purified by silica

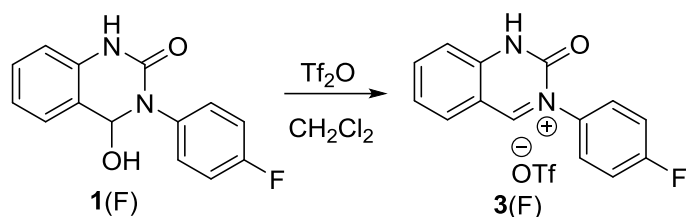
gel column chromatography using petroleum ether/ethyl acetate (3:1, v/v, containing 2% Et₃N) as an eluent to obtain **11** as a white solid (80%). MP: 107.3-108.1 °C. ¹H NMR (DMSO-*d*₆): δ 7.84 (br, 1H), 7.61 (*d*, *J* = 7.6 Hz, 1H), 7.40 (*t*, *J* = 6.4 Hz, 1H), 7.45 – 7.35 (m, 3H), 7.31 (*d*, *J* = 7.6 Hz, 1H), 7.05 (*t*, *J* = 8.4 Hz, 2H), 5.83 (s, 1H), 4.11 – 3.90 (m, 4H), 3.18 (s, 3H). ¹³C NMR (DMSO-*d*₆): δ 159.2, 156.8, 155.3, 142.6, 136.8, 136.4, 131.0, 129.5, 128.3, 127.9, 122.5, 122.4, 115.2, 115.0, 100.0, 65.4, 55.4. ESI-HRMS: *m/z* calculated for C₁₇H₁₇FN₂O₃Na [M + Na]⁺ 339.1113; found: 339.1108.



3-(4-fluorophenyl)-4-hydroxy-1-methyl-3,4-dihydroquinazolin-2(1H)-one: Compound **2(F)** was synthesized from **11** and aqueous HCl according to the general procedure. The crude product was recrystallized from petroleum ether/ethyl

acetate to obtain **2(F)** as a white solid (85%). MP: 171.2-172.3 °C. ¹H NMR (DMSO-*d*₆): δ 7.479 – 7.40 (m, 3H), 7.34 (*d*, *J* = 7.6 Hz, 1H), 7.23 (*t*, *J* = 8.8 Hz, 2H), 7.14 – 7.08 (m, 2H), 6.63 (*d*, *J* = 7.6 Hz, 1H), 5.87 (*d*, *J* = 8.0 Hz, 1H), 3.34 (s, 3H). ¹³C NMR (DMSO-*d*₆): δ 152.4, 137.9, 129.7, 129.5, 129.4, 127.4, 123.5, 122.2, 115.7, 115.5, 113.8, 81.0, 30.6. ESI-HRMS: *m/z* calculated for C₁₅H₁₄FN₂O₂ [M + H]⁺ 273.1039; found: 273.1023.

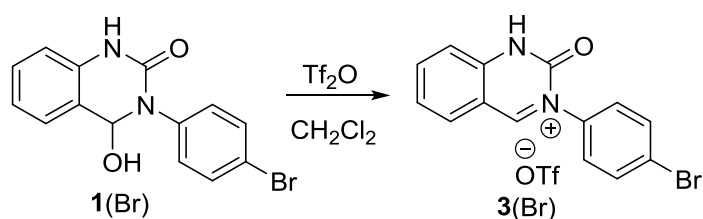
Scheme S3. The Synthesis of Compound **3(F)**



3-(4-fluorophenyl)-2-oxo-1,2-dihydroquinazolin-3-ium trifluoromethanesulfonate:

To a solution of **1(F)** (300 mg, 1.16 mmol) in anhydrous CH₂Cl₂ (50 mL) was added trifluoromethanesulfonic anhydride (1.0 mL). The mixture was stirred at room temperature for 1 h. The solvent was removed under vacuum, and diethyl ether (10 mL) was added to the residual. The resulting precipitates were filtered and washed with diethyl ether to obtain pure **3(F)** as a yellow solid (440 mg, 97%). MP: 230.8.3-231.9 °C. ¹H NMR (CD₃CN): δ 11.55 (br, 1H), 9.71 (s, 1H), 8.30 (t, *J* = 8.4 Hz, 1H), 8.21 (d, *J* = 8.0 Hz, 1H), 7.73-7.67 (m, 4H), 7.48-7.44 (m, 2H). ¹³C NMR (CD₃CN): δ 166.9, 165.0, 162.5, 145.9, 145.7, 145.0, 133.6, 133.6, 133.2, 128.7, 128.6, 126.6, 117.0, 116.7, 116.2, 114.1. ESI-HRMS: *m/z* calculated for C₁₅H₁₄FN₂O₂ [M]⁺ 241.0772; found: 241.0774.

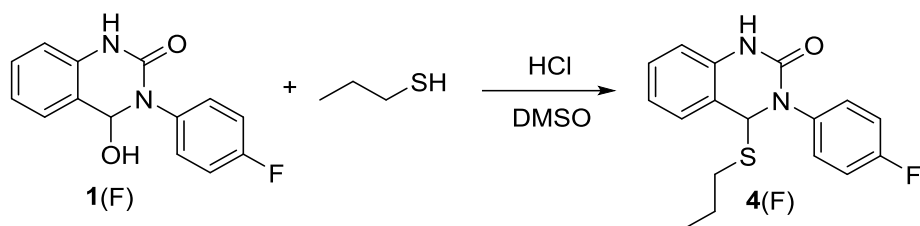
Scheme S4. The Synthesis of Compound **3(Br)**



3-(4-bromophenyl)-2-oxo-1,2-dihydroquinazolin-3-ium

trifluoromethanesulfonate Compound **3(Br)** was synthesized from **1(Br)** (100 mg, 0.31 mmol) by using the similar procedure as **3(F)** to obtain a yellow solid (134 mg, 95%). MP: 245.6-246.3 °C. ¹H NMR (CD₃CN): δ 11.62 (br, 1H), 9.69 (s, 1H), 8.31-8.26 (m, 2H), 8.20 (d, *J* = 8.0 Hz, 1H), 7.86 (d, *J* = 8.8 Hz, 2H), 7.70-7.64 (m, 2H), 7.57 (d, *J* = 7.2 Hz, 1H). ¹³C NMR (CD₃CN) δ 166.7, 146.0, 145.5, 145.10, 136.6, 133.2, 133.0, 128.1, 126.6, 125.10, 116.3, 114.2. ESI-HRMS: *m/z* calculated for C₁₄H₁₀BrN₂O [M]⁺ 300.9971; found: 300.9973.

Scheme S5. The Synthesis of Compound **4(F)**



To a solution of **1(F)** (200 mg, 0.78 mmol) in DMSO (10 mL) was added 1-propanethiol (177 mg, 2.32 mmol) and aqueous HCl (3 mL). The reaction was stirred at r.t. for 14 h. The mixture was extracted with EtOAc (3 × 30 ml) and washed with saturated aqueous NaHCO₃. The organic phase was dried over MgSO₄ and concentrated under vacuum. The crude product was purified by silica gel column chromatography using petroleum ether/ethyl acetate (9:1, v/v, containing 2% Et₃N) as an eluent to afford **3(F)** as a white solid (240 mg, 98 %). MP: 59.5-60.1 °C. ¹H NMR (CD₃CN): δ 7.90 (br, 1H), 7.50 – 7.45 (m, 2H), 7.29 – 7.24 (m, 2H), 7.20 – 7.14 (m, 2H), 7.04, (td, *J* = 8.4, 1.2 Hz, 1H) 6.90 (d, *J* = 8.0 Hz, 1H), 6.05 (s, 1H), 2.45 – 2.38 (m, 1H), 2.34 – 2.27 (m, 1H), 1.44 – 1.35 (m, 1H), 0.82 (d, *J* = 7.2 Hz, 1H). ¹³C NMR (CD₃CN): δ 162.5, 160.0, 152.1, 137.4, 137.3, 136.8, 130.4, 130.3, 128.9, 126.2, 122.1, 120.3, 115.5, 115.3, 113.7, 67.8, 31.0, 22.7, 12.8. ESI-HRMS: *m/z* calculated for C₁₇H₁₇FN₂OSNa [M + Na]⁺ 339.0938; found: 339.0939.

^1H NMR and ^{13}C NMR Spectra

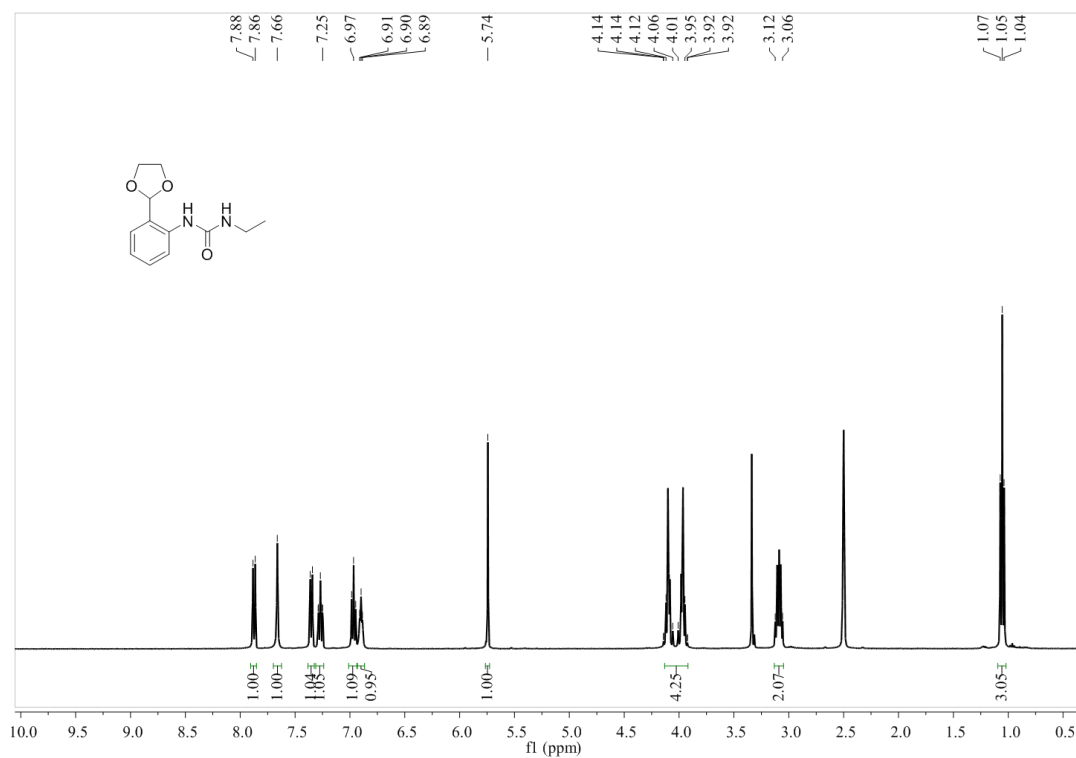


Figure S1. ^1H NMR spectrum of 9(Et) in $\text{DMSO-}d_6$.

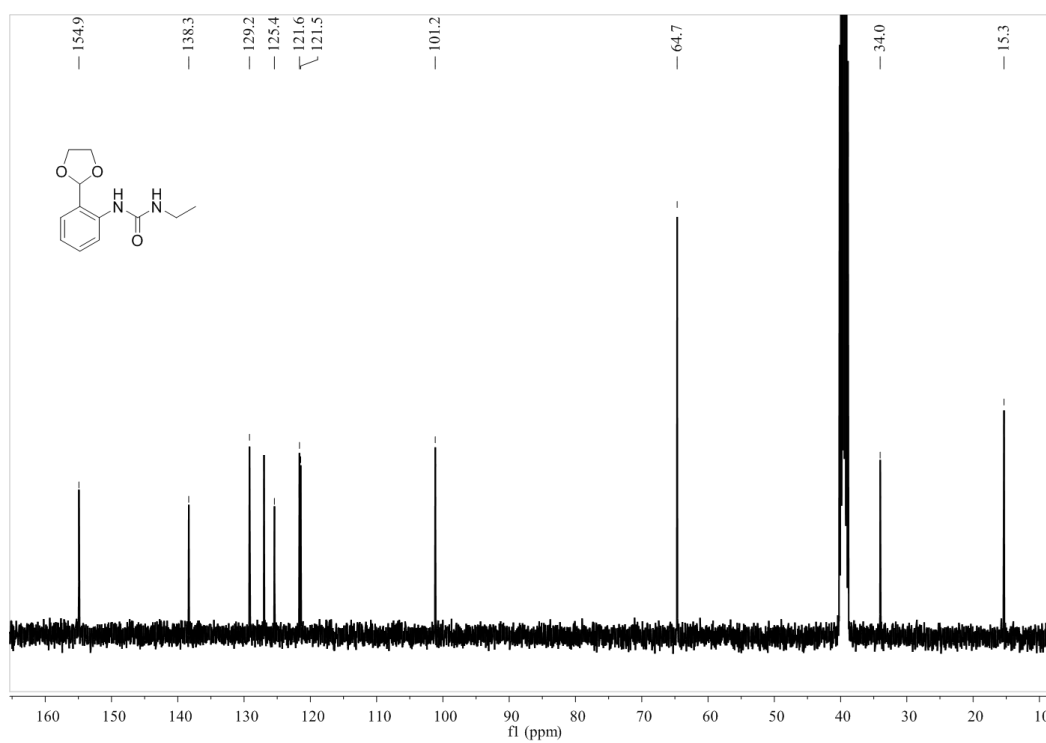


Figure S2. ^{13}C NMR spectrum of 9(Et) in $\text{DMSO-}d_6$.

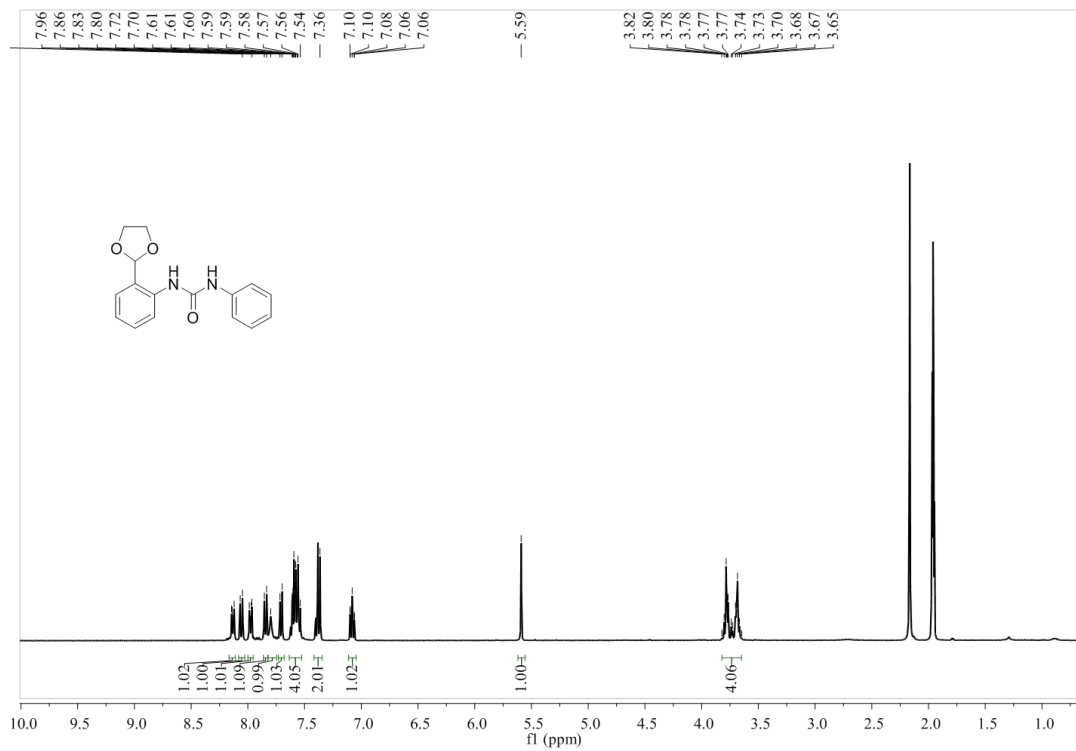


Figure S3. ^1H NMR spectrum of **9(H)** in CD_3CN .

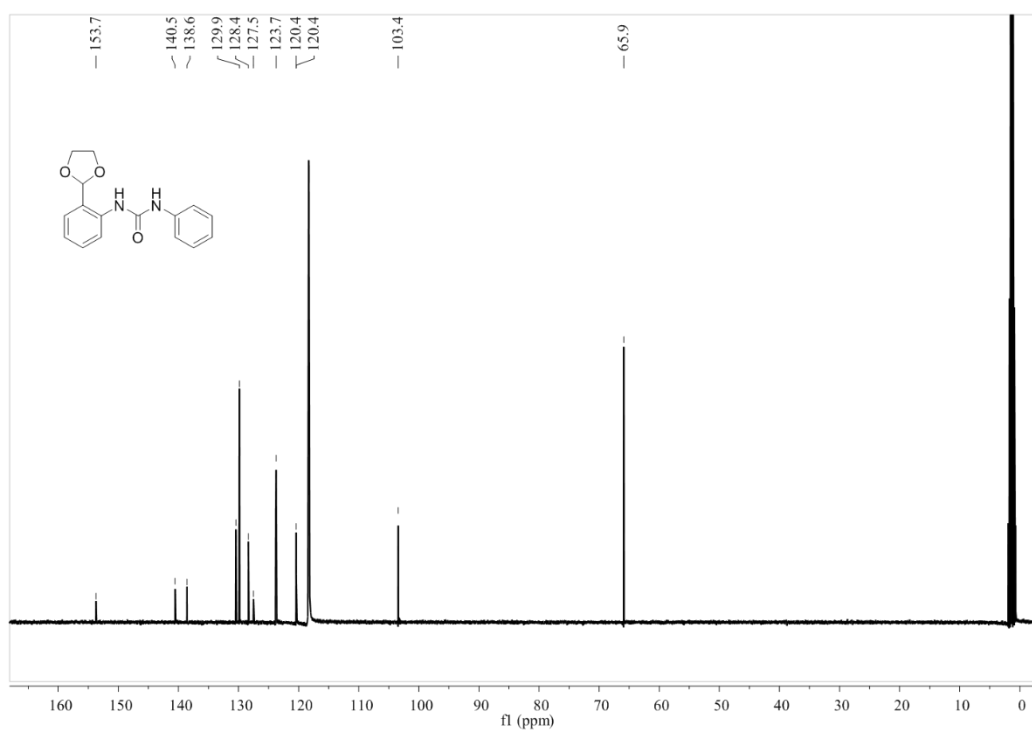


Figure S4. ^{13}C NMR spectrum of **9(H)** in CD_3CN .

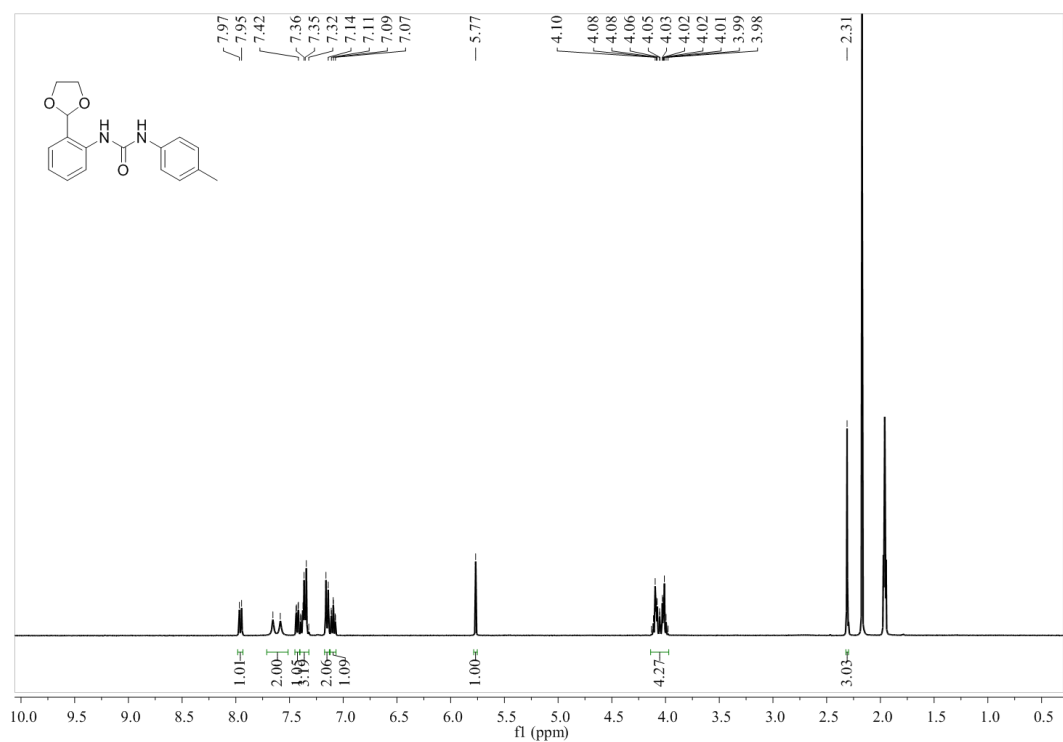


Figure S5. ¹H NMR spectrum of **9(Me)** in CD₃CN.

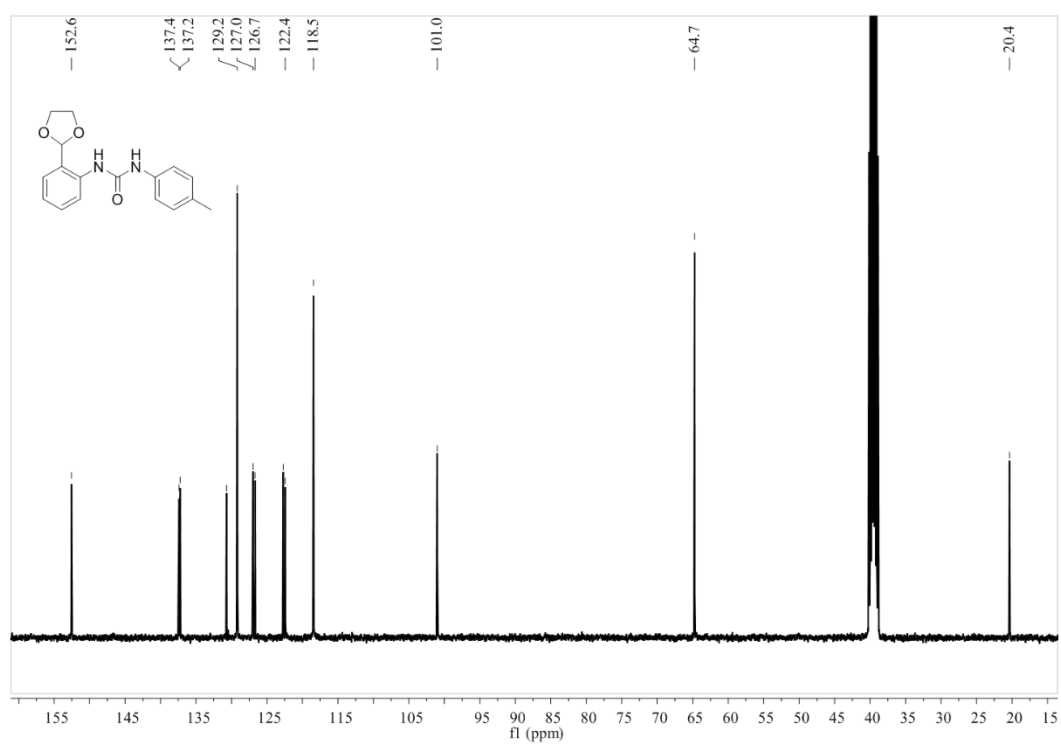


Figure S6. ¹³C NMR spectrum of **9(Me)** in DMSO-*d*₆.

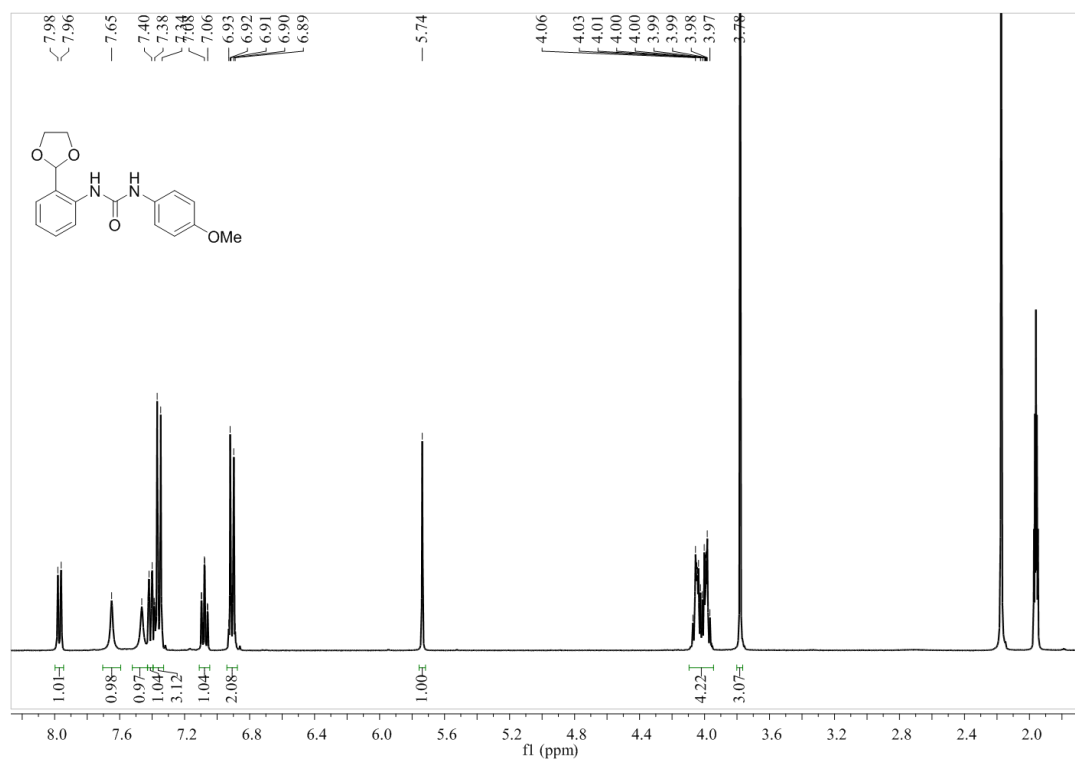


Figure S7. ¹H NMR spectrum of **9(OMe)** in CD₃CN.

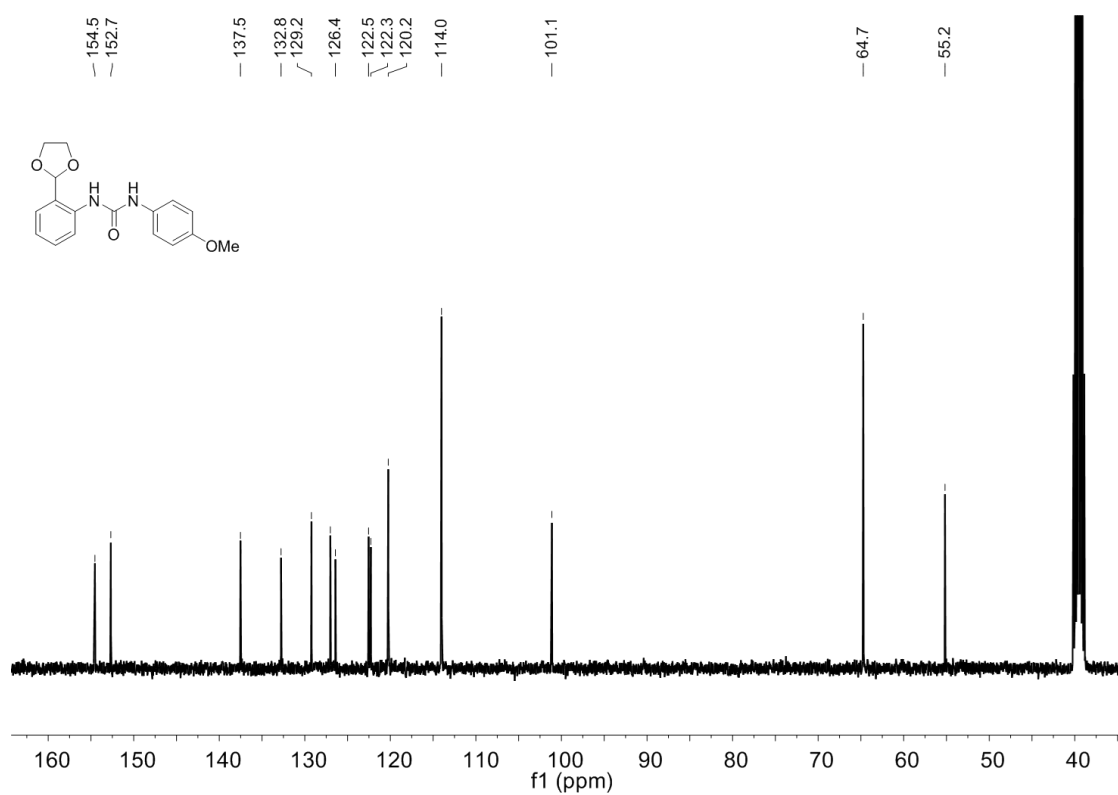


Figure S8. ¹³C NMR spectrum of **9(OMe)** in DMSO-*d*₆.

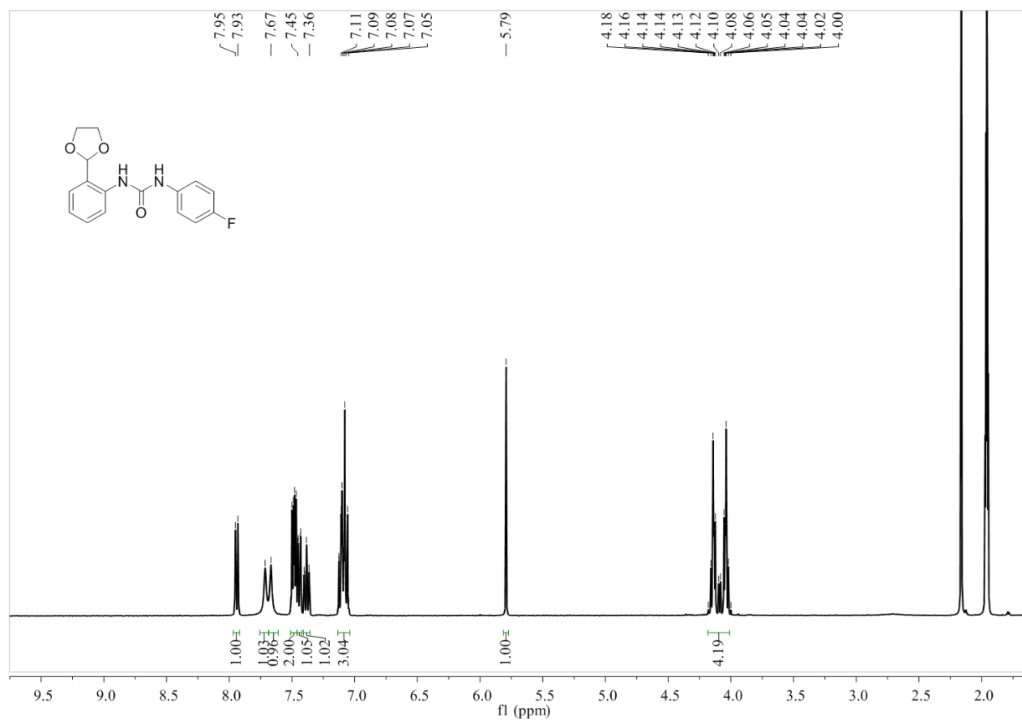


Figure S9. ¹H NMR spectrum of 9(F) in CD₃CN.

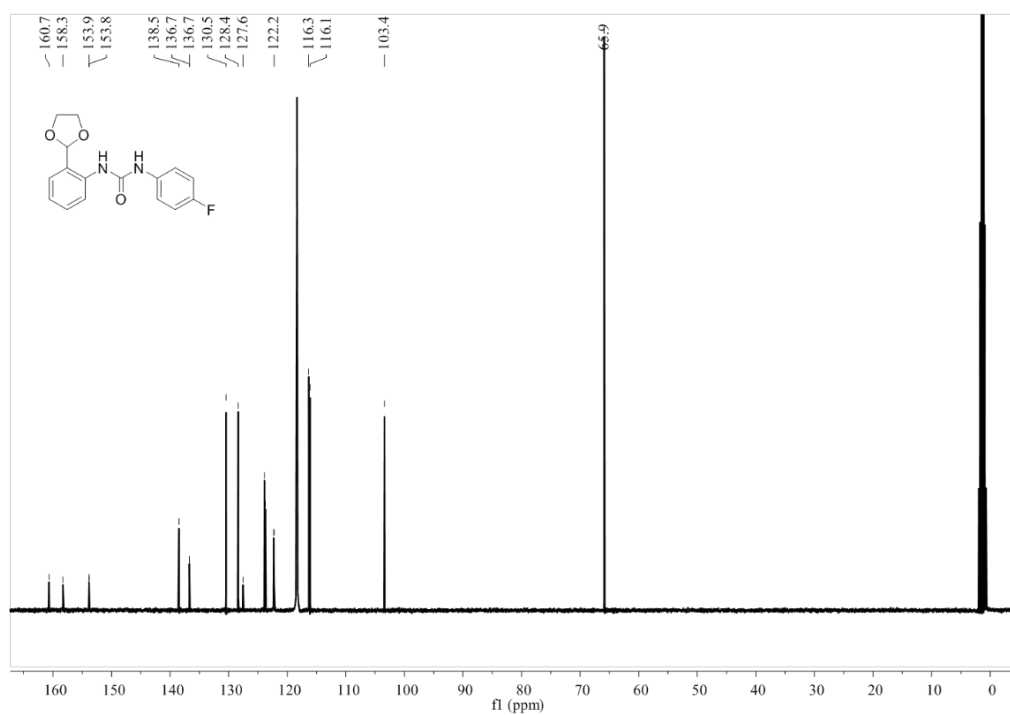


Figure S10. ¹³C NMR spectrum of 9(F) in CD₃CN.

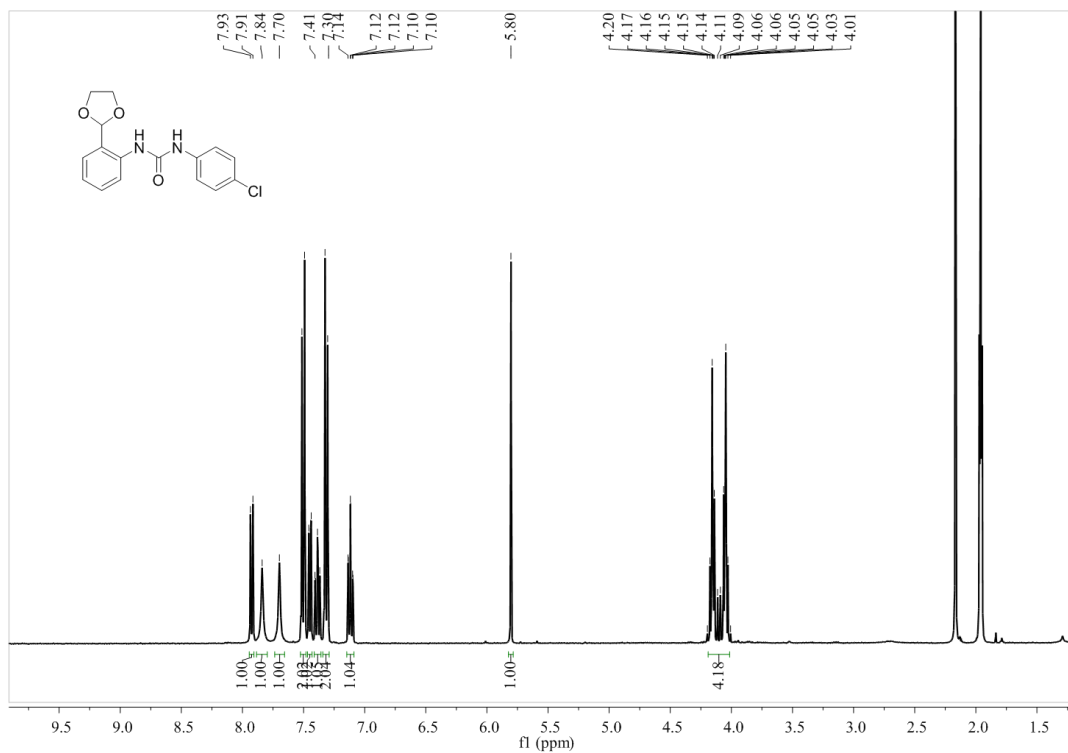


Figure S11. ¹H NMR spectrum of **9(Cl)** in CD₃CN.

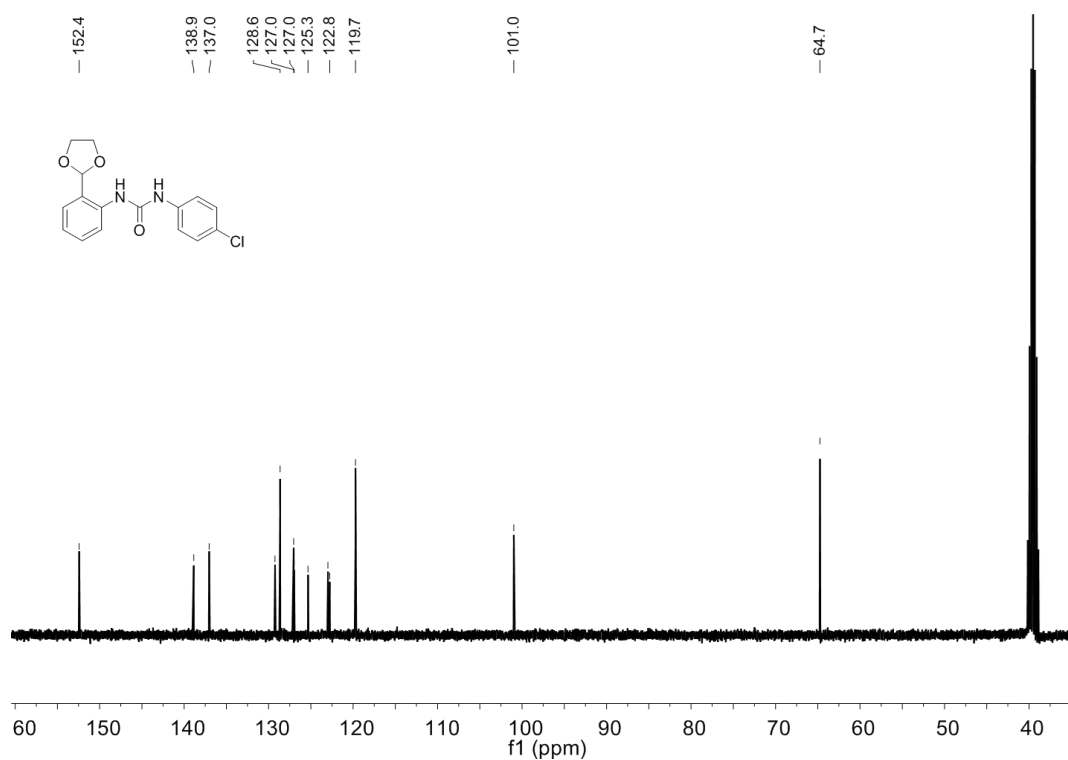


Figure S12. ¹³C NMR spectrum of **9(Cl)** in DMSO-*d*₆.

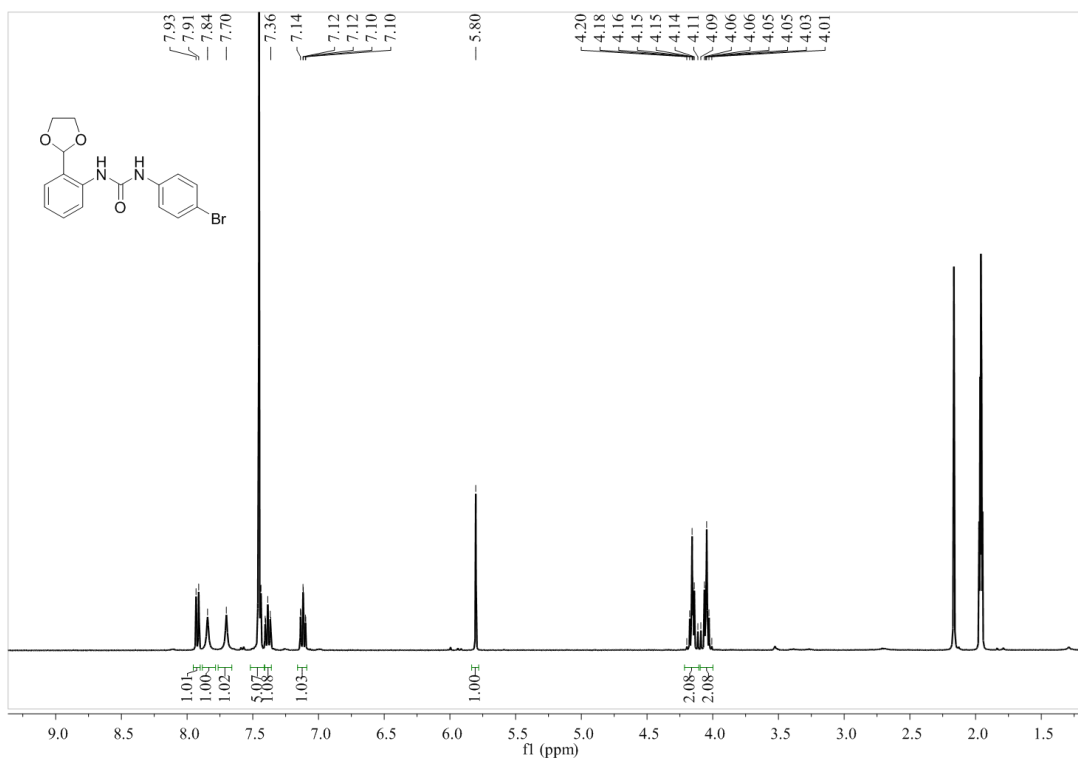


Figure S13. ^1H NMR spectrum of **9(Br)** in CD_3CN .

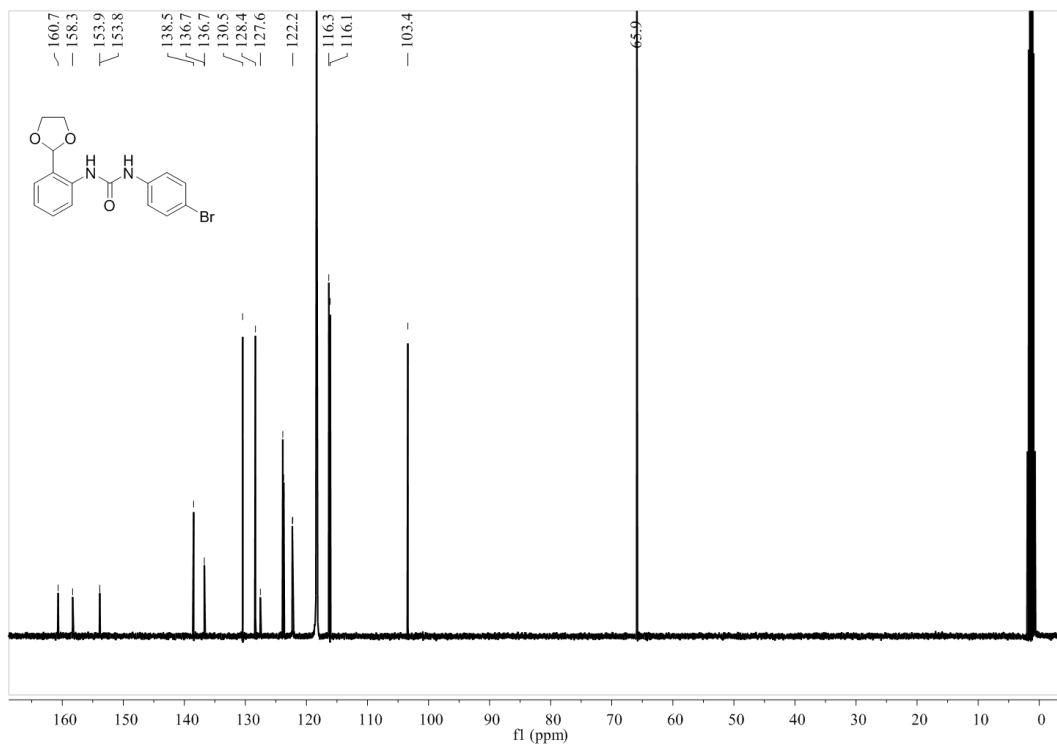


Figure S14. ^{13}C NMR spectrum of **9(Br)** in CD_3CN .

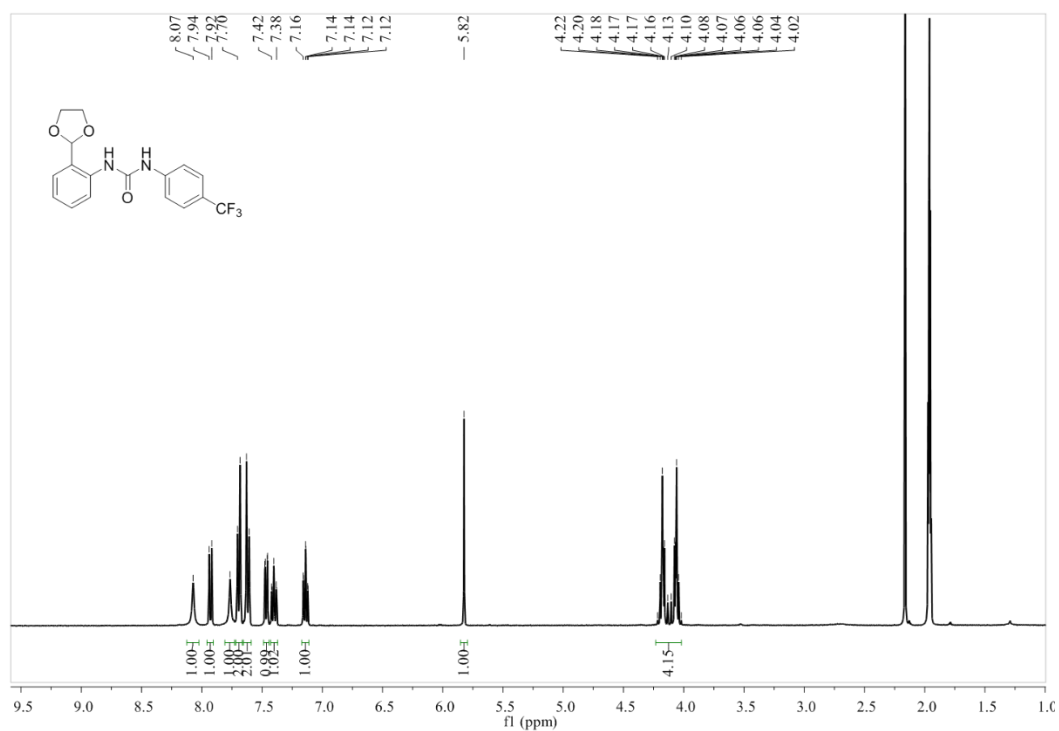


Figure S15. ^1H NMR spectrum of **9**(CF₃) in CD₃CN.

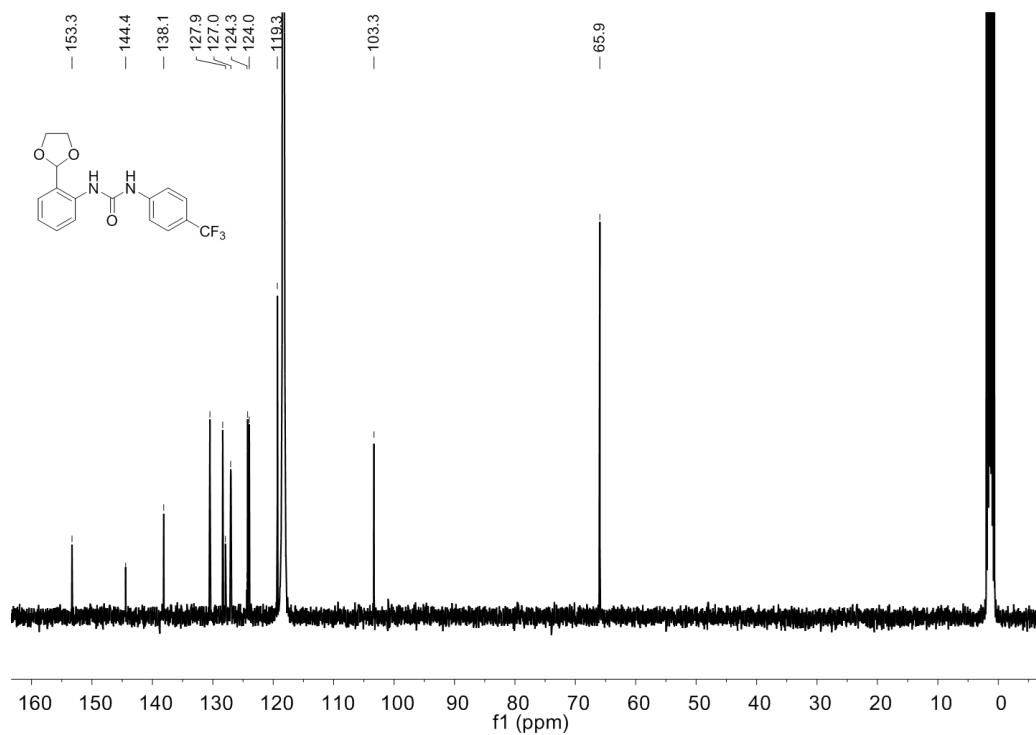


Figure S16. ^{13}C NMR spectrum of **9**(CF₃) in CD₃CN.

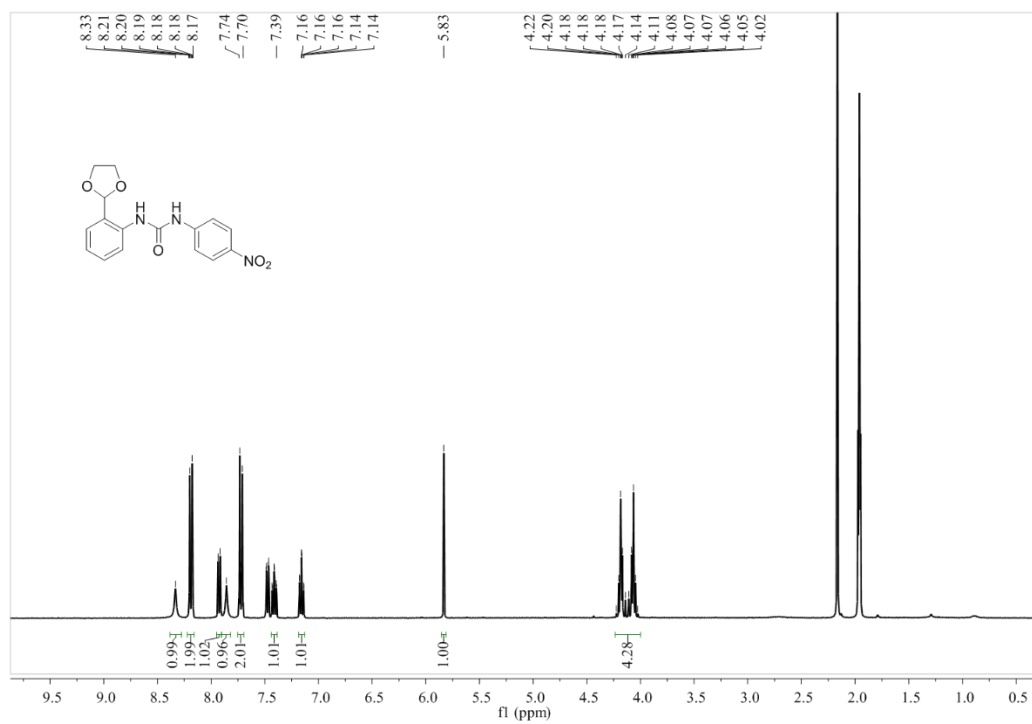


Figure S17. ¹H NMR spectrum of **9**(NO₂) in CD₃CN.

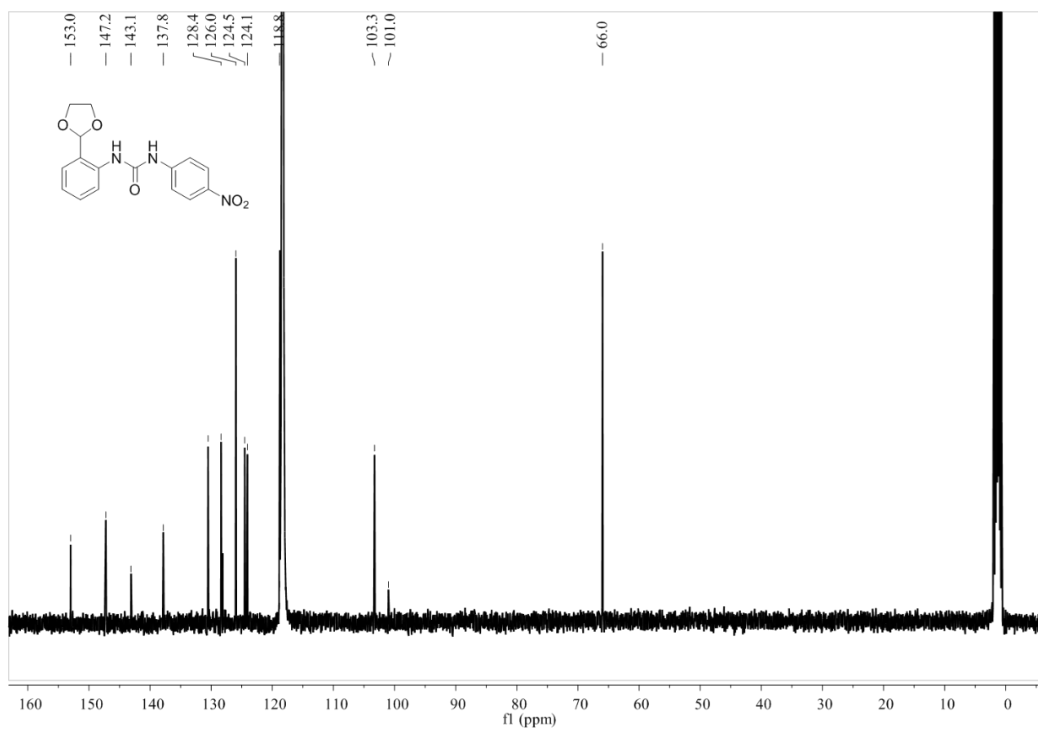


Figure S18. ¹³C NMR spectrum of **9**(NO₂) in CD₃CN.

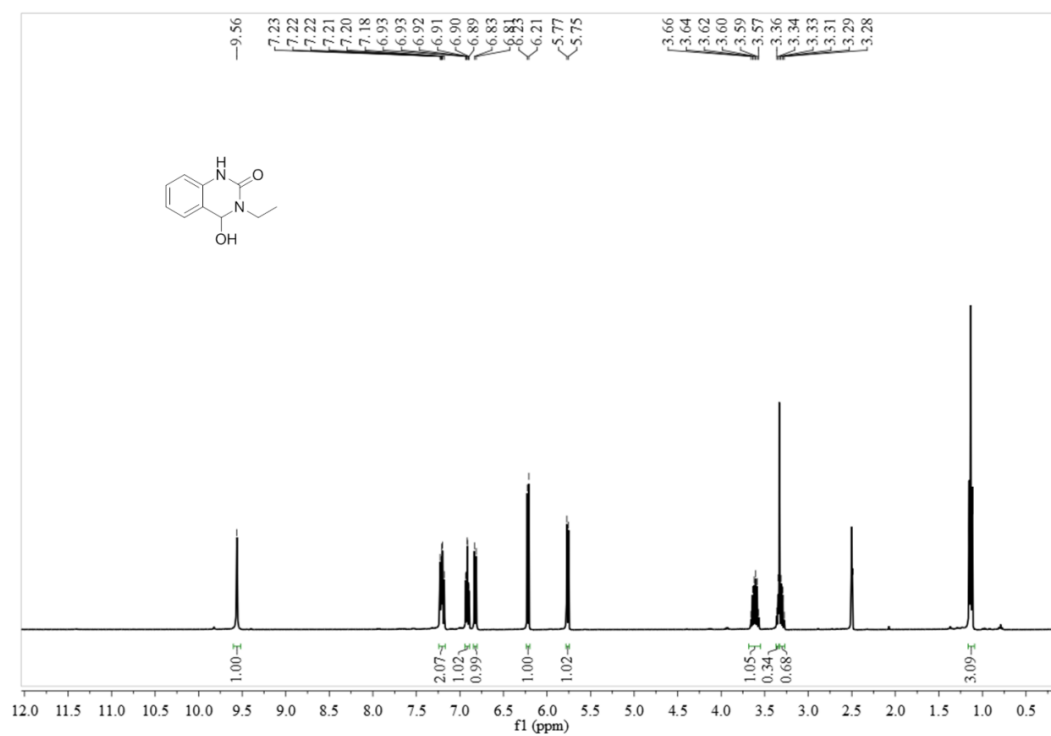


Figure S19. ^1H NMR spectrum of **1**(Et) in $\text{DMSO-}d_6$.

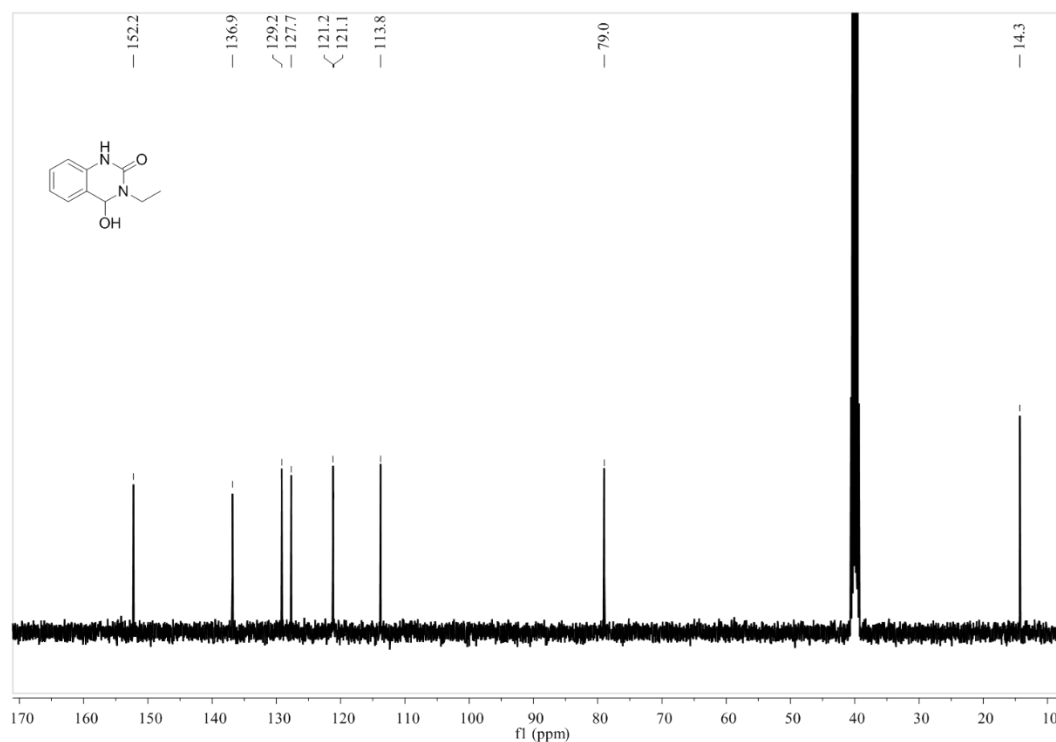


Figure S20. ^{13}C NMR spectrum of **1**(Et) in $\text{DMSO-}d_6$.

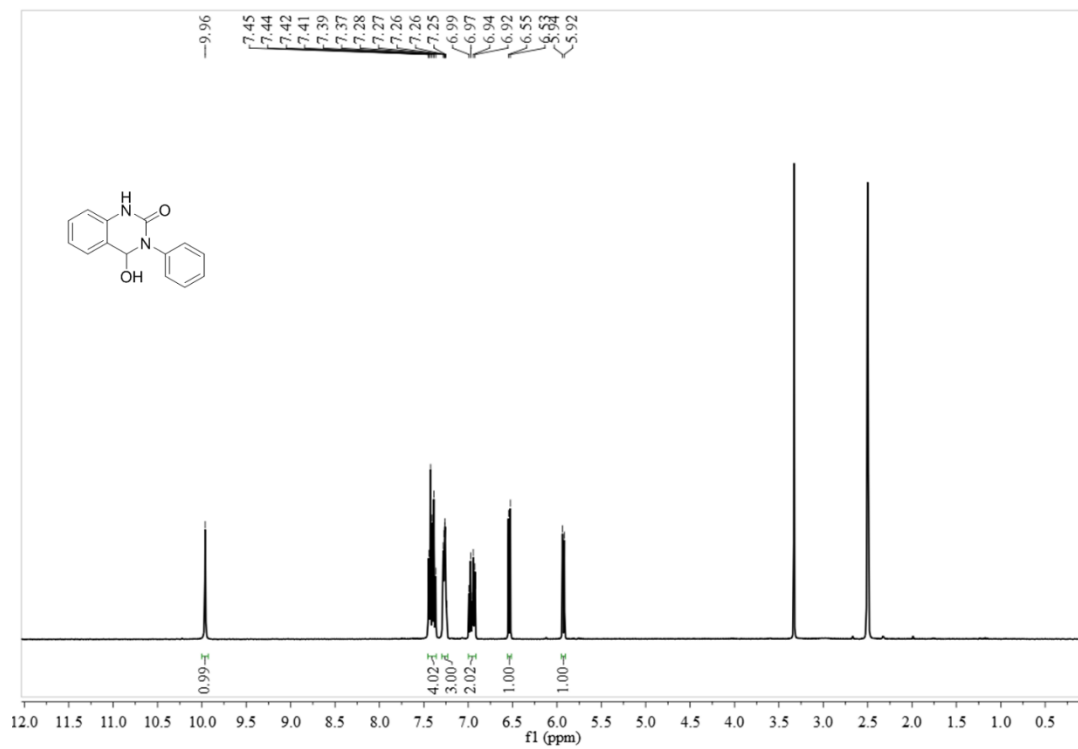


Figure S21. ^1H NMR spectrum of 1(H) in $\text{DMSO-}d_6$.

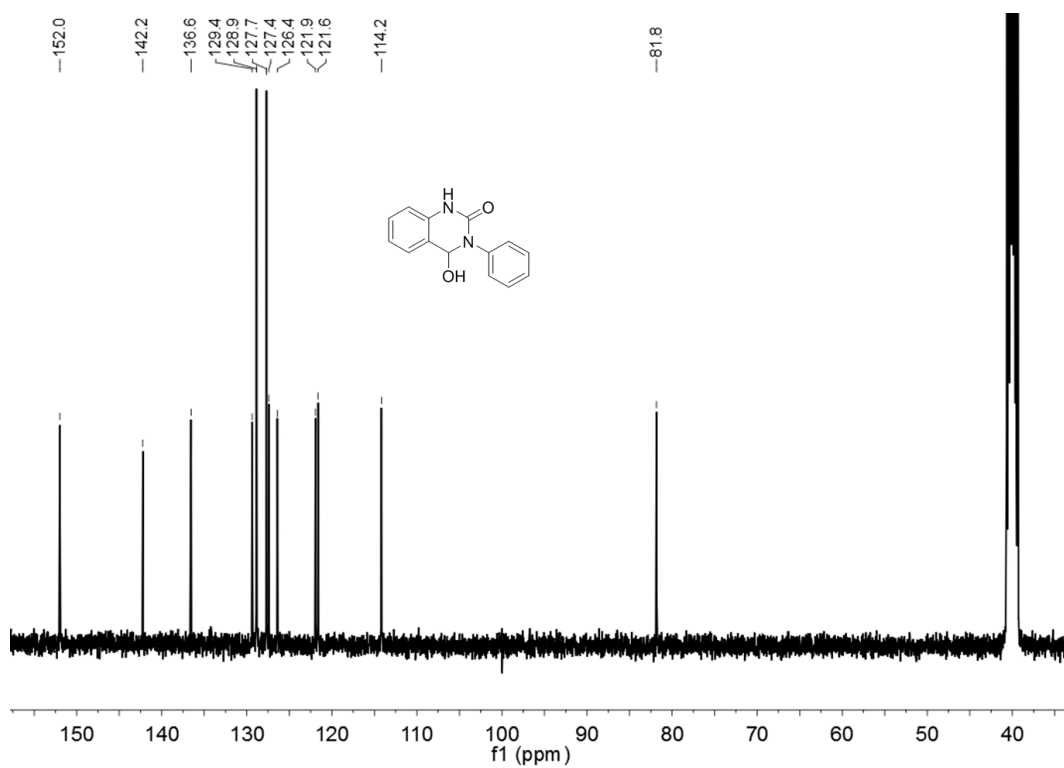


Figure S22. ^{13}C NMR spectrum of 1(H) in $\text{DMSO-}d_6$.

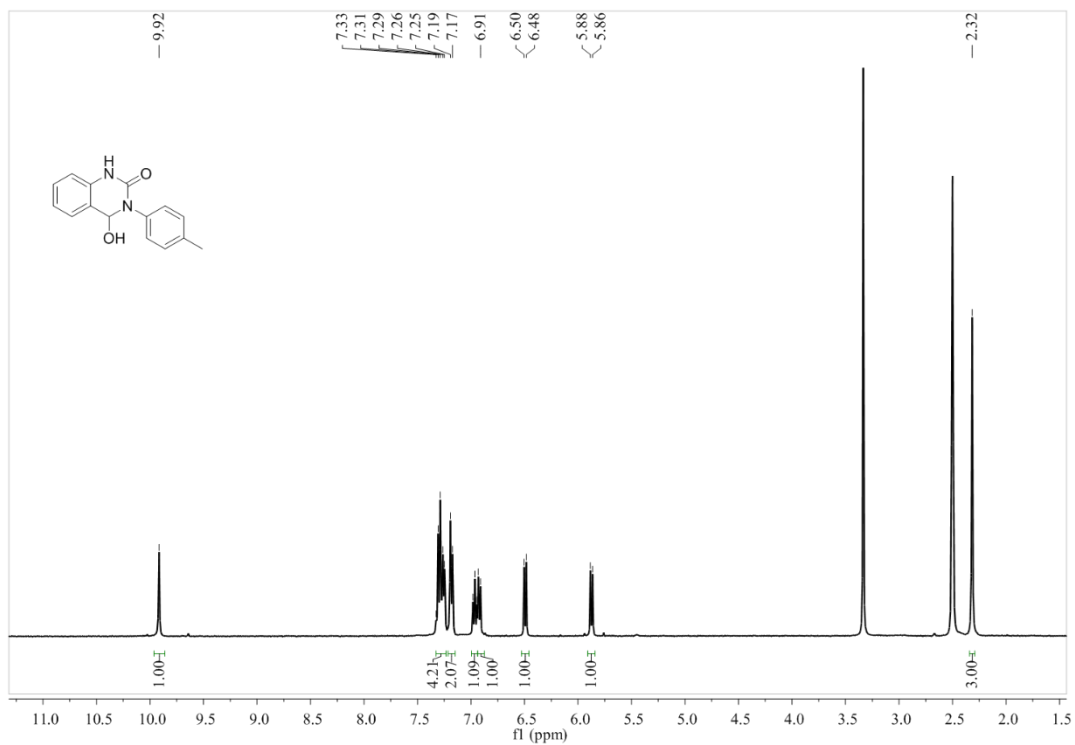


Figure S23. ^1H NMR spectrum of **1(Me)** in $\text{DMSO-}d_6$.

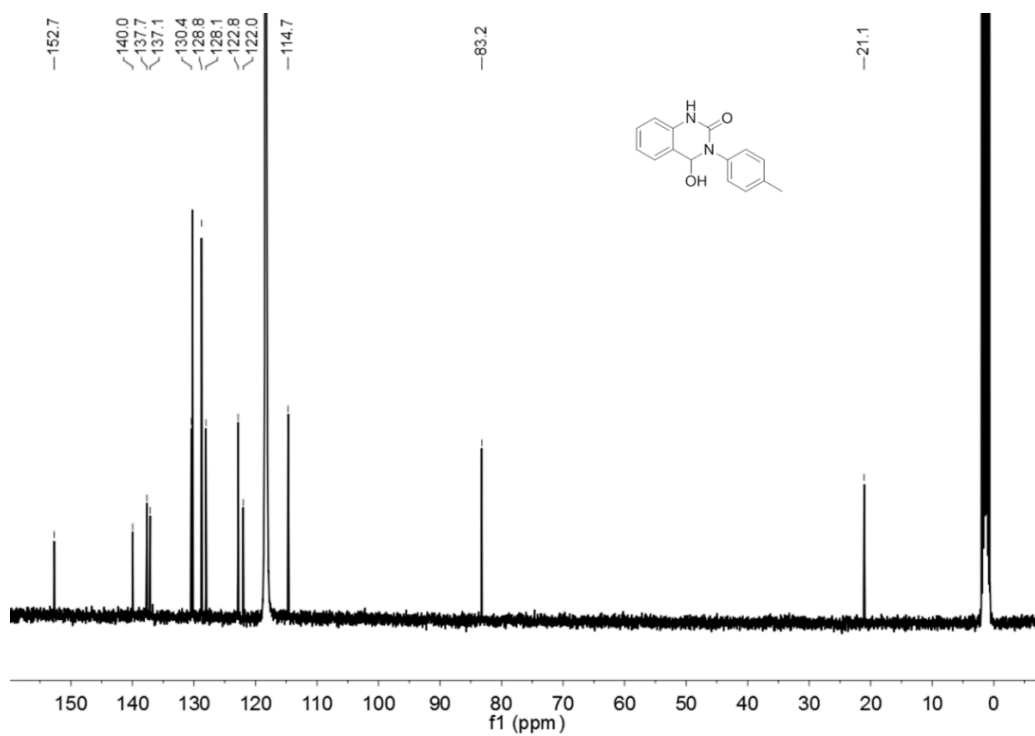


Figure S24. ^{13}C NMR spectrum of **1(Me)** in CD_3CN .

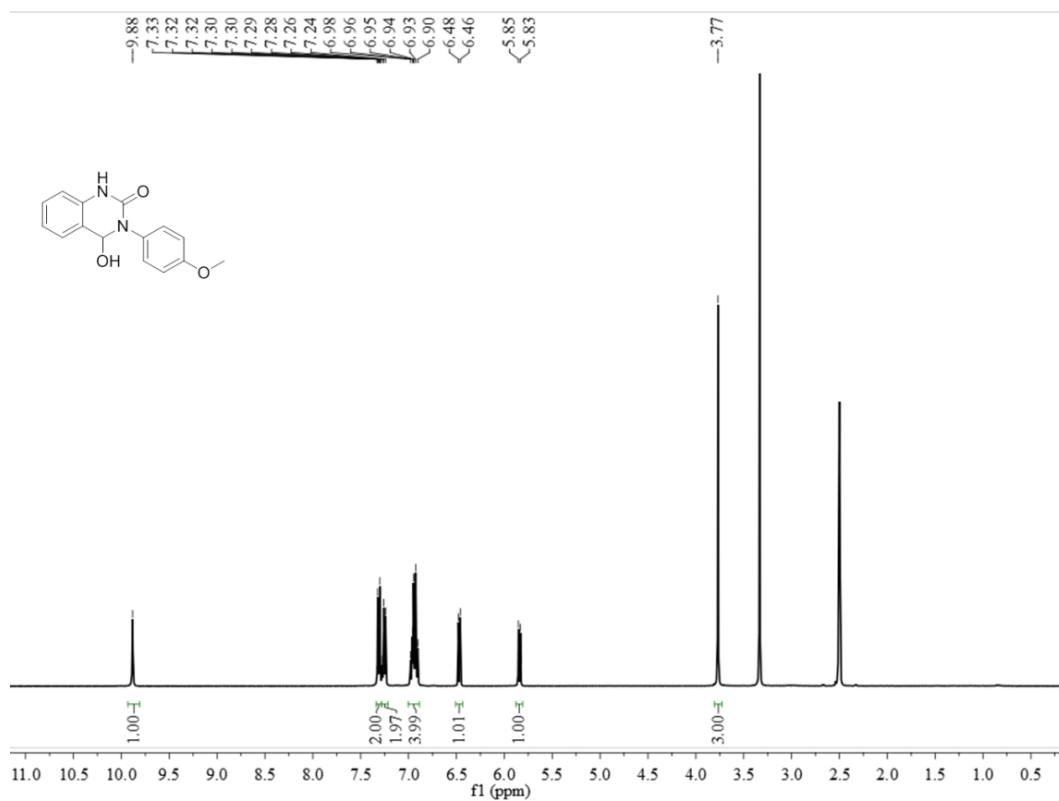


Figure S25. ^1H NMR spectrum of 1(OMe) in $\text{DMSO-}d_6$.

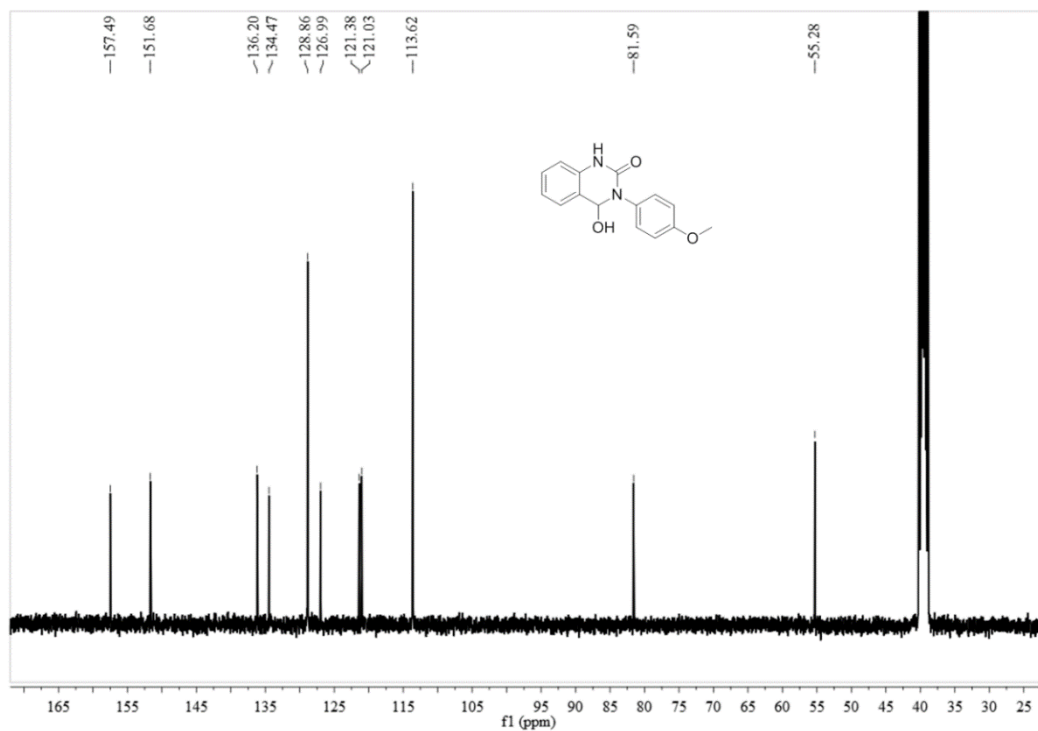


Figure S26. ^{13}C NMR spectrum of 1(OMe) in $\text{DMSO-}d_6$.

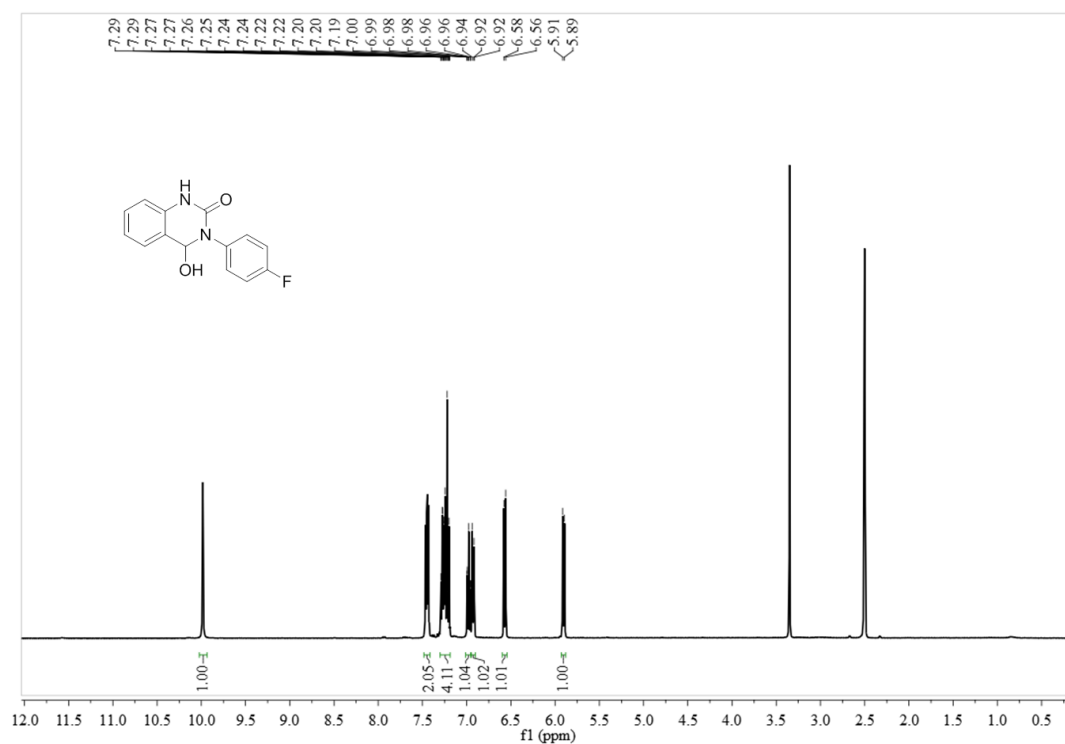


Figure S27. ¹H NMR spectrum of 1(F) in DMSO-*d*₆.

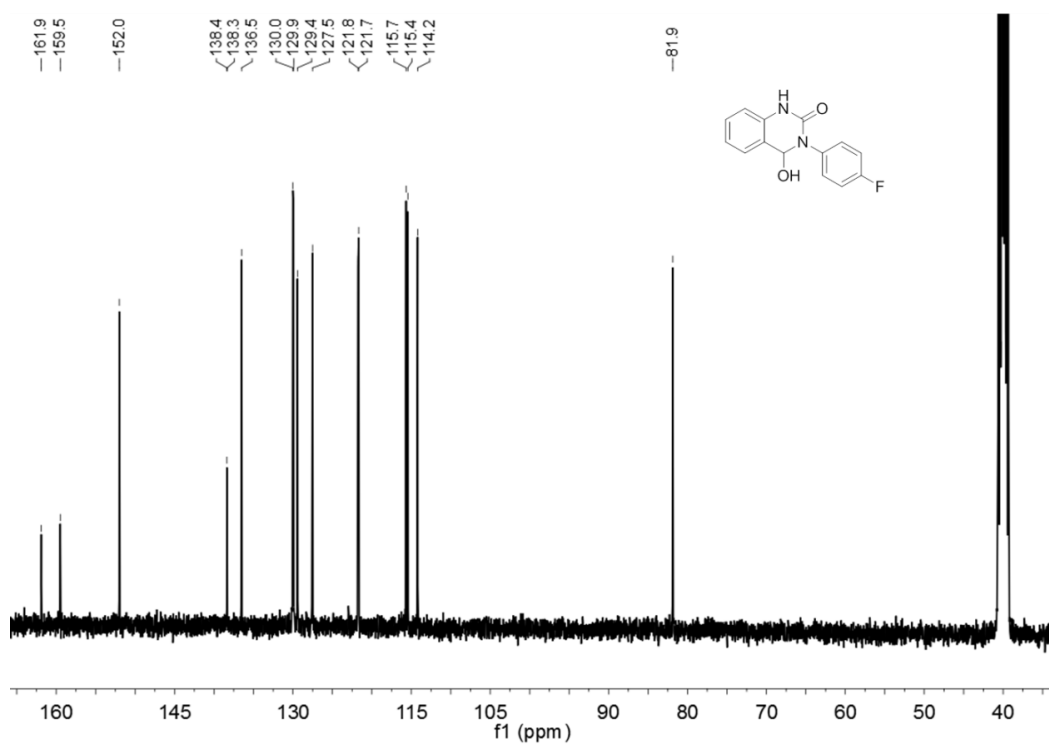


Figure S28. ¹³C NMR spectrum of 1(F) in DMSO-*d*₆.

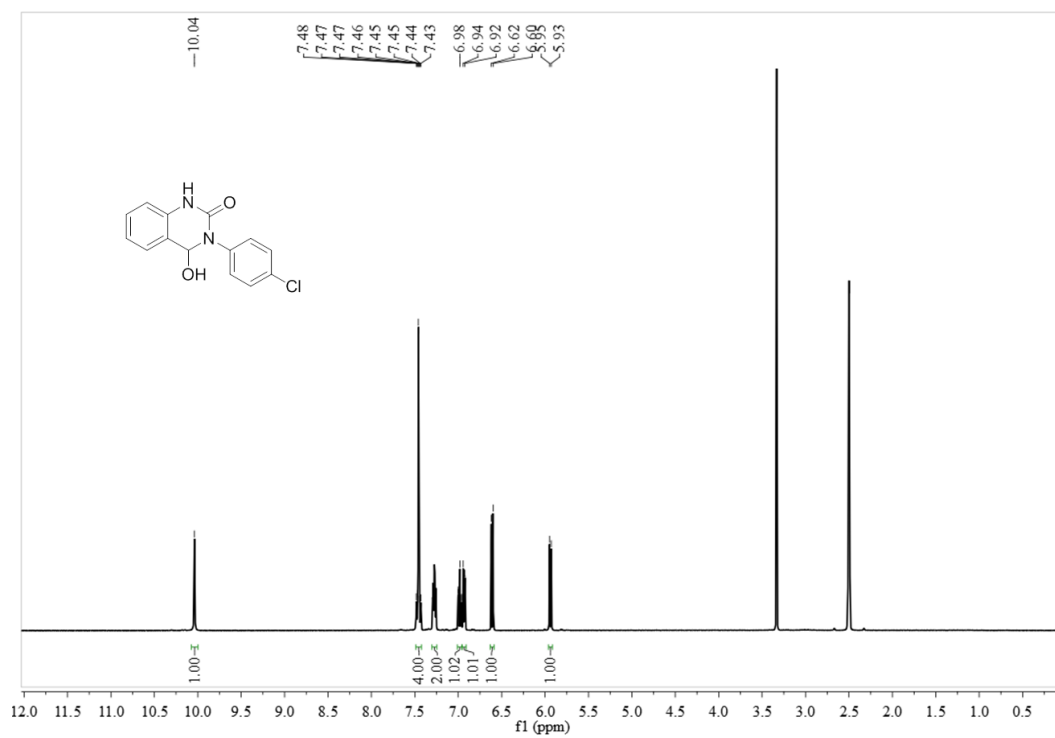


Figure S29. ^1H NMR spectrum of **1(Cl)** in $\text{DMSO-}d_6$.

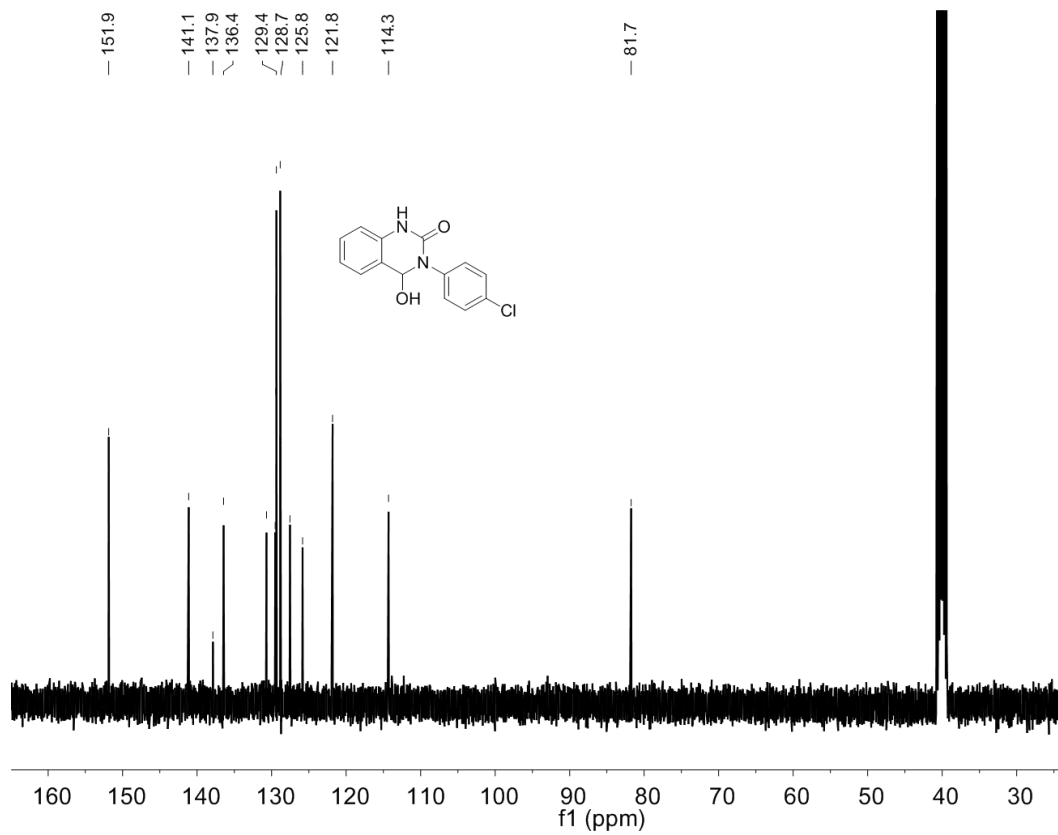


Figure S30. ^{13}C NMR spectrum of **1(Cl)** in $\text{DMSO-}d_6$.

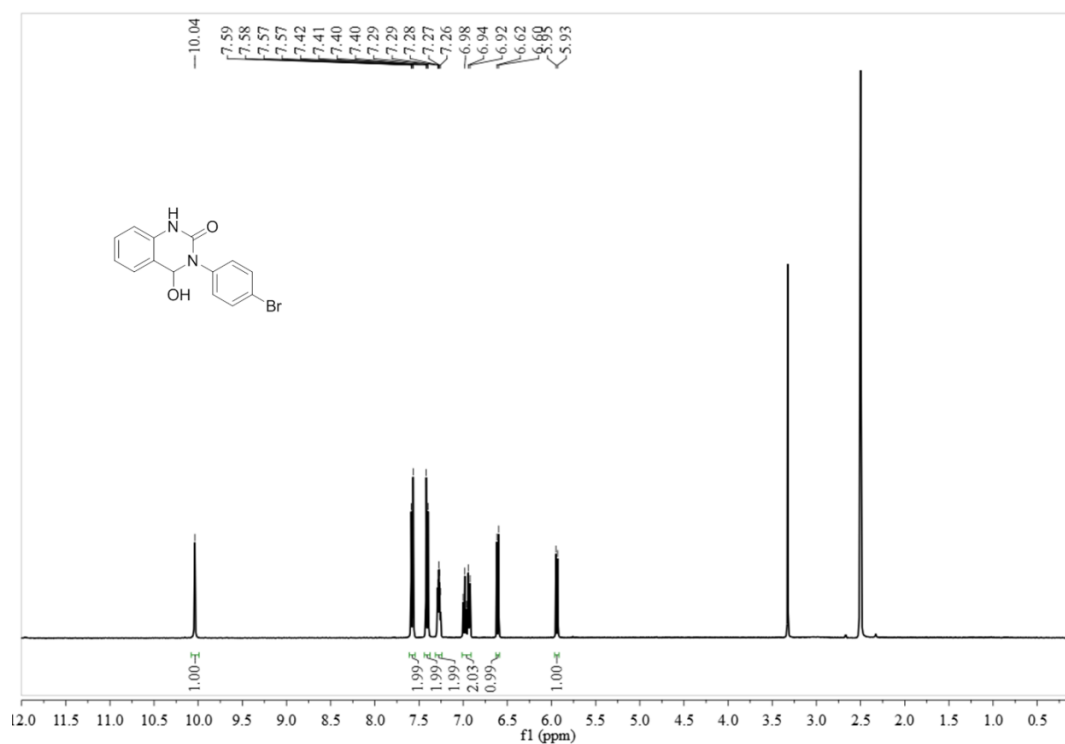


Figure S31. ^1H NMR spectrum of **1(Br)** in $\text{DMSO-}d_6$.

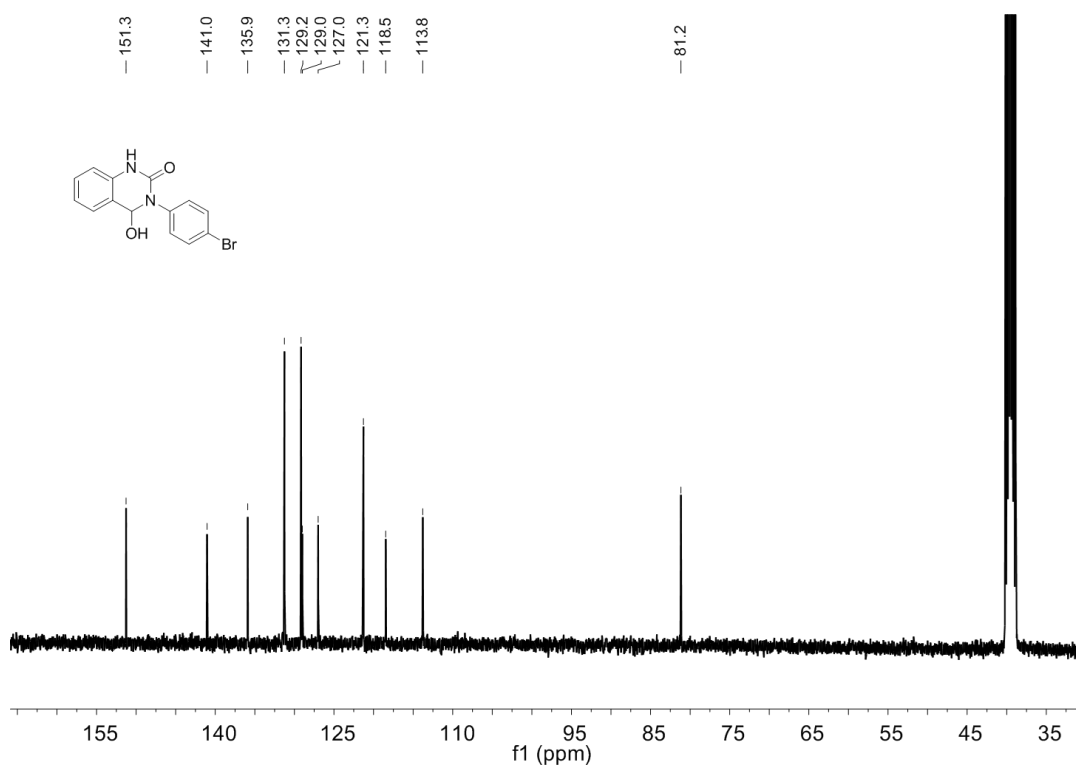


Figure S32. ^{13}C NMR spectrum of **1(Br)** in $\text{DMSO-}d_6$.

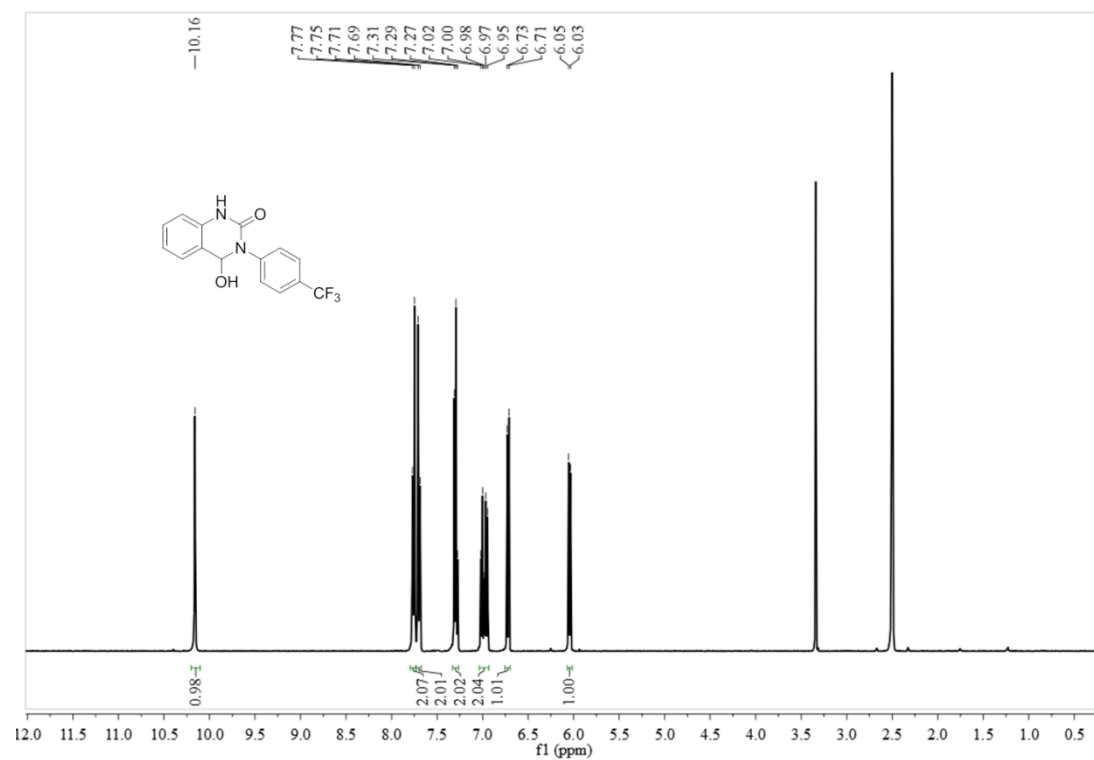


Figure S33. ¹H NMR spectrum of 1(CF₃) in DMSO-*d*₆.

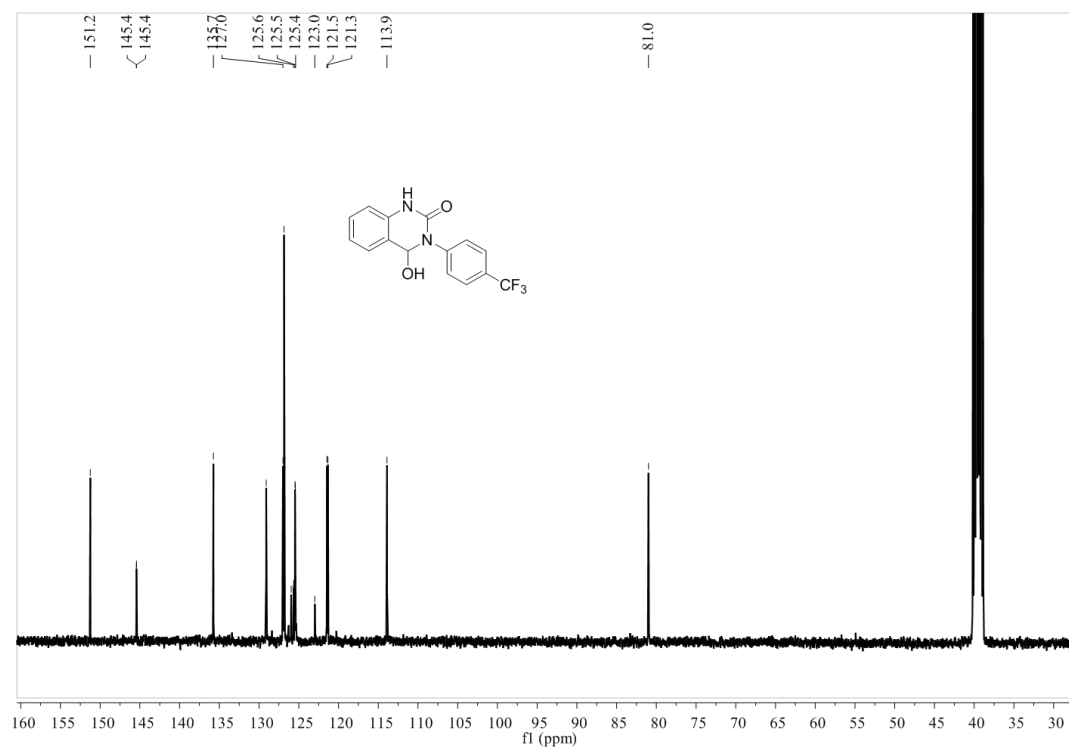


Figure S34. ¹³C NMR spectrum of 1(CF₃) in DMSO-*d*₆.

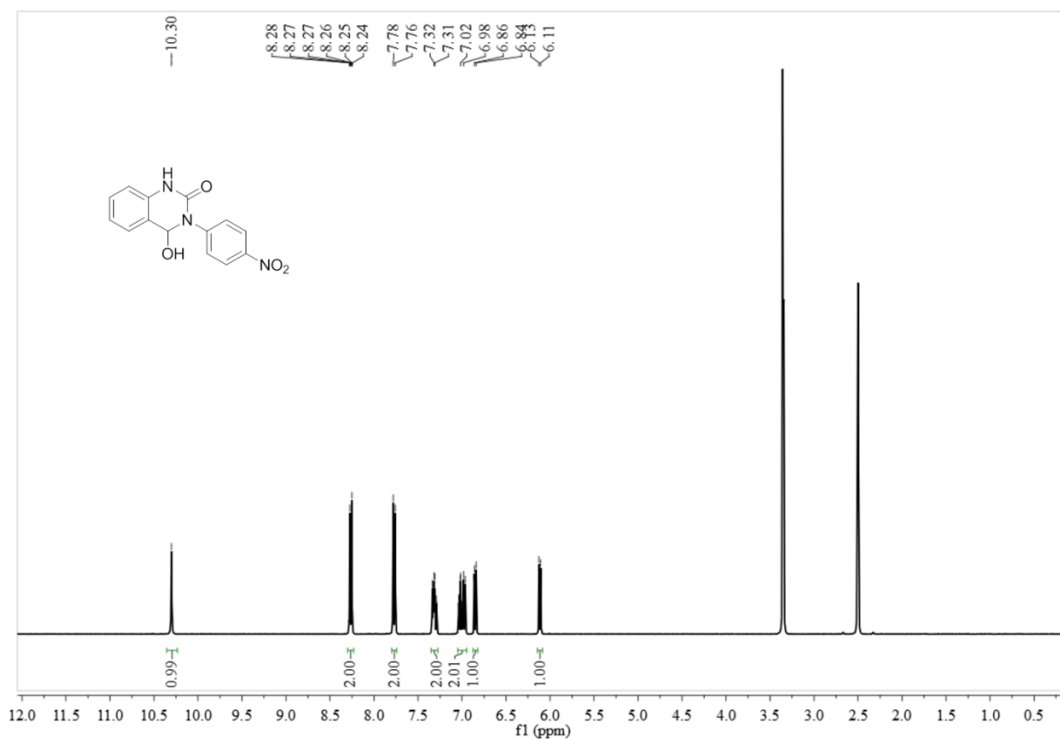


Figure S35. ¹H NMR spectrum of **1**(NO₂) in DMSO-*d*₆.

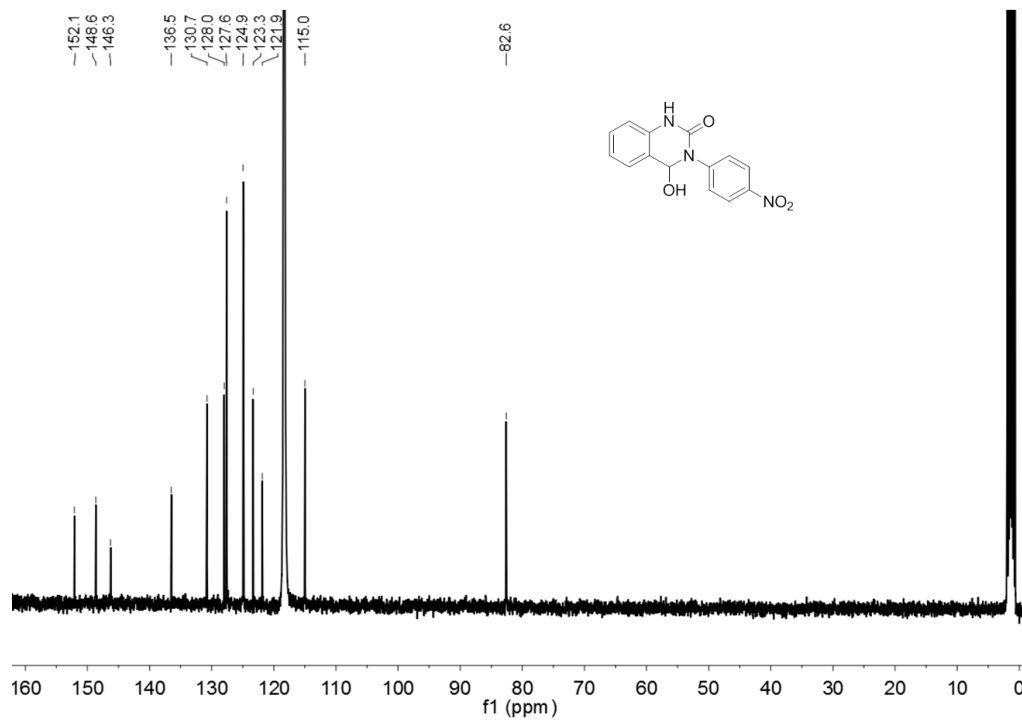


Figure S36. ¹³C NMR spectrum of **1**(NO₂) in CD₃CN.

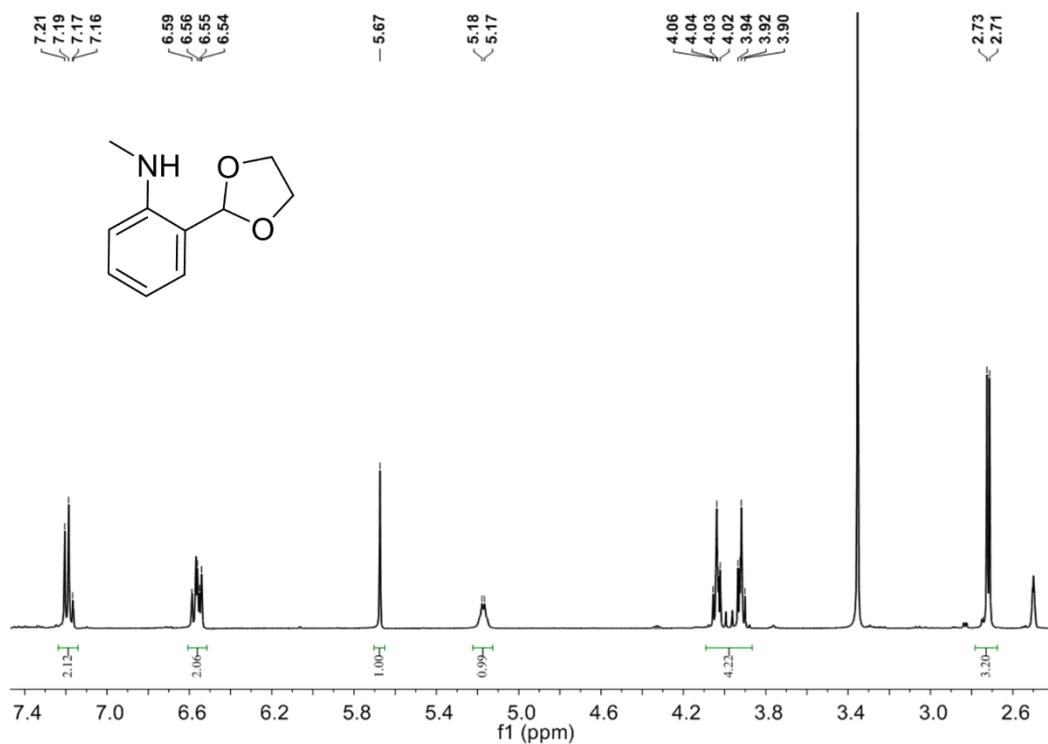


Figure S37. ¹H NMR spectrum of **10** in DMSO-*d*₆.

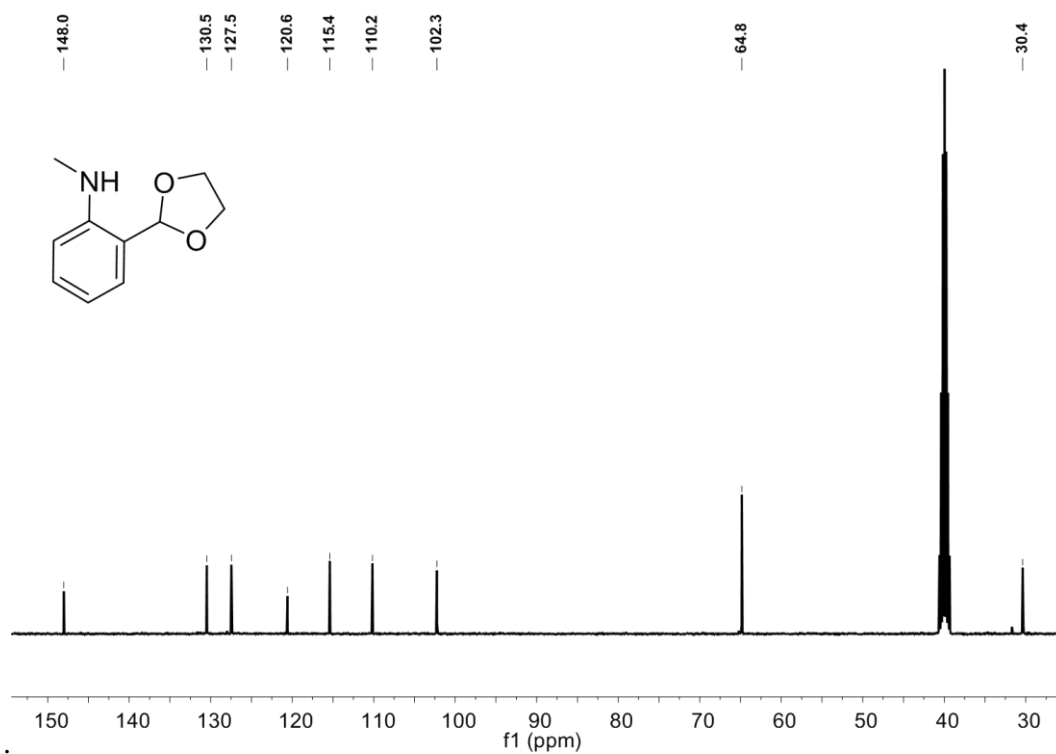


Figure S38. ¹³C NMR spectrum of **10** in DMSO-*d*₆.

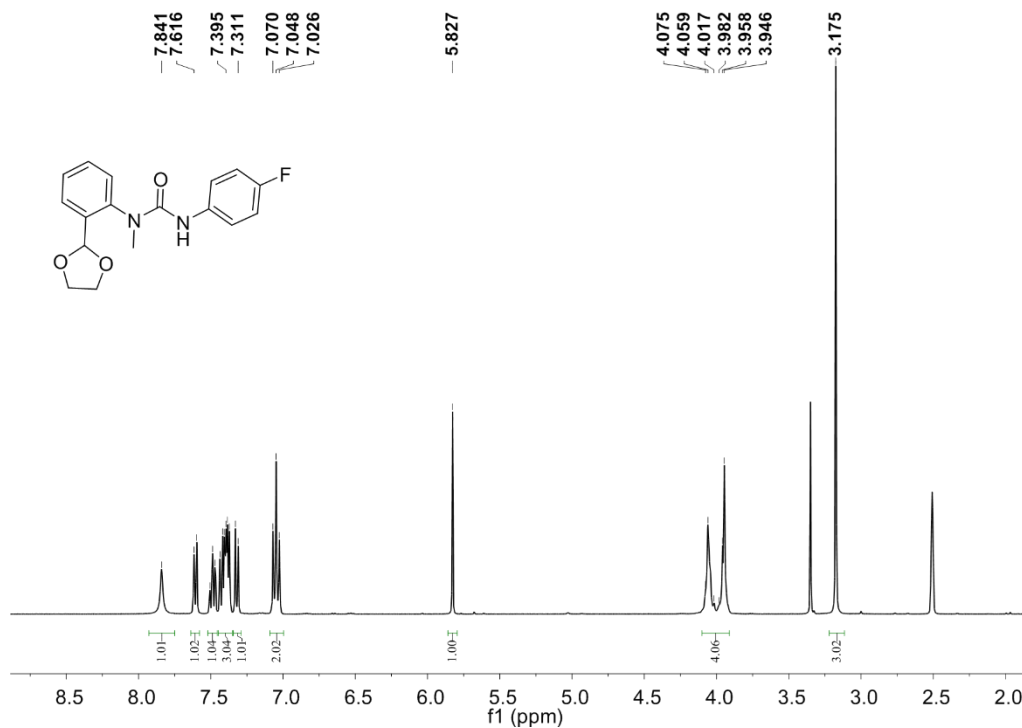


Figure S39. ¹H NMR spectrum of **11** in DMSO-*d*₆.

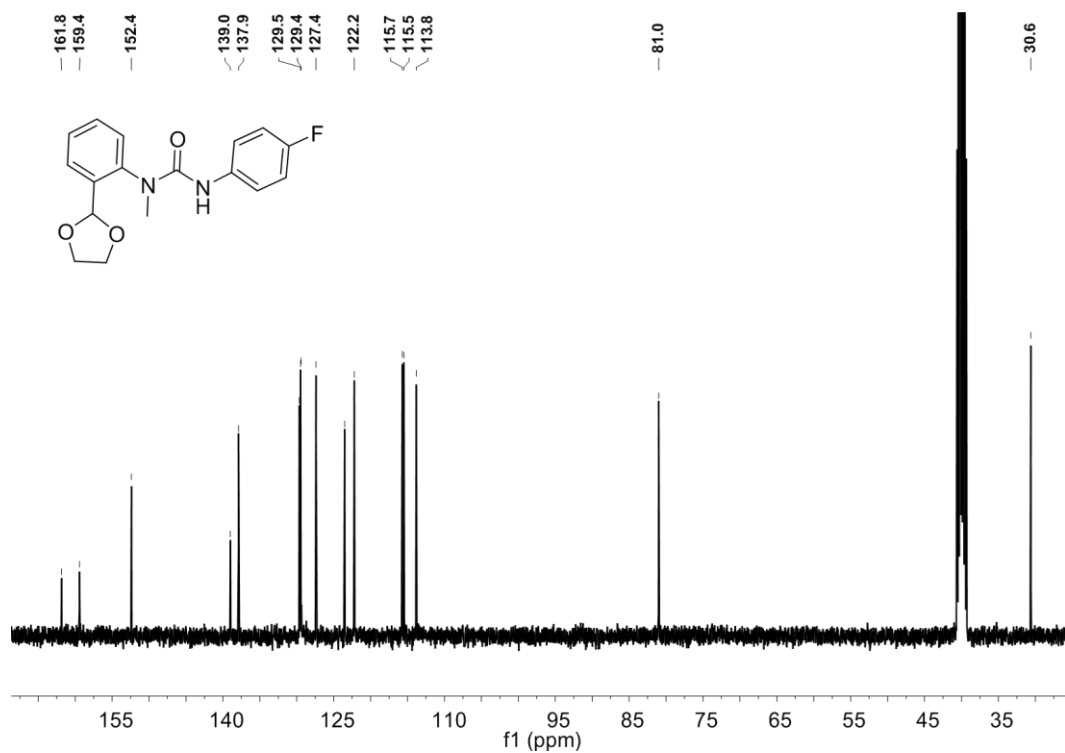


Figure S40. ¹³C NMR spectrum of **11** in DMSO-*d*₆.

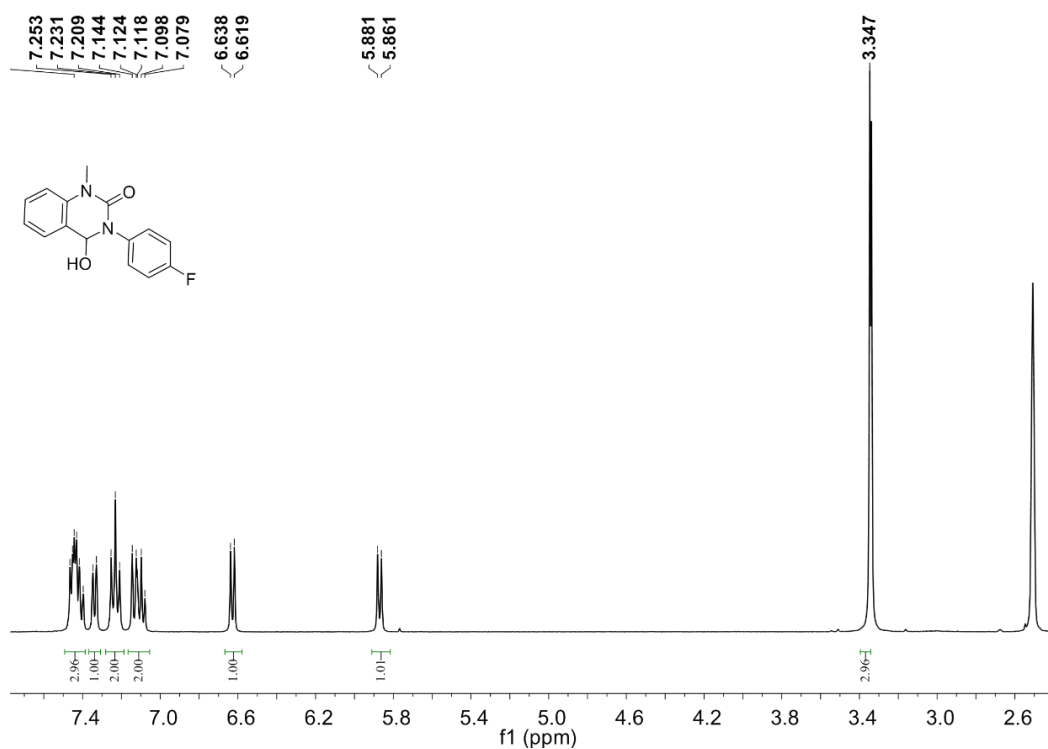


Figure S41. ¹H NMR spectrum of 2(F) in DMSO-*d*₆.

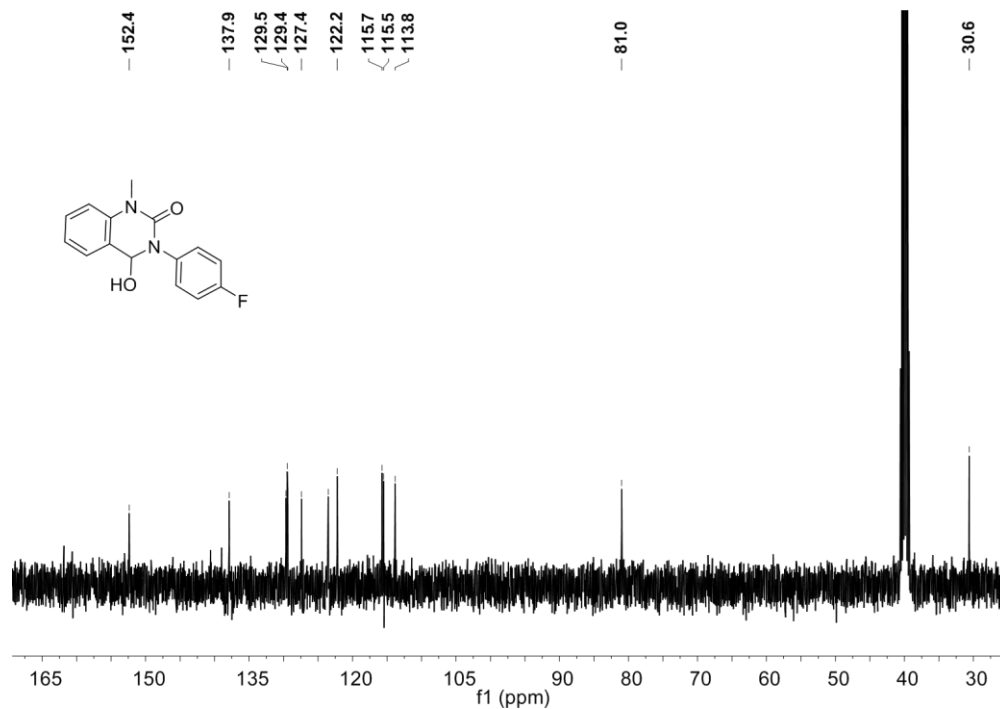


Figure S42. ¹³C NMR spectrum of 2(F) in DMSO-*d*₆.

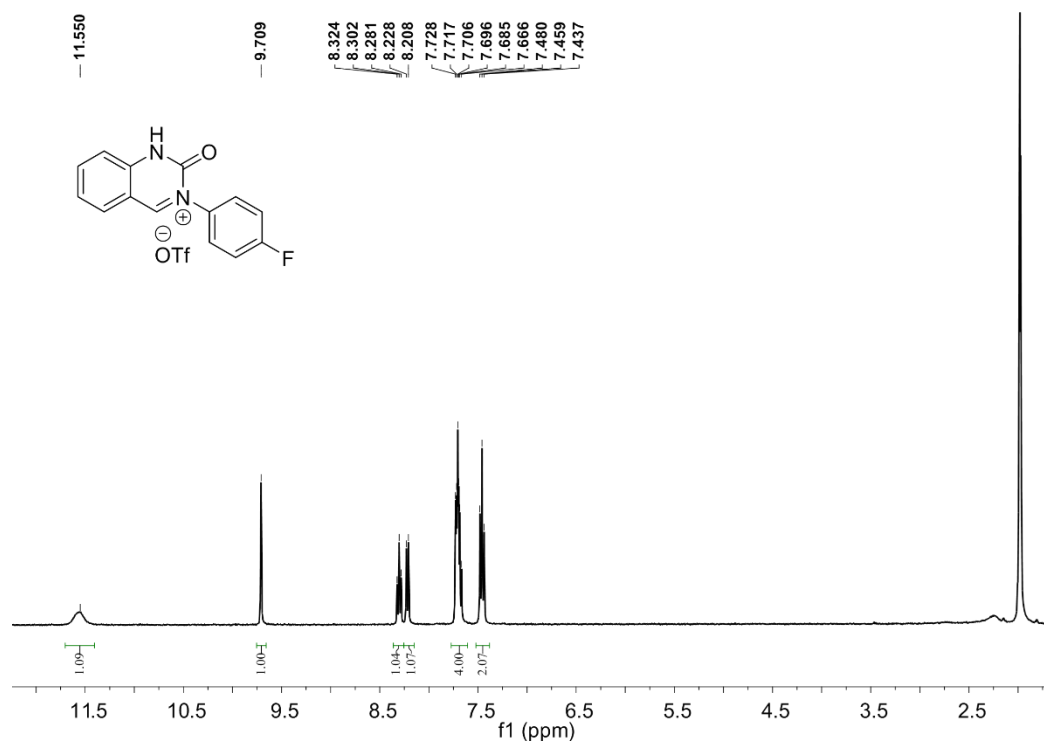


Figure S43. ¹H NMR spectrum of 3(F) in CD₃CN.

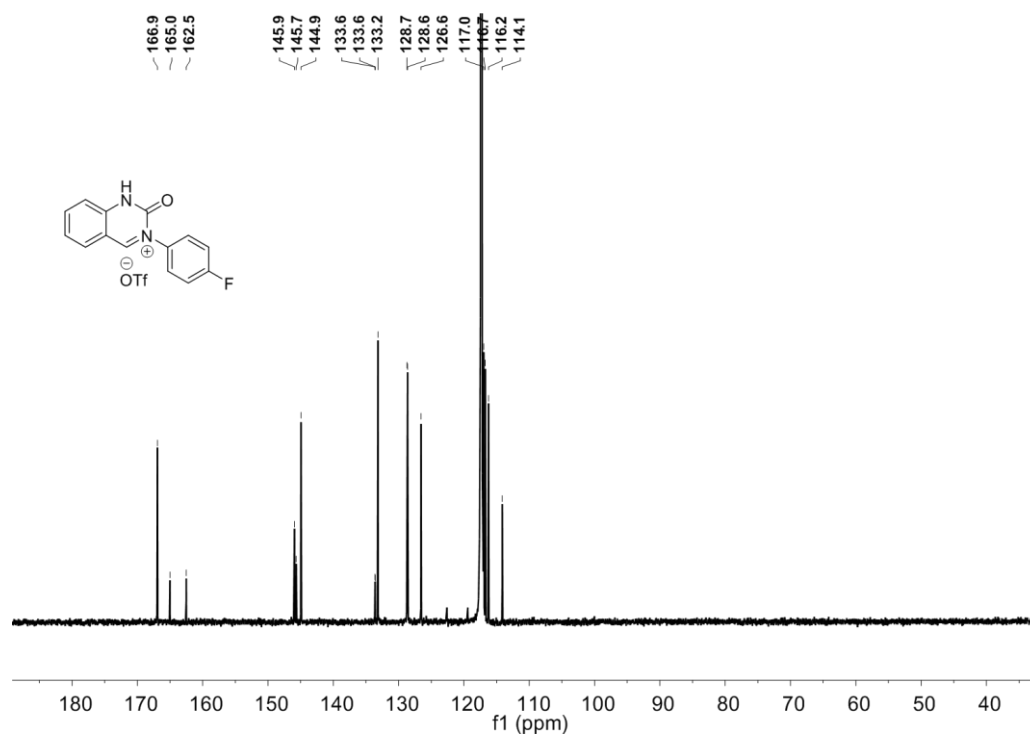


Figure S44. ¹³C NMR spectrum of 3(F) in CD₃CN.

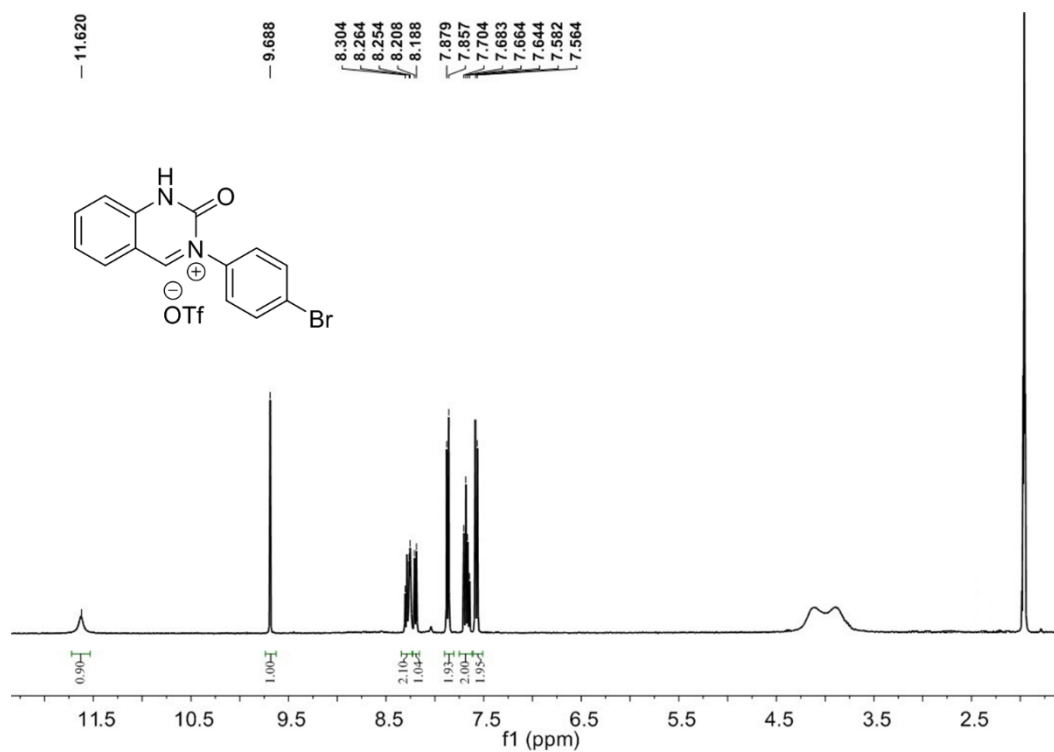


Figure S45. ^1H NMR spectrum of 3(Br) in CD_3CN .

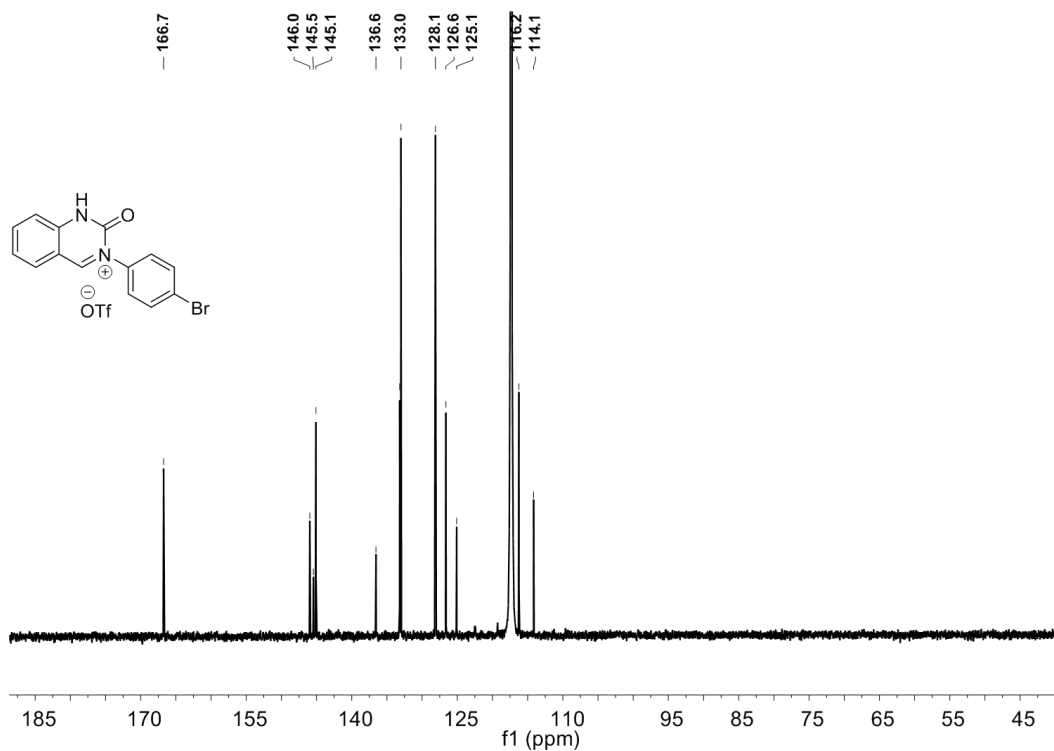


Figure S46. ^{13}C NMR spectrum of 3(Br) in CD_3CN .

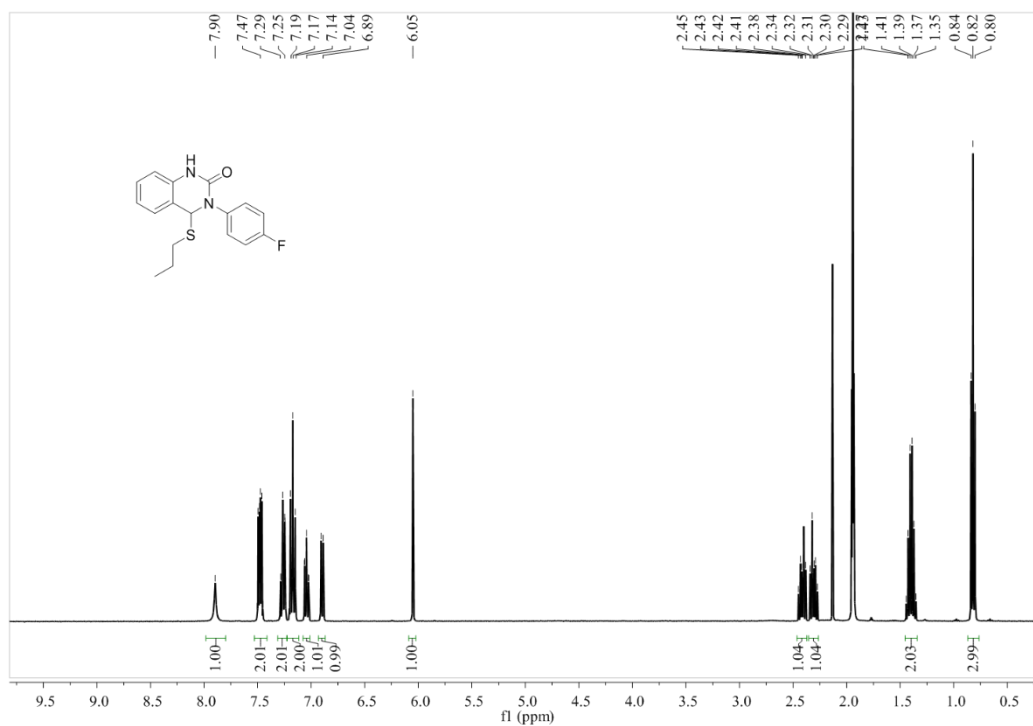


Figure S47. ^1H NMR spectrum of 4(F) in CD_3CN .

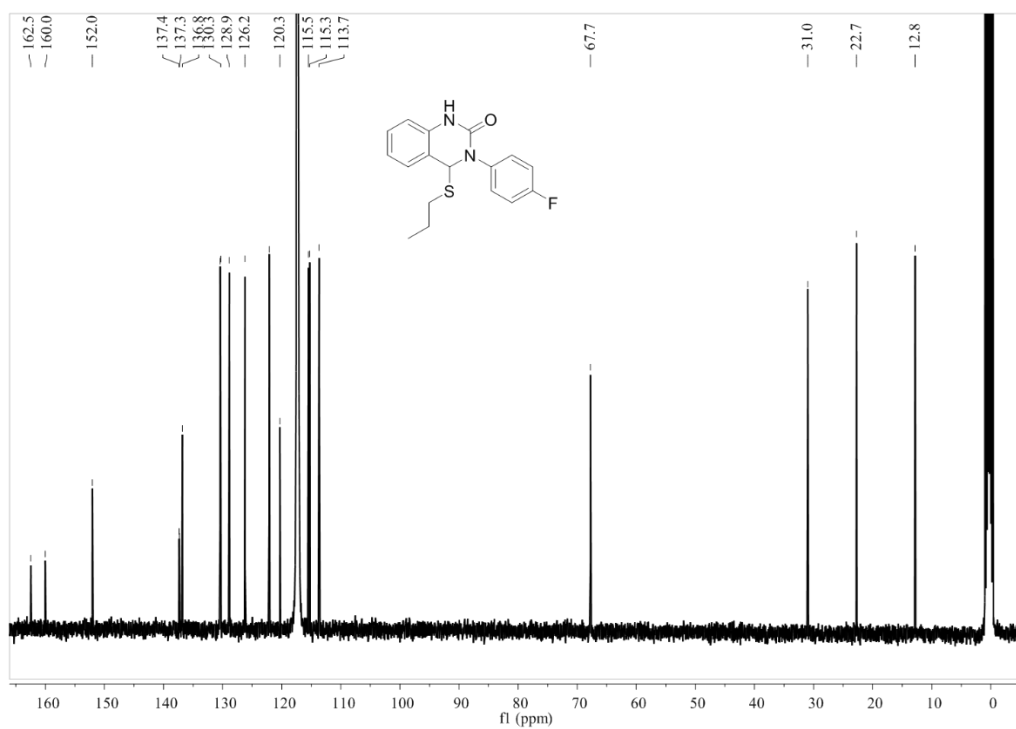


Figure S48. ^{13}C NMR spectrum of 4(F) in CD_3CN .

X-ray Crystallography

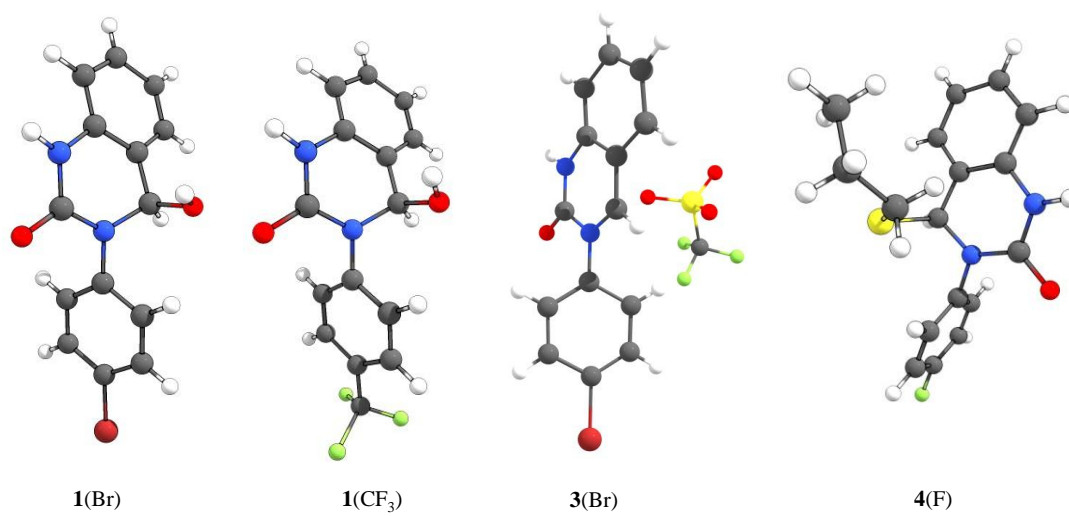


Figure S49. Crystal structures of **1(Br)**, **1(CF₃)**, and **3(Br)**, and **4(F)**.

Table S1. Summary of crystallographic data.

| Compound | 1(Br) | 1(CF₃) | 3(Br) | 4(F) |
|--|--|--|--|--|
| Formula | C ₁₄ H ₁₁ N ₂ O ₂ Br | C ₁₅ H ₁₁ N ₂ O ₂ F ₃ | C ₁₅ H ₁₀ N ₂ O ₄ F ₃ BrS | C ₁₇ H ₁₇ N ₂ OFS |
| Formula weight | 319.16 | 308.26 | 451.22 | 316.40 |
| <i>T</i> /K | 173(2) | 173(4) | 173 | 293(2) |
| Crystallization | dichloromethan | dichloromethane | acetonitrile | acetonitrile |
| Color | white | colorless | white | white |
| Crystal system | monoclinic | monoclinic | monoclinic | monoclinic |
| Space group | <i>P</i> 2 ₁ / <i>c</i> | <i>P</i> 2 ₁ / <i>c</i> | <i>C</i> 2/ <i>c</i> | <i>P</i> 2 ₁ / <i>n</i> |
| <i>a</i> / Å | 6.516(1) | 6.489(10) | 22.646(5) | 9.785(3) |
| <i>b</i> / Å | 9.521(2) | 9.467(2) | 12.591(3) | 8.479(3) |
| <i>c</i> / Å | 20.424(4) | 21.306(3) | 12.272(3) | 19.199(7) |
| <i>α</i> / ° | 90.000 | 90.000 | 90.000 | 90.000 |
| <i>β</i> / ° | 95.165(2) | 94.633(10) | 95.852(4) | 95.155(3) |
| <i>γ</i> / ° | 90.000 | 90.000 | 90.000 | 90.000 |
| <i>V</i> / Å ³ | 1261.9(4) | 1304.8(4) | 3480.9(13) | 1586.6(9) |
| <i>Z</i> | 4 | 4 | 8 | 4 |
| <i>D</i> _x / g cm ⁻³ | 1.680 | 1.569 | 1.722 | 1.325 |
| <i>μ</i> / mm ⁻¹ | 3.048 | 0.747 | 2.536 | 1.252 |
| <i>F</i> (000) | 637 | 634 | 1792 | 667 |
| <i>θ</i> range / ° | 3.04 to 60.28 | 3.62 to 60.33 | 2.43 to 27.49 | 4.02 to 50.52 |
| GOF on <i>F</i> ² | 1.037 | 1.044 | 0.927 | 1.079 |
| <i>R</i> ₁ [<i>I</i> > 2σ(<i>I</i>)] | 0.0238 | 0.0411 | 0.0321 | 0.0573 |
| <i>wR</i> ₂ (all data) | 0.0621 | 0.1064 | 0.0839 | 0.1693 |

3. Response toward Base, Anion, and Acid

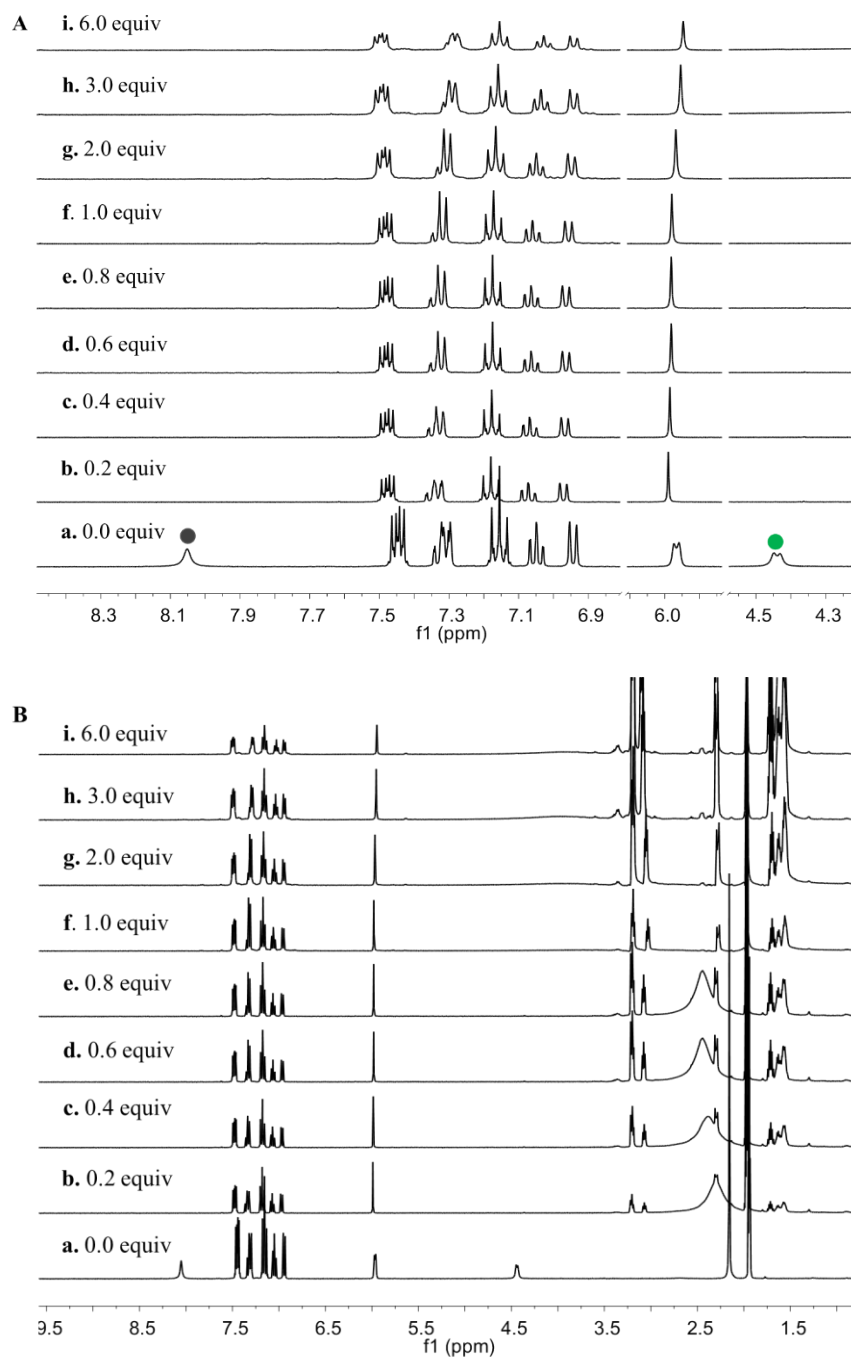
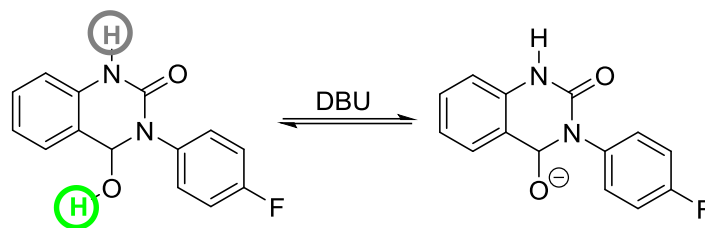


Figure S50. (A) Partial ^1H NMR spectra of **1(F)** with the addition of DBU (0.0 – 6.0 equiv) in CD_3CN ; (B) The full NMR spectra of panel A.

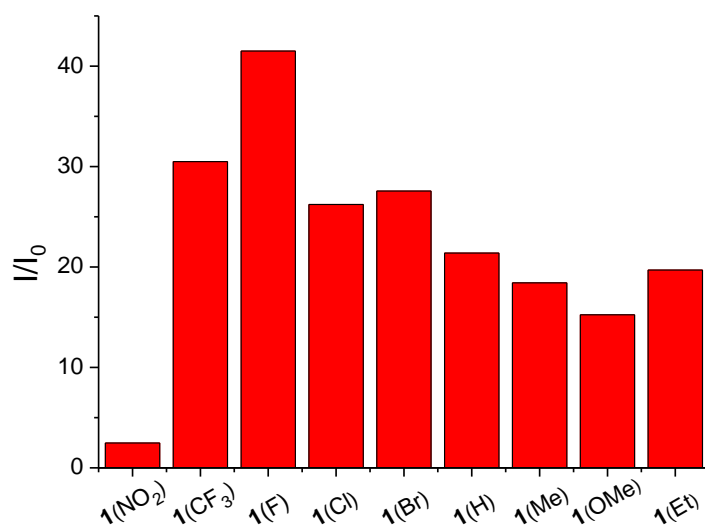


Figure S51. Ratios of the intensity changes at 419 nm (B) of **1**(NO₂), **1**(CF₃), **1**(F), **1**(Cl), **1**(Br), **1**(H), **1**(Me), **1**(OCH₃), and **1**(Et) (50 μM) with the addition of DBU (50.0 equiv) in CH₃CN ($\lambda_{\text{ex}} = 355$ nm).

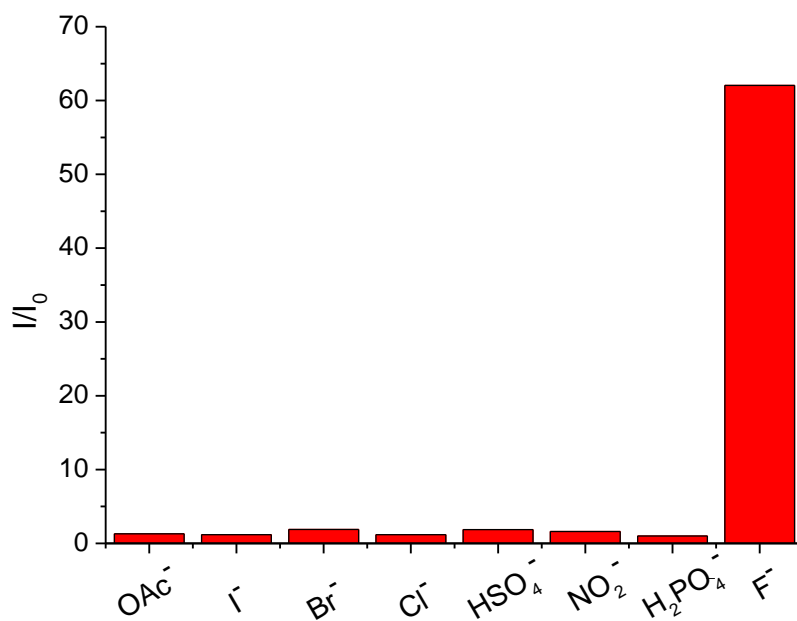
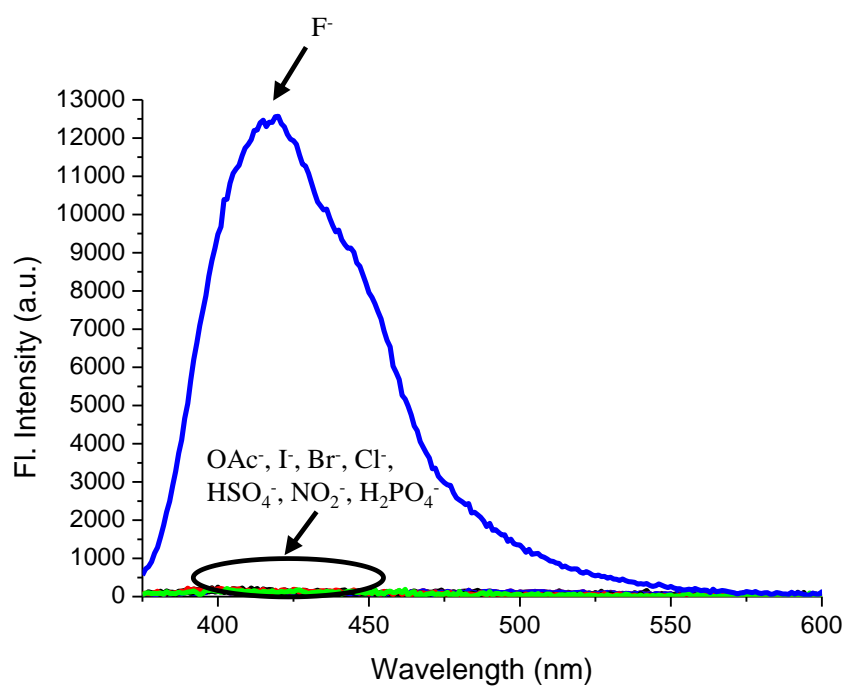


Figure S52. Fluorescence spectra (A) and ratios of the intensity changes at 419 nm (B) of **1(F)** with the addition of various anions (10.0 equiv) in CH_3CN ($\lambda_{ex} = 355$ nm).

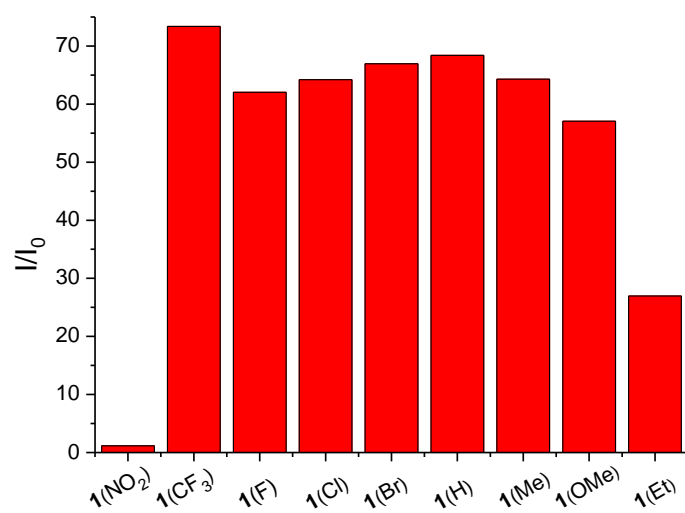


Figure S53. Ratios of the intensity changes at 419 nm (B) of **1**(NO₂), **1**(CF₃), **1**(F), **1**(Cl), **1**(Br), **1**(H), **1**(Me), **1**(OCH₃), and **1**(Et) (50 μ M) with the addition of TBAF (10.0 equiv) in CH₃CN ($\lambda_{\text{ex}} = 355$ nm).

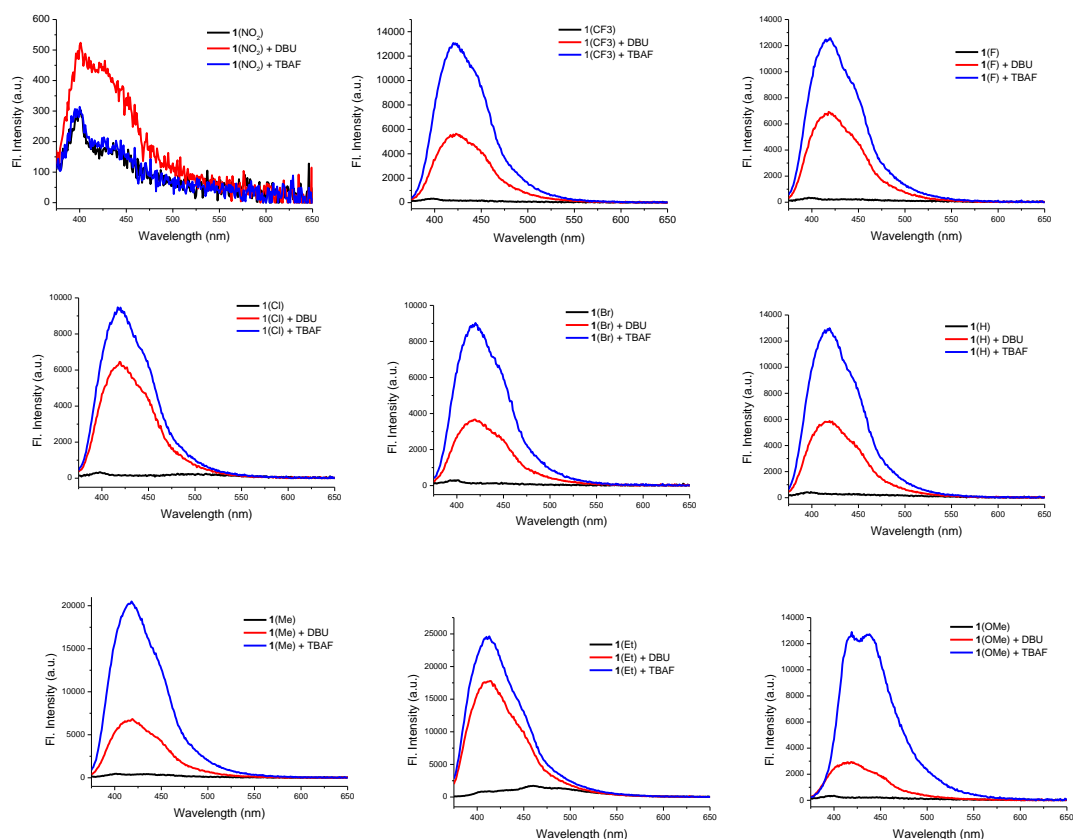


Figure S54. Fluorescence spectra **1**(NO₂), **1**(CF₃), **1**(F), **1**(Cl), **1**(Br), **1**(H), **1**(Me), **1**(OCH₃), and **1**(Et) (50 μM) with the addition of DBU (50.0 equiv) and TBAF (10.0 equiv) in CH₃CN ($\lambda_{\text{ex}} = 355$ nm). This figure shows the emission spectra of Figure S51 and S53.

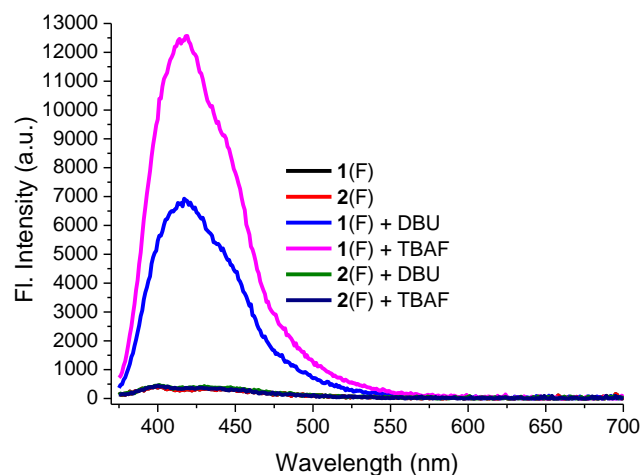


Figure S55. Fluorescence spectra of **1**(F) and **2**(F) (50 μM) with the addition of TBAF (10.0 equiv) or DBU (50.0 equiv) in CH₃CN ($\lambda_{\text{ex}} = 355$ nm).

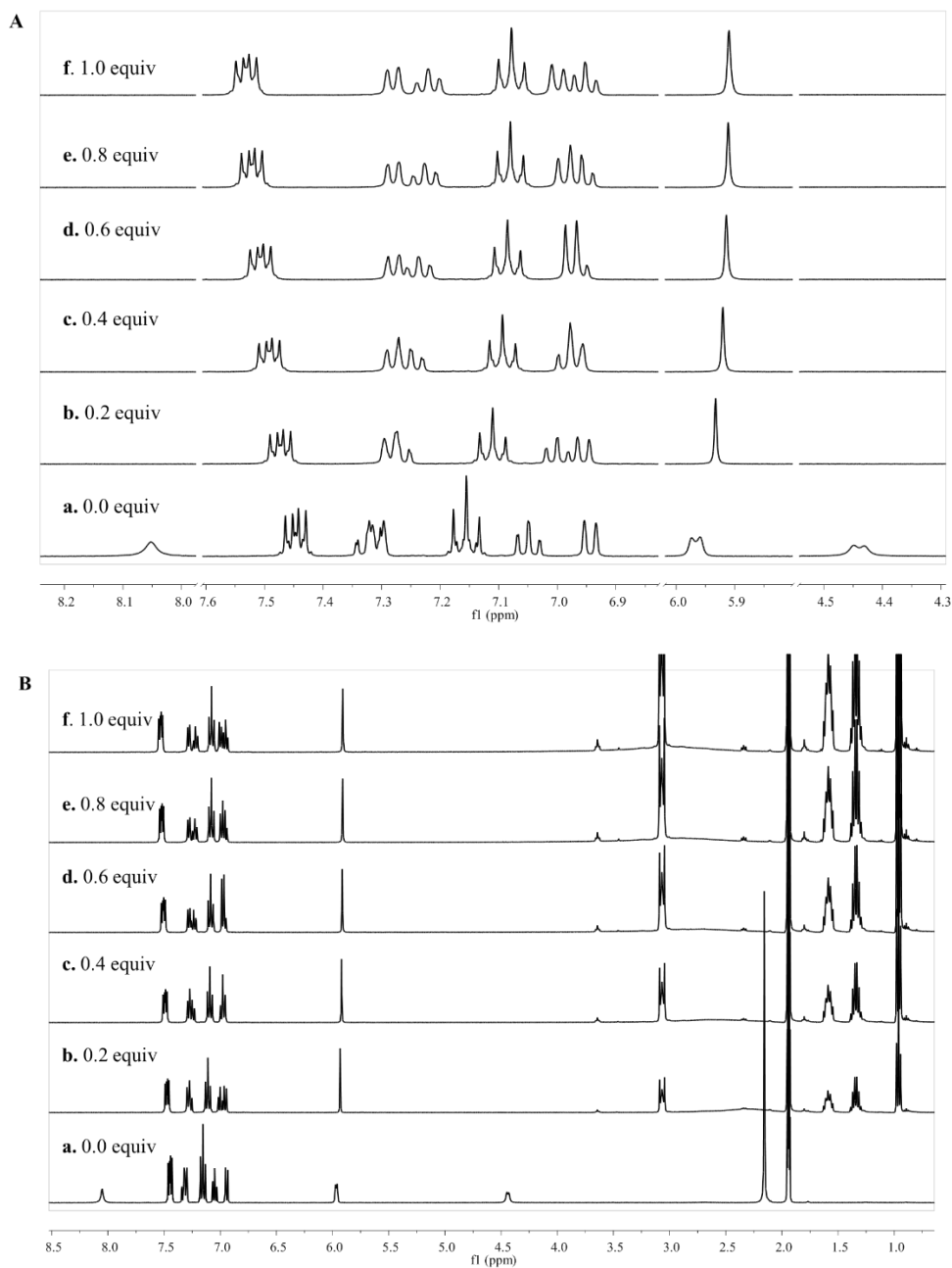
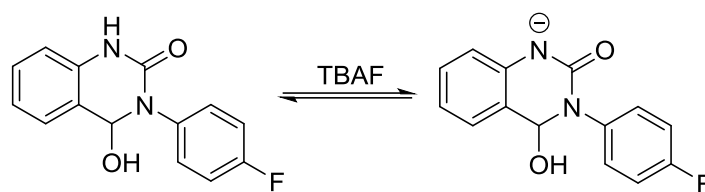


Figure S56. (A) Partial ^1H NMR spectra of **1(F)** with the addition of tetrabutylammonium fluoride (TBAF) (0.0 – 1.0 equiv) in CD_3CN ; (B) The full NMR spectra of panel A.

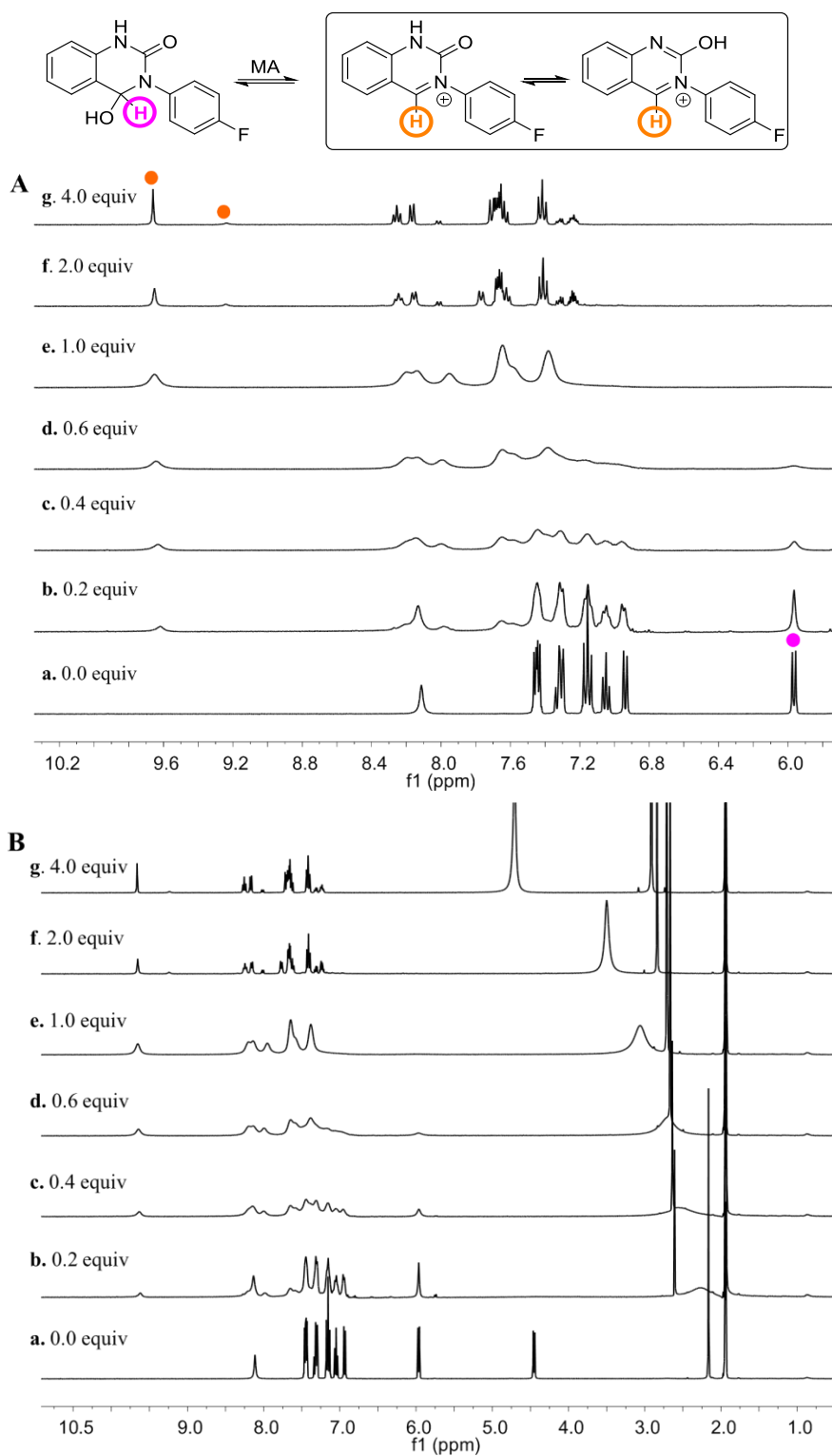


Figure S57. (A) ^1H NMR spectra of **1(F)** with the addition of methanesulfonic acid (MA, 0.0 – 4.0 equiv) in CD_3CN ; (B) The full NMR spectra of panel A.

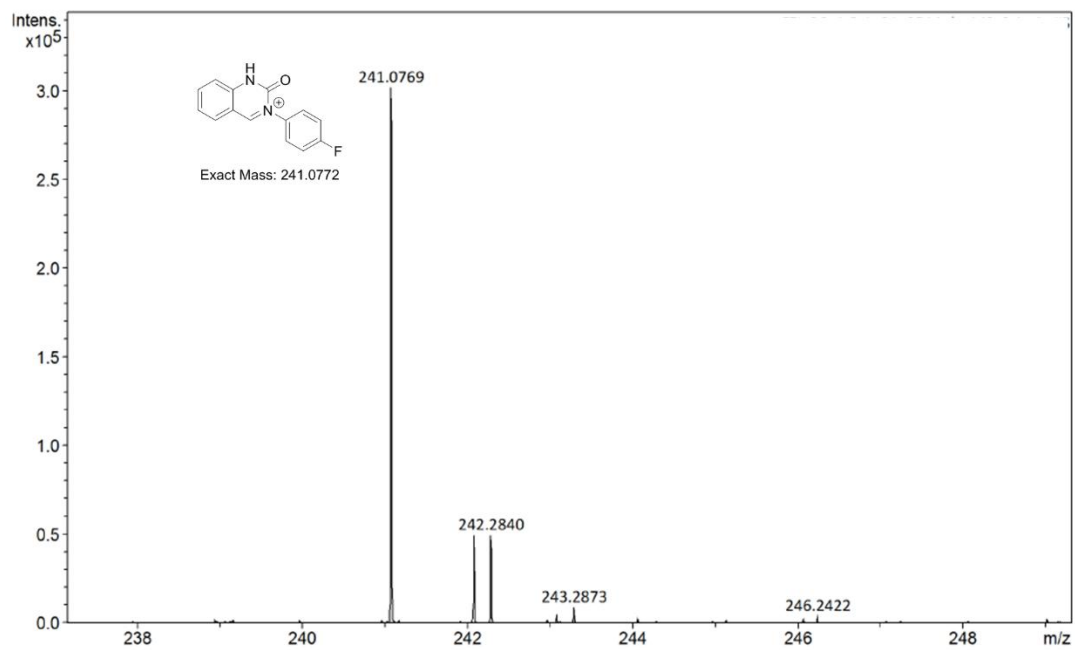


Figure S58. ESI mass spectrum of ion **3(F)** in CH₃CN.

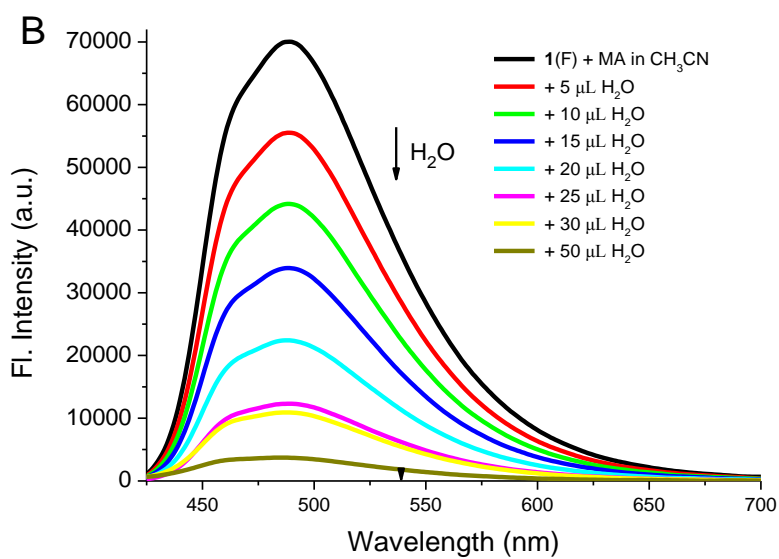
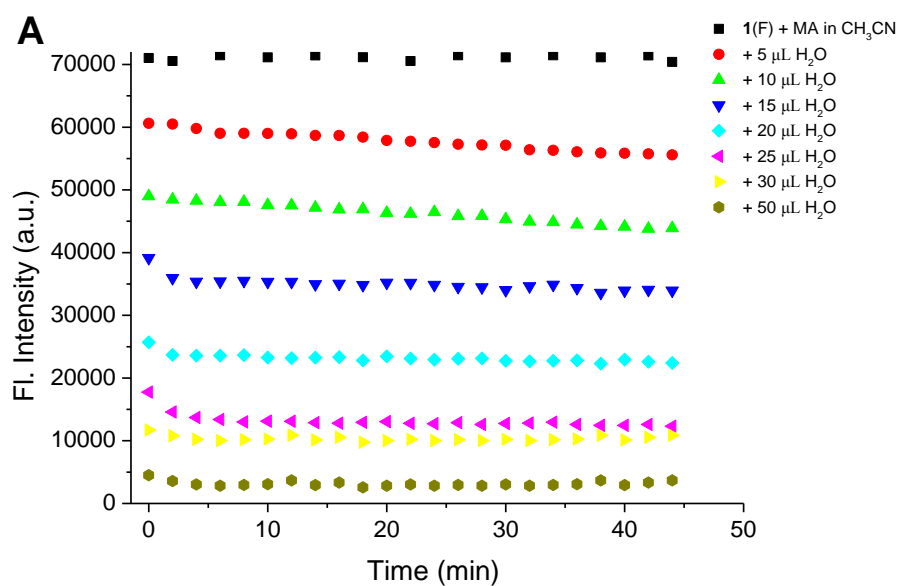


Figure S59. The change of fluorescence intensity at 486 nm over time (A) and fluorescence spectra (B) of **1(F)** (50 μM) with the addition of MA (20 equiv) in CH₃CN (1.0 mL), followed by the titration of H₂O ($\lambda_{\text{ex}} = 400$ nm).

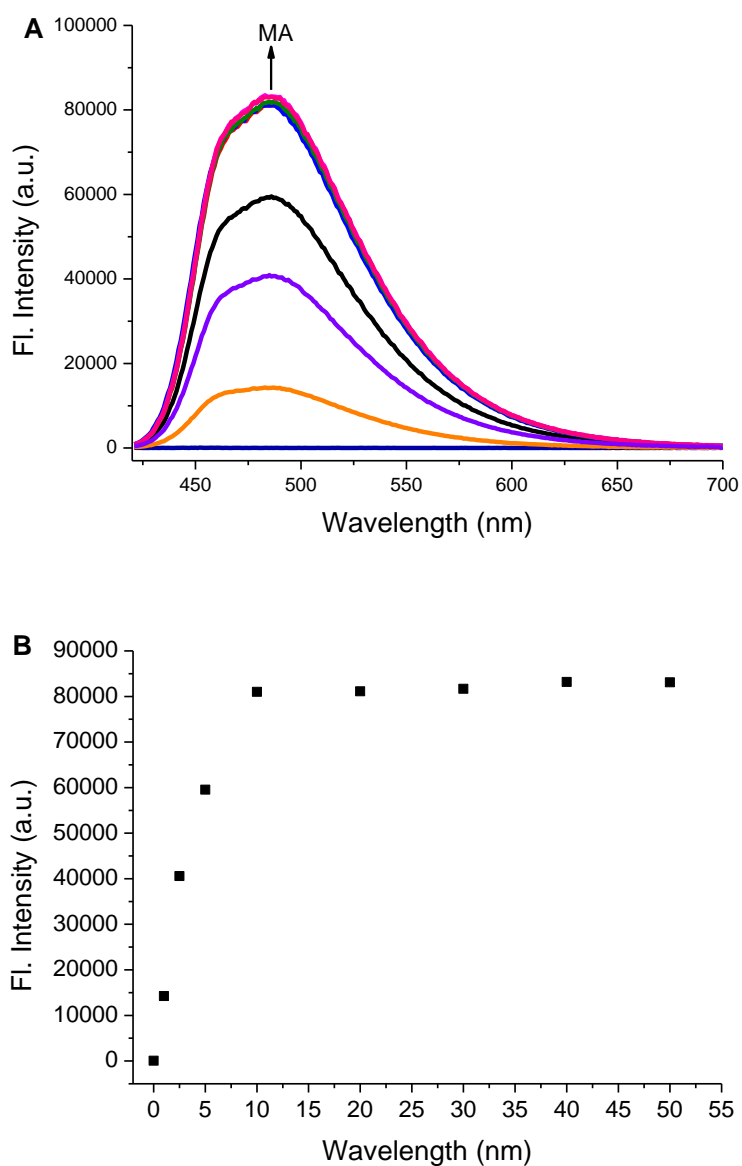
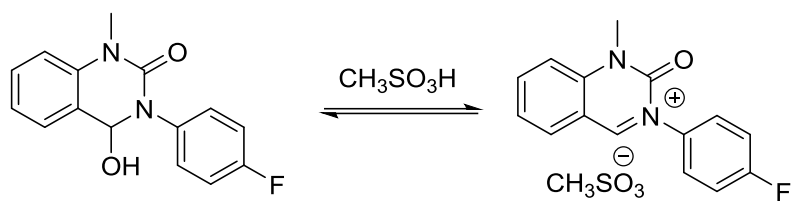


Figure S60. Fluorescence spectra of **2(F)** ($50 \mu\text{M}$) with the titration of MA (0–50.0 equiv) in CH_3CN ($\lambda_{\text{ex}} = 400 \text{ nm}$) (A), and the change of emission intensity at 486 nm (B).

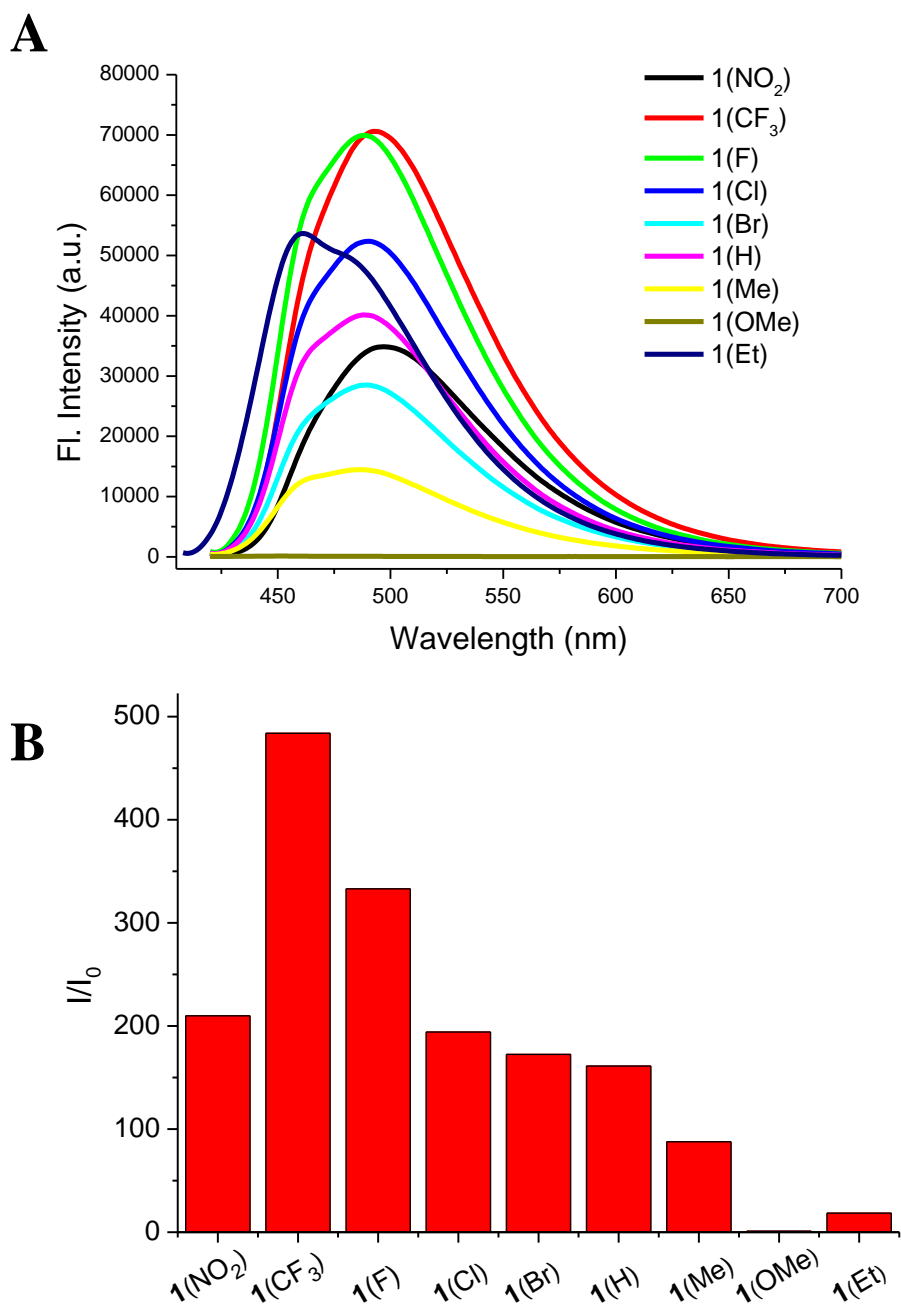


Figure S61. Fluorescence spectra (A) and ratios of the intensity changes at 486 nm (B) of **1**(NO₂), **1**(CF₃), **1**(F), **1**(Cl), **1**(Br), **1**(H), **1**(Me), **1**(OCH₃), and **1**(Et) (50 μM) with the addition of MA (50.0 equiv) in CH₃CN ($\lambda_{\text{ex}} = 400$ nm for **1**(NO₂) – **1**(OCH₃) and $\lambda_{\text{ex}} = 388$ nm for **1**(Et)).

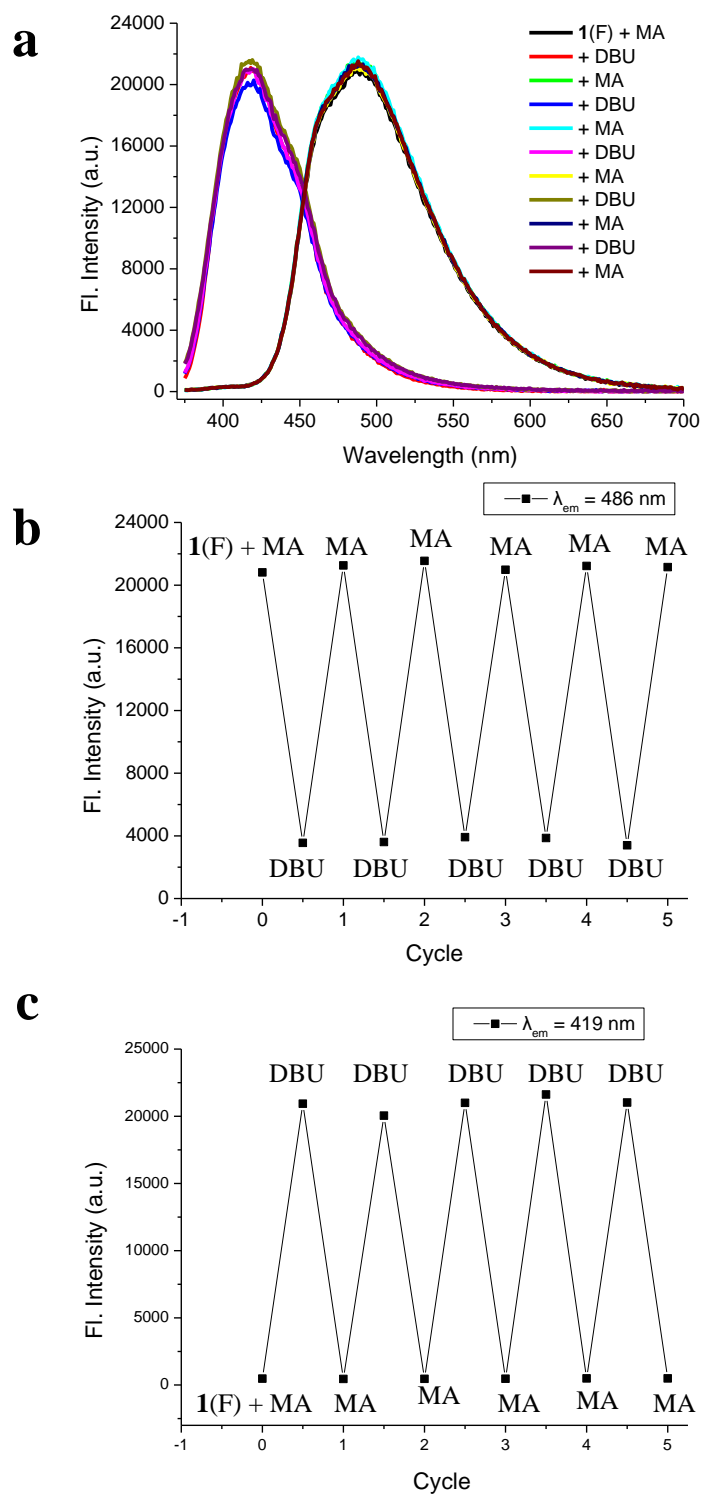


Figure S62. (a) Fluorescence spectra of **1(F)** (50 μ M) with the addition of 2.0 equiv MA, followed by consecutive addition of DBU (100 equiv) and MA (100 equiv) in CH_3CN ; (b) Fluorescence response at 486 nm of the solution; (c) Fluorescence response at 419 nm of the solution.

4. Dynamic Covalent Reactions

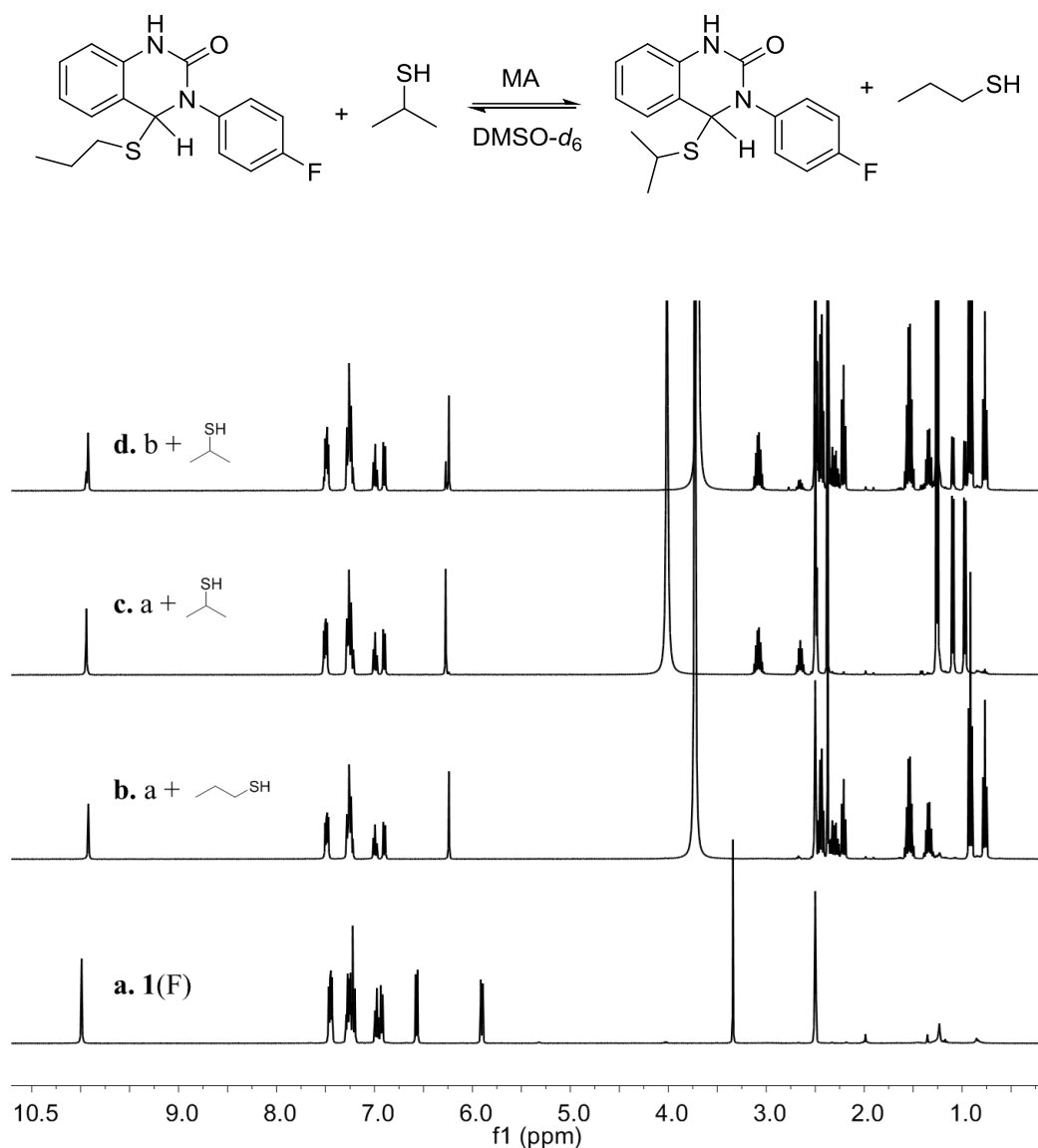


Figure S63. ¹H NMR spectra of dynamic thiol exchange in the presence of MA (1.0 equiv) in DMSO-*d*₆. (a) **1(F)**; (b) the reaction of **1(F)** with 1-propanethiol (3.0 equiv); (c) the reaction of **1(F)** with 2-propanethiol (3.0 equiv); (d) the addition of 2-propanethiol (3.0 equiv) into panel b. This figure shows full NMR spectra of Figure 4A in the main text.

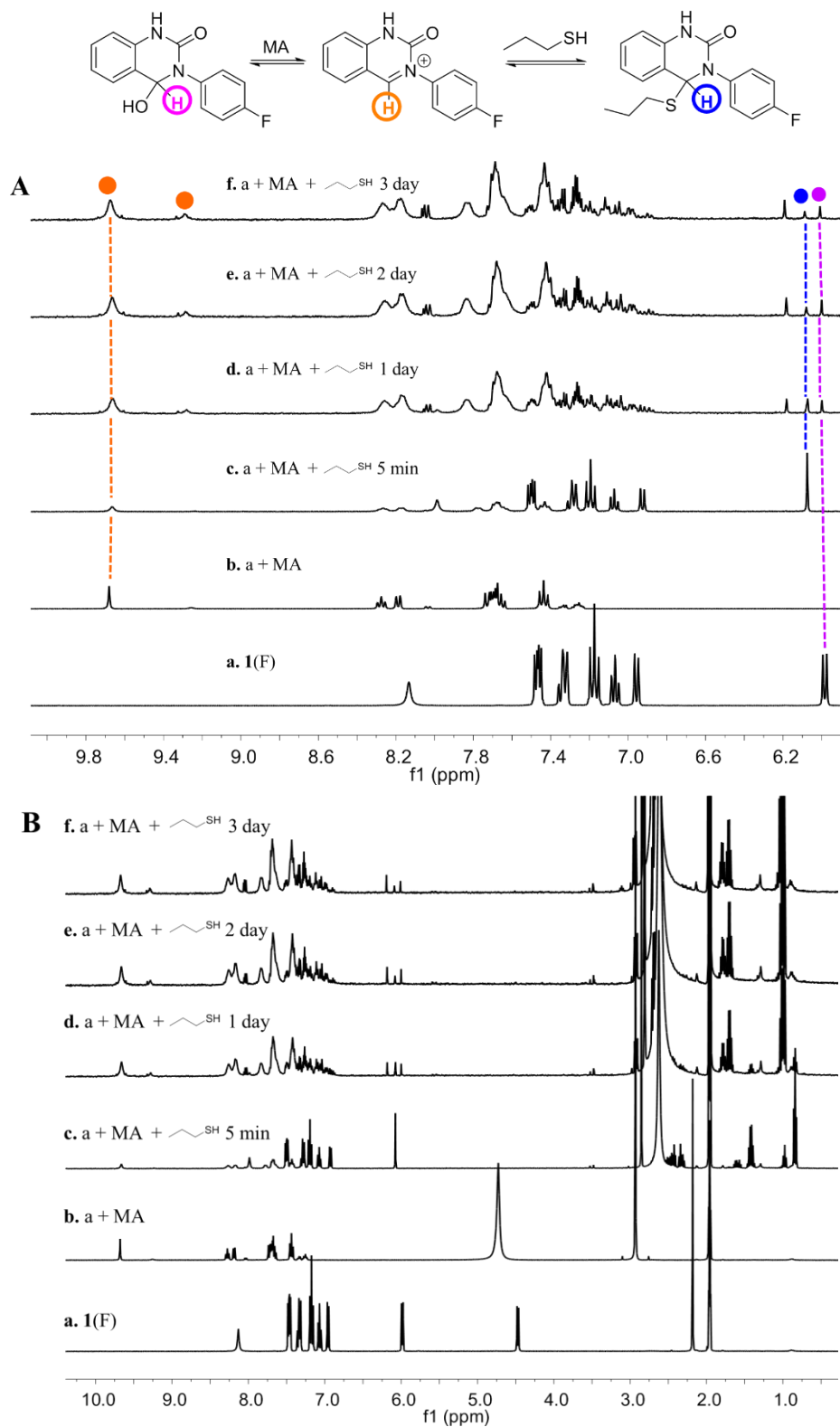


Figure S64. (A) Partial ^1H NMR spectra of the dynamic covalent reaction of **1**(F) with 1-propanethiol (3.0 equiv) in the presence of MA (1.0 equiv) in CD_3CN . (a) **1**(F); (b) **1**(F) with the addition of MA (4.0 equiv); (c, d, e, f) the reaction of **1**(F) with 1-propanethiol at varied time. (B) The full NMR spectra of panel A.

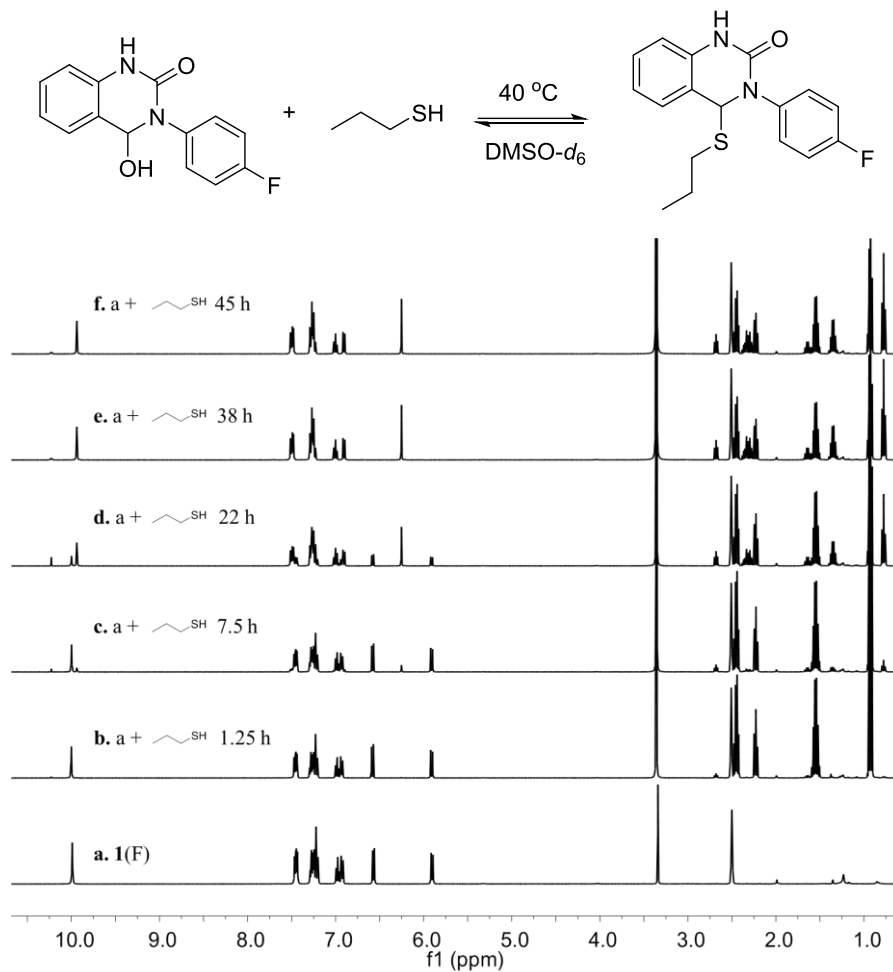


Figure S65. ¹H NMR spectra of the reaction between **1(F)** and 1-propanethiol (3.0 equiv) at 40 °C at varied time in DMSO-*d*₆. The equilibrium was reached after 38 h.

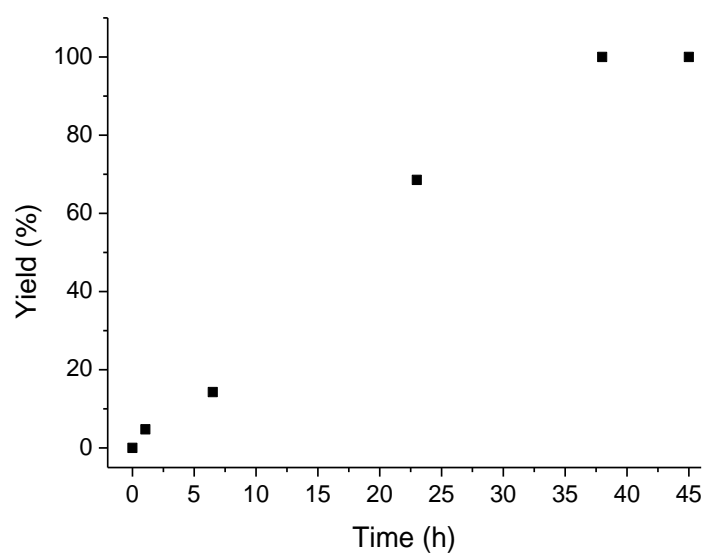


Figure S66. The yield of the reaction between **1(F)** and 1-propanethiol (3.0 equiv) at 40 °C at varied time in DMSO-*d*₆.

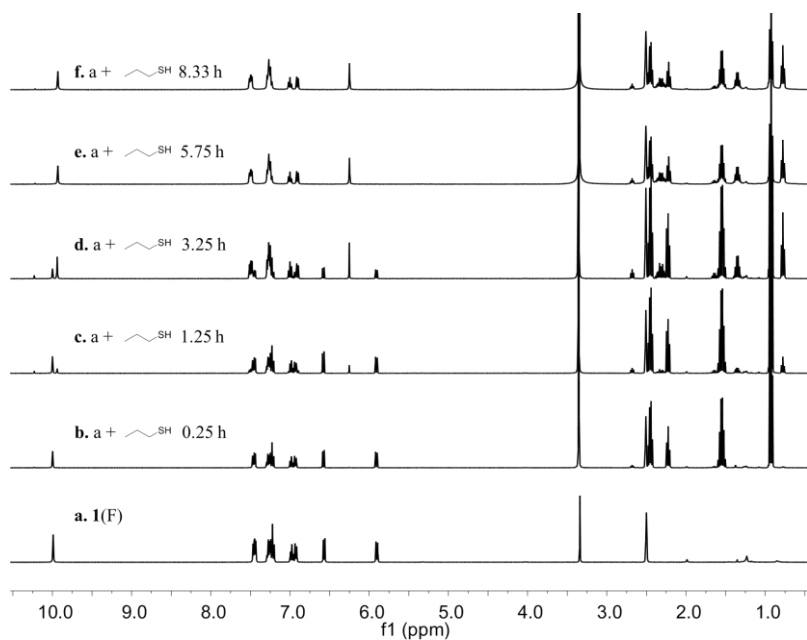
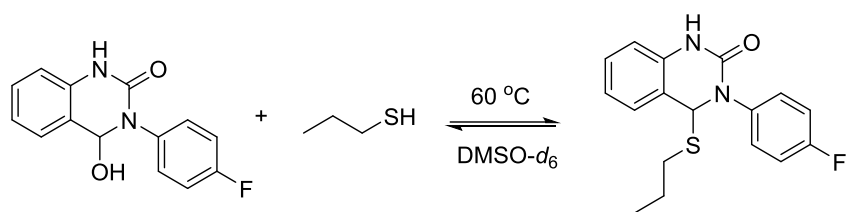


Figure S67. ¹H NMR spectra of the reaction between 1(F) and 1-propanethiol (3.0 equiv) at 60 °C at varied time in DMSO-*d*₆. The equilibrium was reached after 5.75 h.

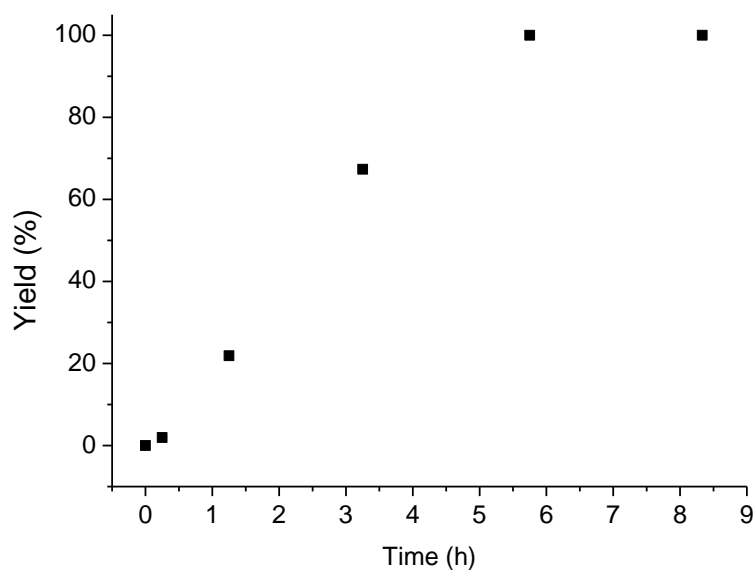


Figure S68. The yield of the reaction between 1(F) and 1-propanethiol (3.0 equiv) at 60 °C at varied time in DMSO-*d*₆.

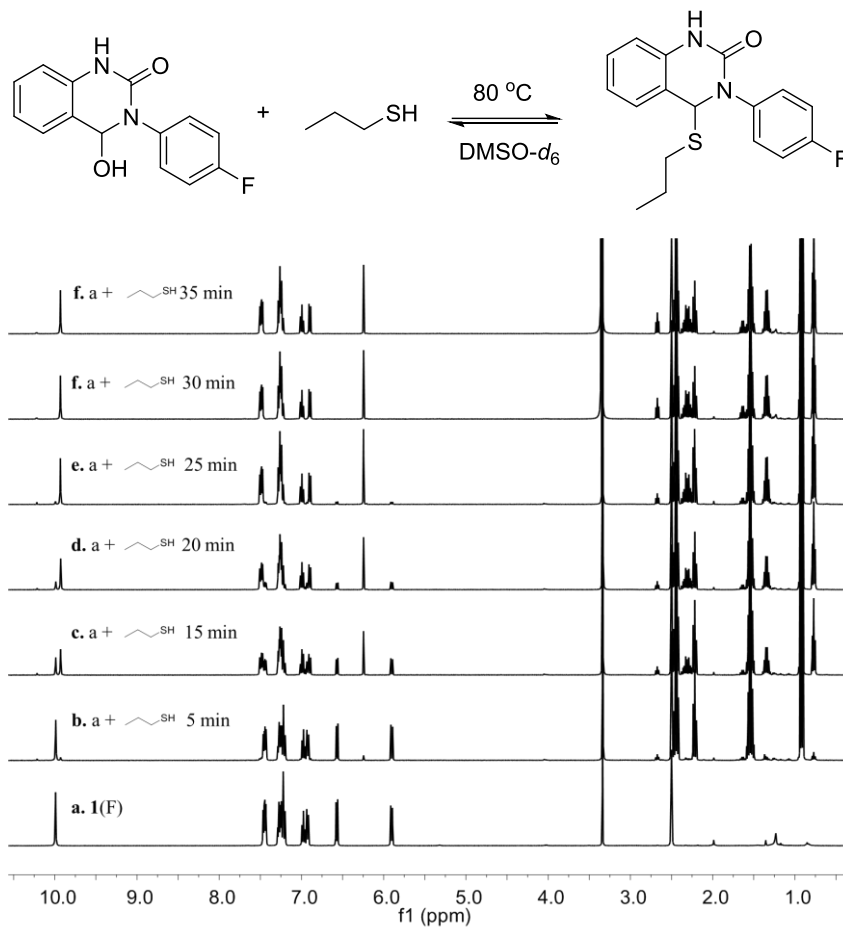


Figure S69. ¹H NMR spectra of the reaction between **1(F)** and 1-propanethiol (3.0 equiv) at 80 °C at varied time in DMSO-*d*₆. The equilibrium was reached after 30 min.

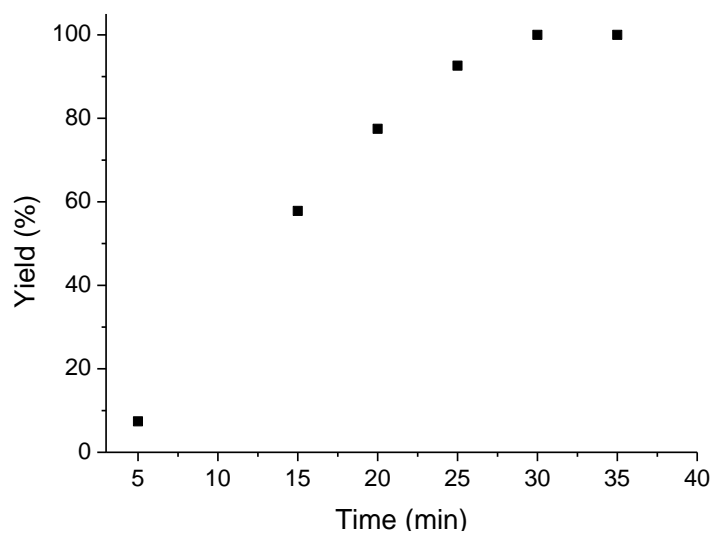


Figure S70. The yield of the reaction between **1(F)** and 1-propanethiol (3.0 equiv) at 80 °C at varied time in DMSO-*d*₆.

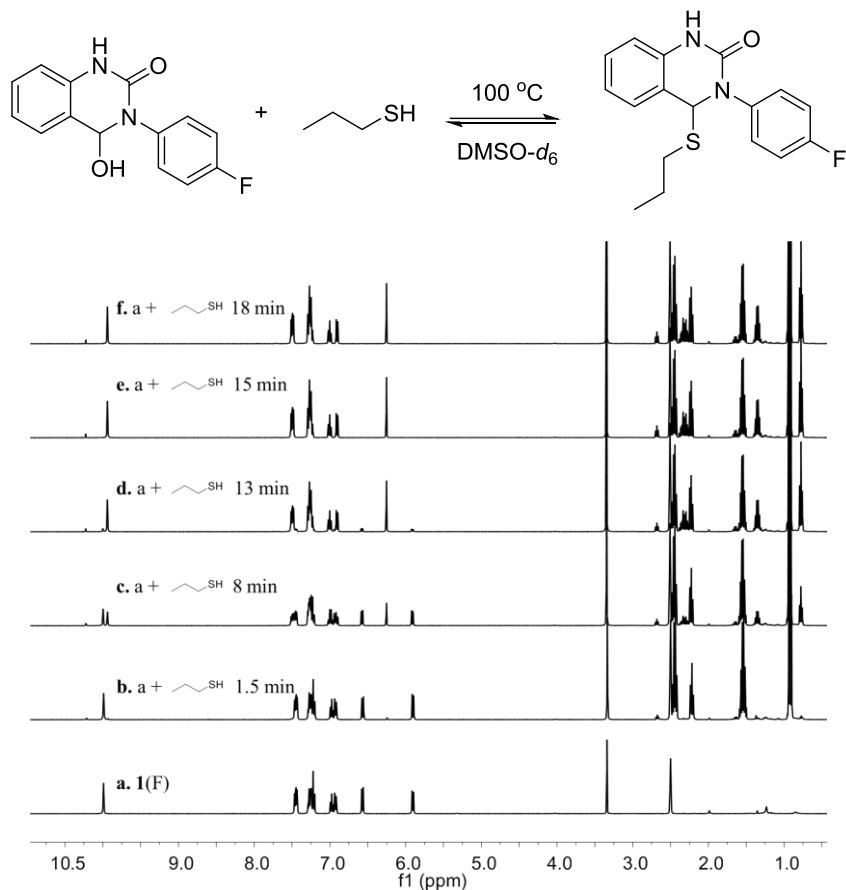


Figure S71. ^1H NMR spectra of the reaction between **1(F)** and 1-propanethiol (3.0 equiv) at 100 °C at varied time in $\text{DMSO-}d_6$. The equilibrium was reached after 15 min.

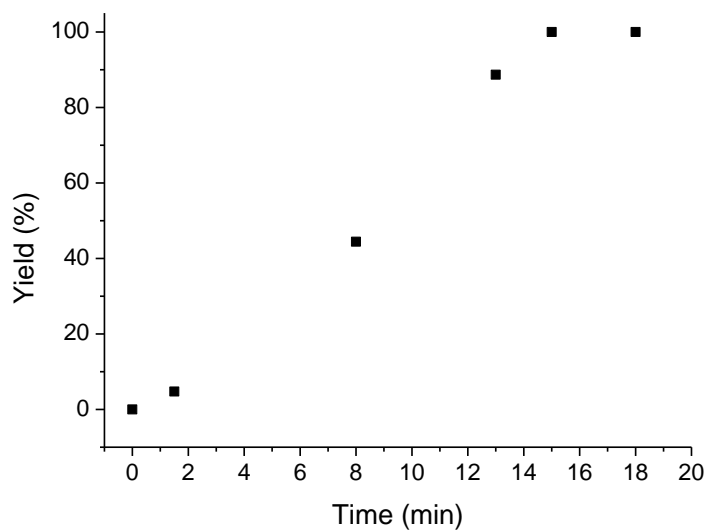


Figure S72. The yield of the reaction between **1(F)** and 1-propanethiol (3.0 equiv) at 100 °C at varied time in $\text{DMSO-}d_6$.

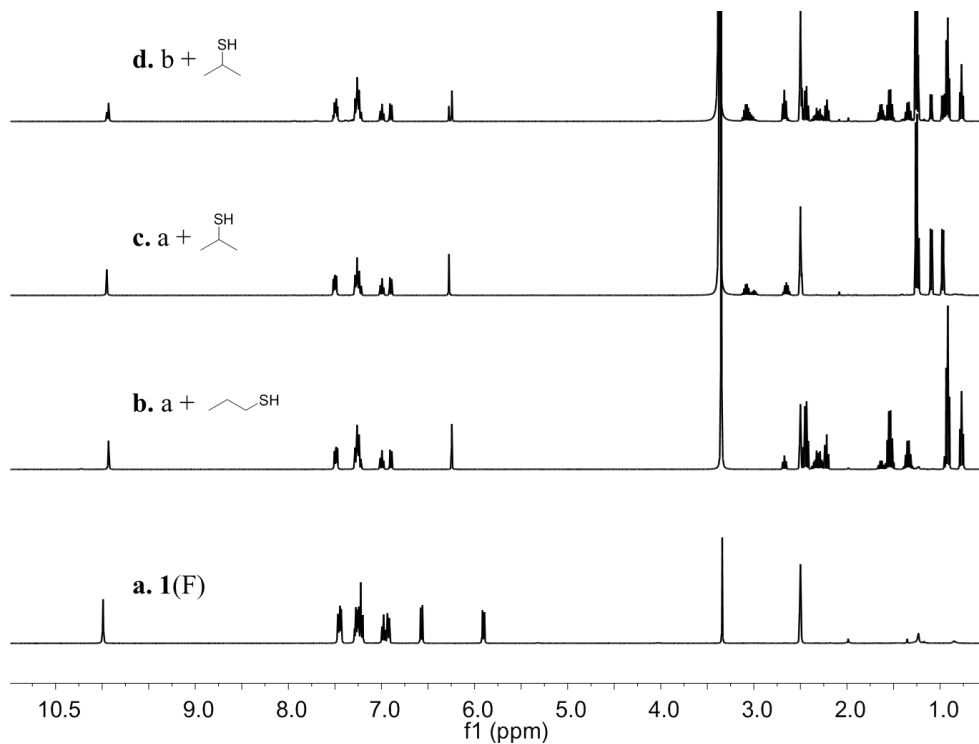
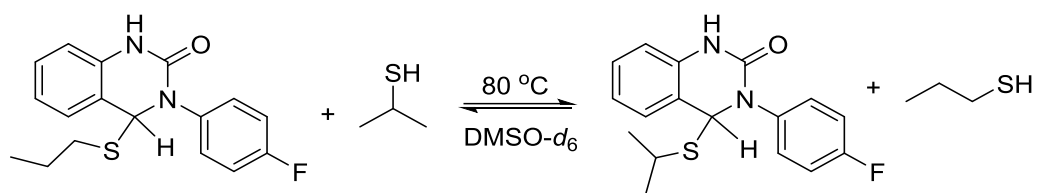


Figure S73. ¹H NMR spectra of dynamic thiol exchange at 80 °C in DMSO-*d*₆. (a) **1(F)**; (b) the reaction of **1(F)** with 1-propanethiol (3.0 equiv); (c) the reaction of **1(F)** with 2-propanethiol (3.0 equiv); (d) the addition of 2-propanethiol (3.0 equiv) into panel b.

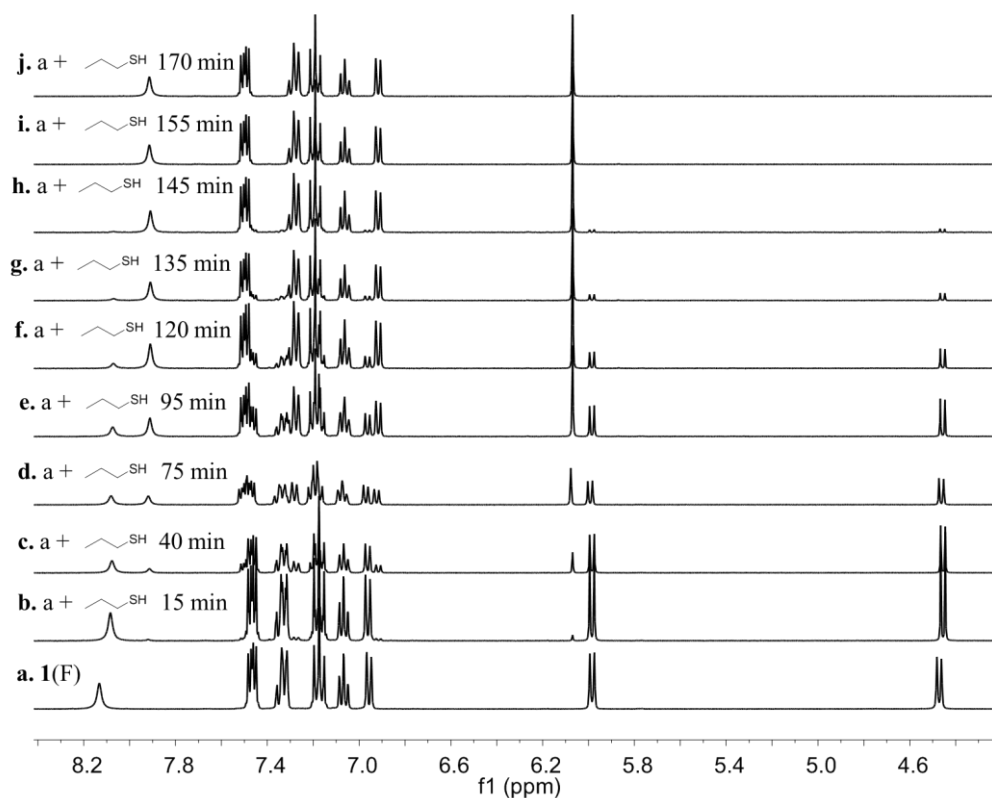


Figure S74. ^1H NMR spectra of the reaction between **1(F)** and 1-propanethiol (3.0 equiv) at 60 °C at varied time in CD_3CN . The equilibrium was reached after 155 min.

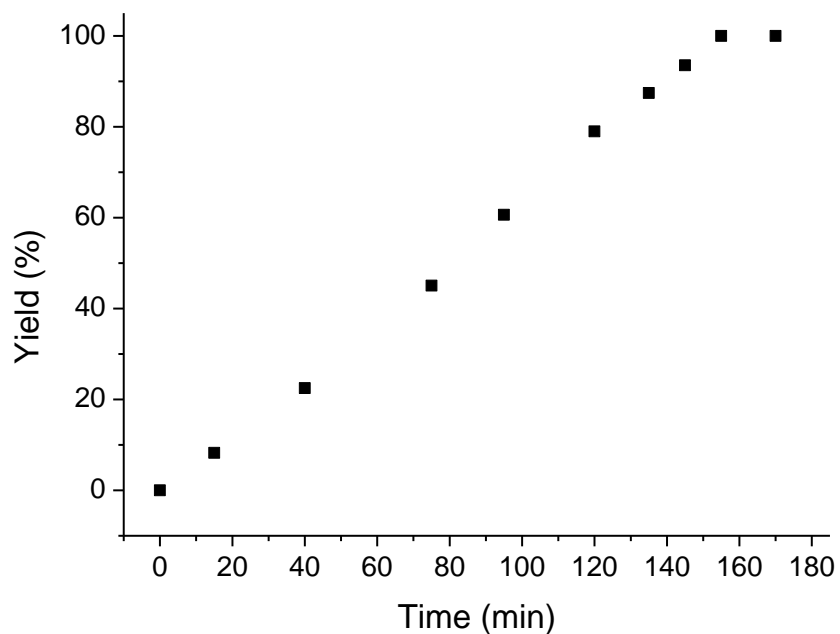


Figure S75. The yield of the reaction between **1(F)** and 1-propanethiol (3.0 equiv) at 60 °C at varied time in CD_3CN .

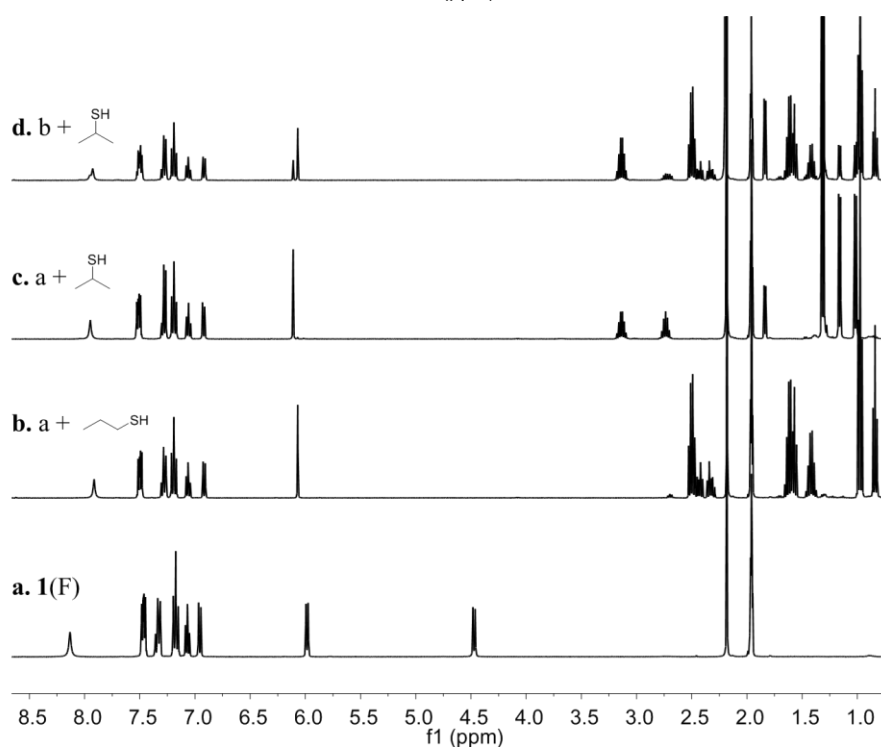
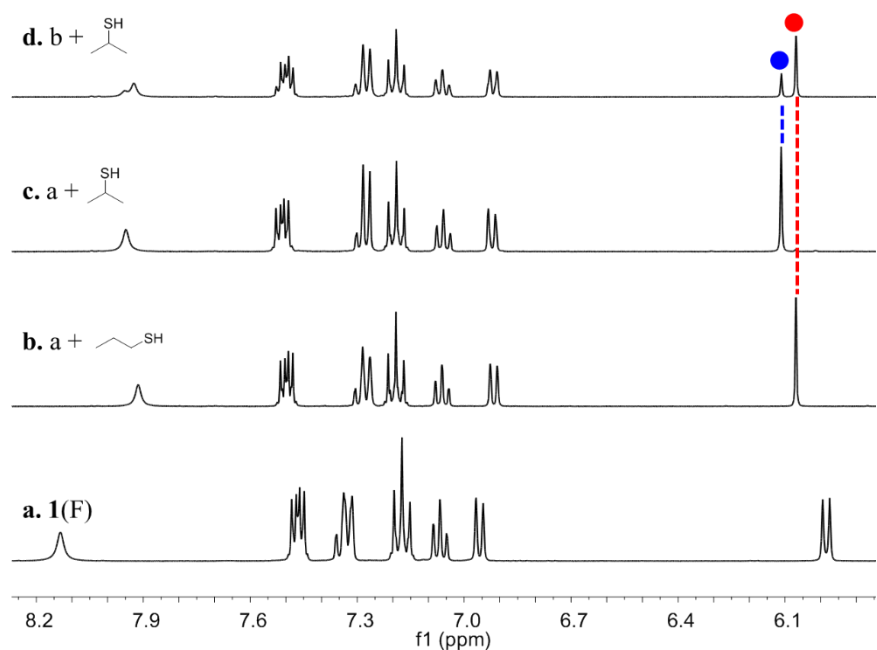
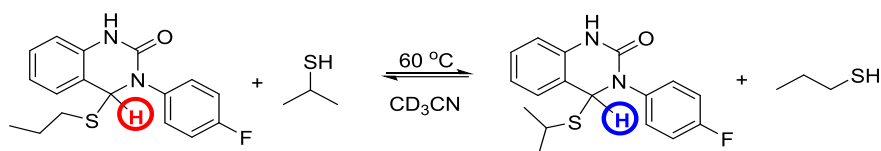


Figure S76. (A) Partial ^1H NMR spectra of dynamic thiol exchange at $60\text{ }^\circ\text{C}$ in CD_3CN . (a) **1(F)**; (b) the reaction of **1(F)** with 1-propanethiol (3.0 equiv); (c) the reaction of **1(F)** with 2-propanethiol (3.0 equiv); (d) the addition of 2-propanethiol (3.0 equiv) into panel b. (B) The full NMR spectra of panel A.

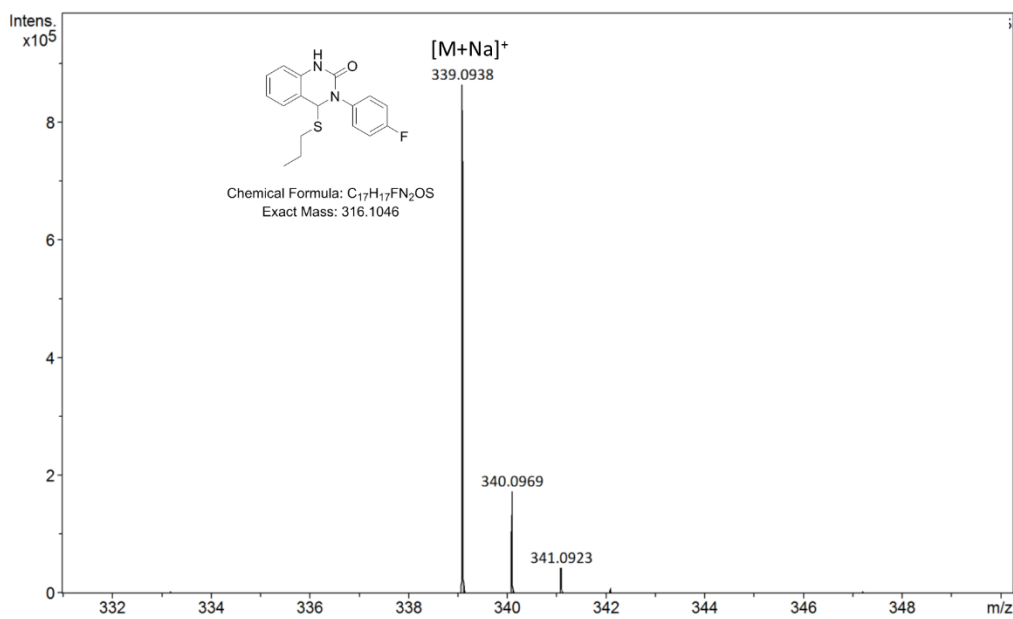


Figure S77. ESI mass spectrum of the reaction between **1(F)** and 1-propanethiol in the presence of MA in DMSO-*d*₆.

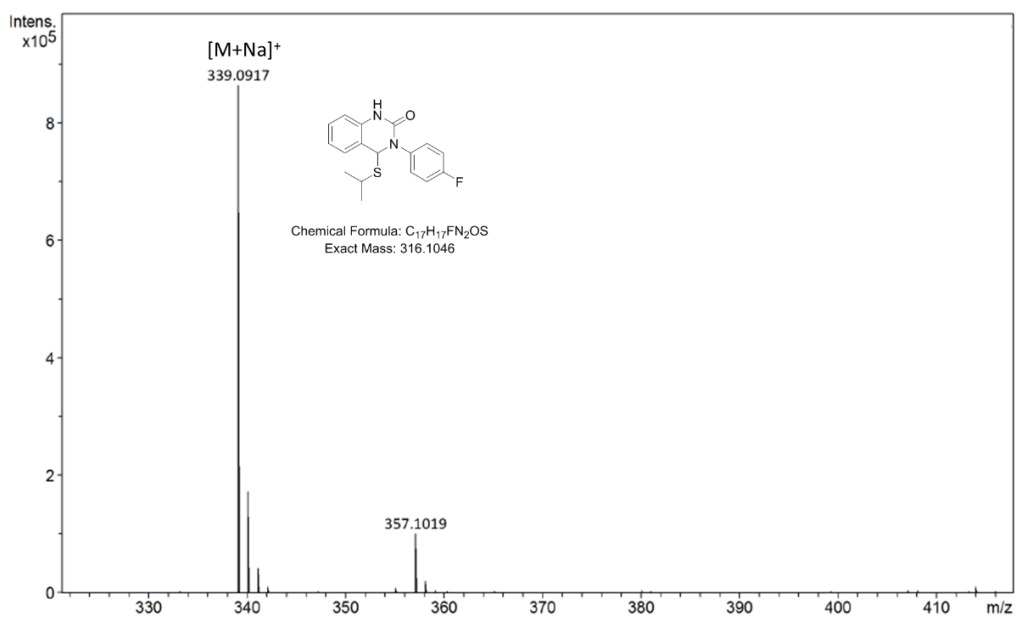


Figure S78. ESI mass spectrum of the reaction of **1(F)** and 2-propanethiol in the presence of MA in DMSO-*d*₆.

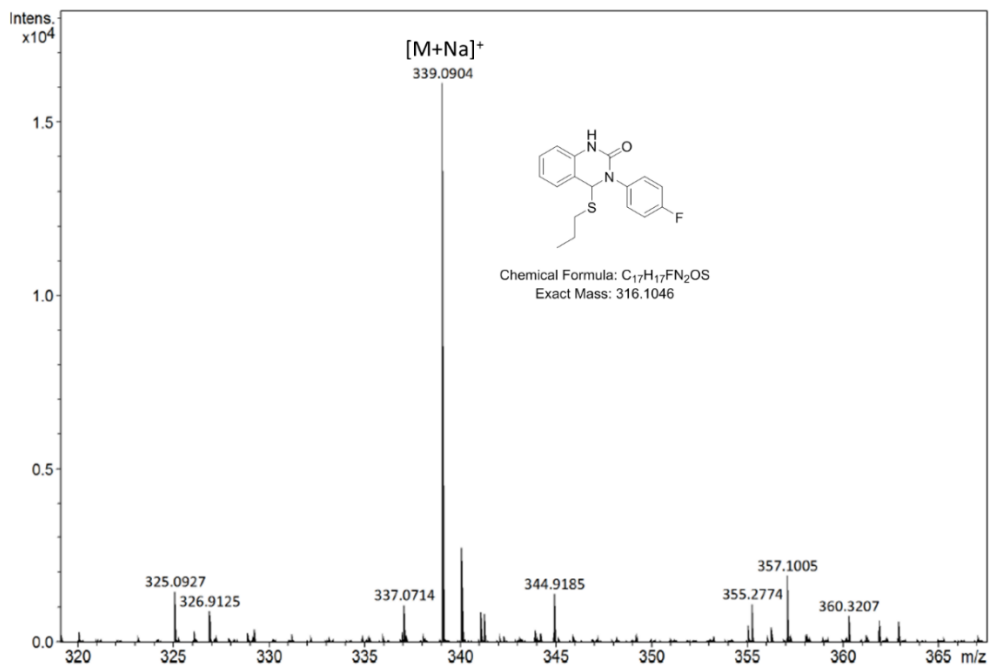


Figure S79. ESI mass spectrum of the reaction of **1(F)** and 1-propanethiol at 80 °C in DMSO-*d*₆.

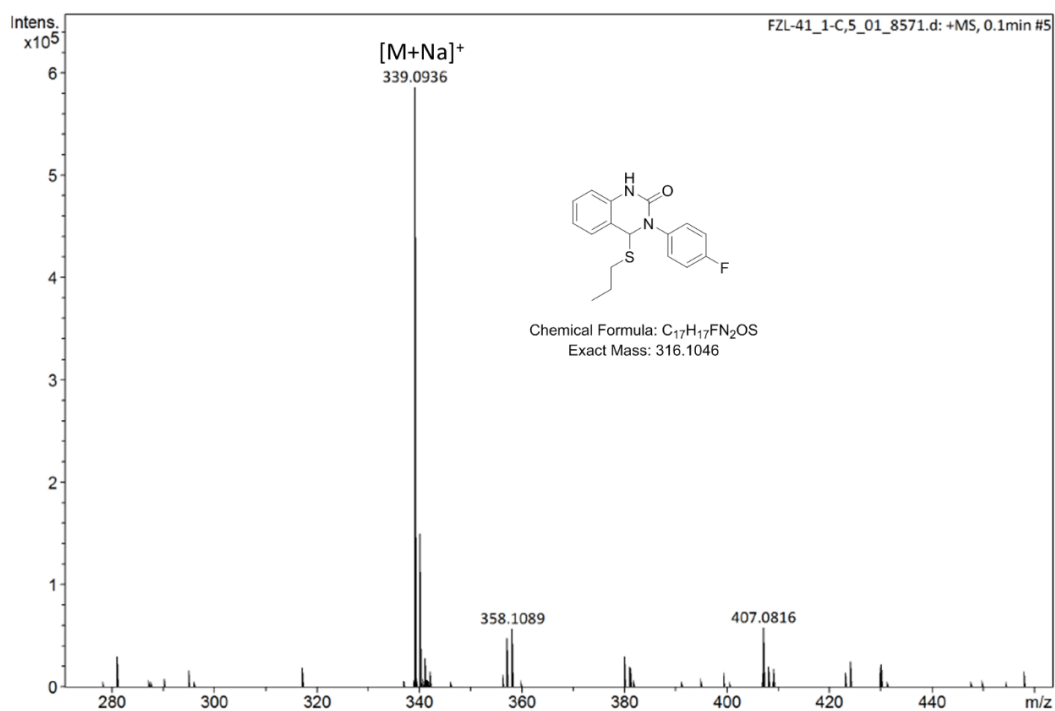


Figure S80. ESI mass spectrum of dynamic covalent reaction between **1(F)** and 1-propanethiol at 60 °C in CD₃CN.

5. Thermally Activated Fluorescence

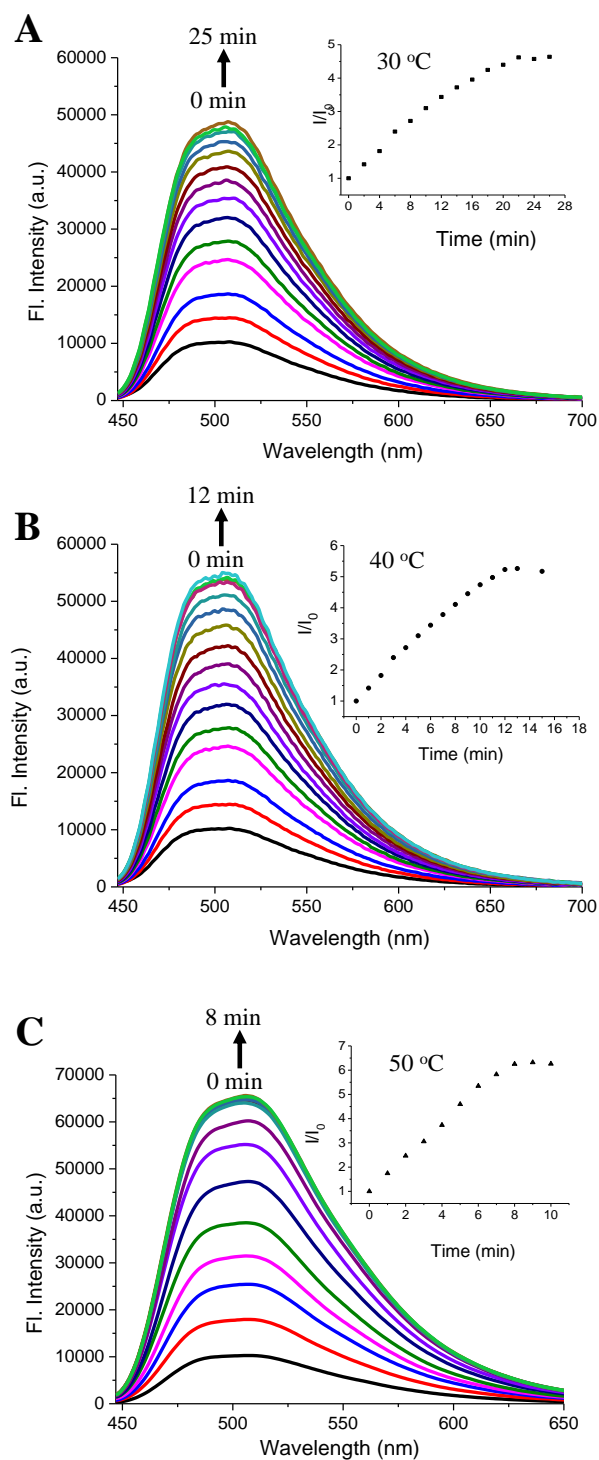


Figure S81. Fluorescence spectra of **1(F)** (50 μ M) with heating at 30 °C (A), 40 °C (B), and 50 °C in CH_3CN at varied time. Inset: time traced intensity response at 510 nm ($\lambda_{\text{ex}} = 427$ nm).

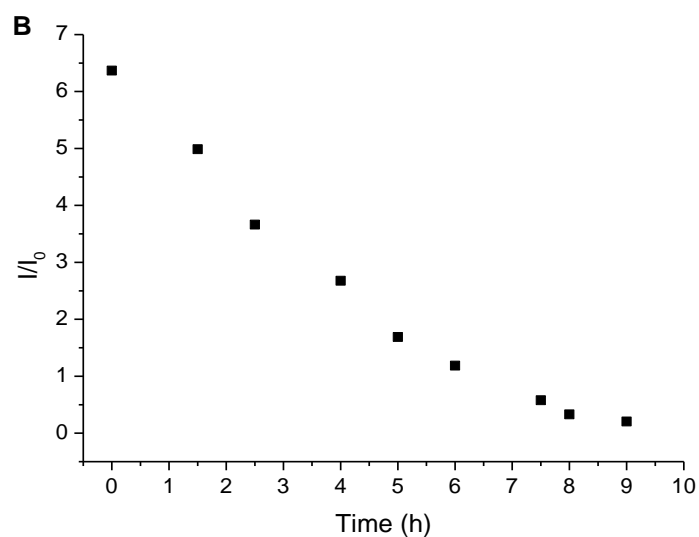
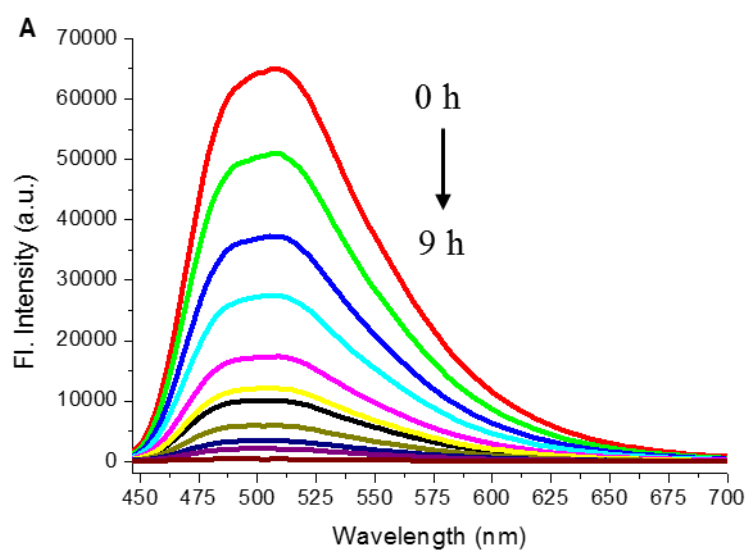


Figure S82. (A) Fluorescence spectra of a solution (50 μM) of thermally activated **1(F)** in CH_3CN during a natural cooling process from 50 $^\circ\text{C}$ to 25 $^\circ\text{C}$ at varied time; (B) intensity response at 510 nm at varied time ($\lambda_{\text{ex}} = 427$ nm).

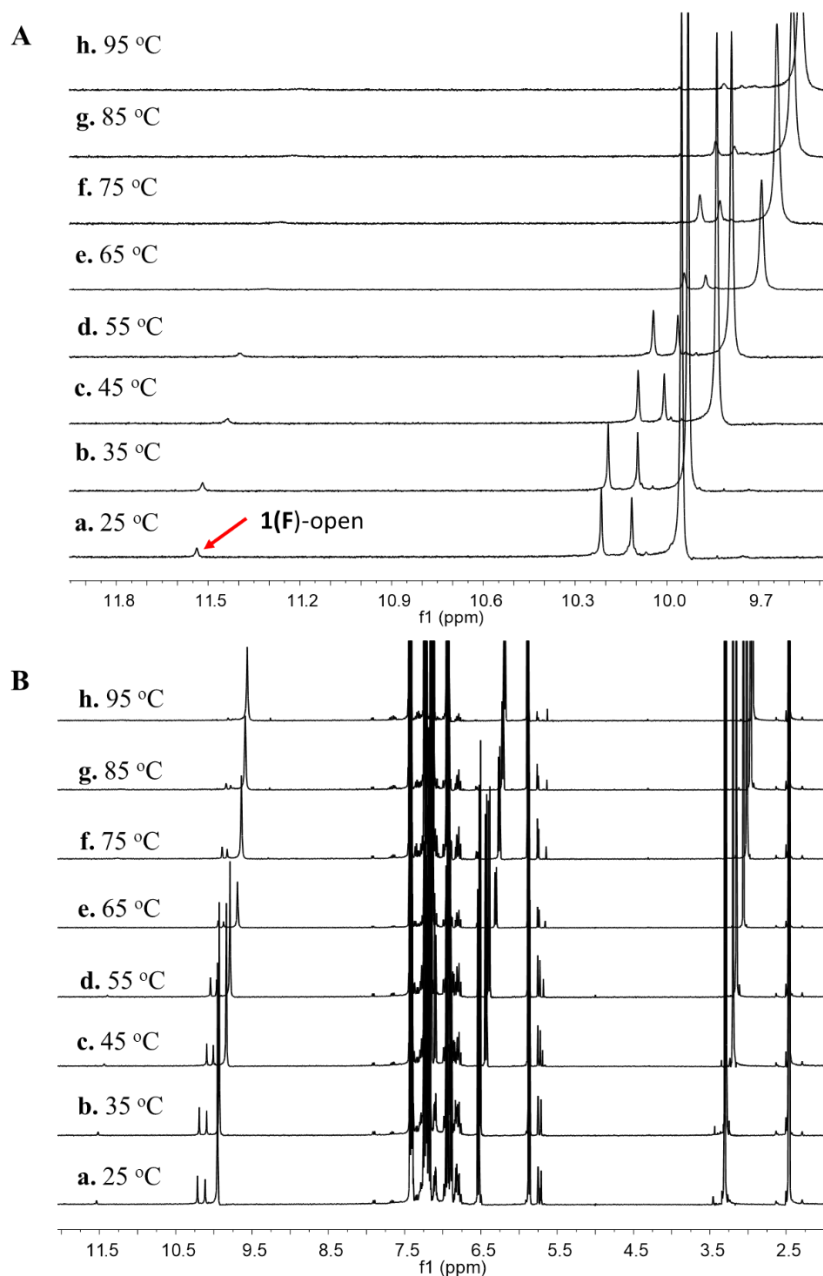
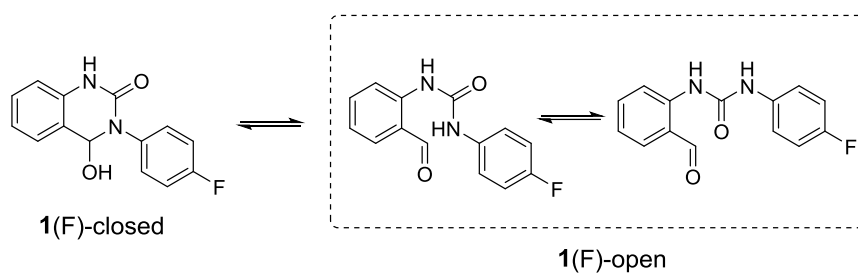


Figure S83. VT- ^1H NMR spectra of activated **1(F)** in $\text{DMSO-}d_6$. The data indicates the emergence of open form of **1(F)** in activated **1(F)**, which was obtained by heating **1(F)** powder under vacuum for 12 hour.

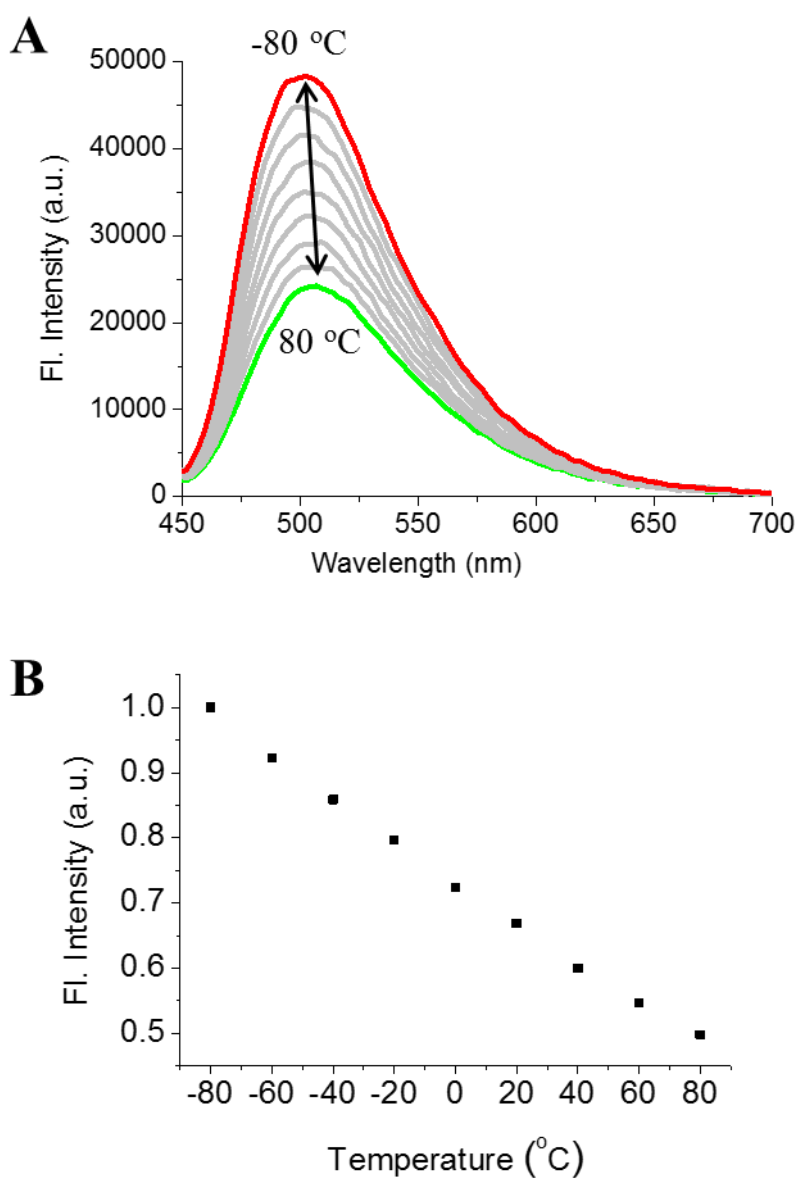


Figure S84. Fluorescence spectra (A) and ratios of the intensity changes at 509 nm (B) of solid **1(F)** at varied temperature ($\lambda_{\text{ex}} = 365$ nm).

6. Chemical Cascade Reactions

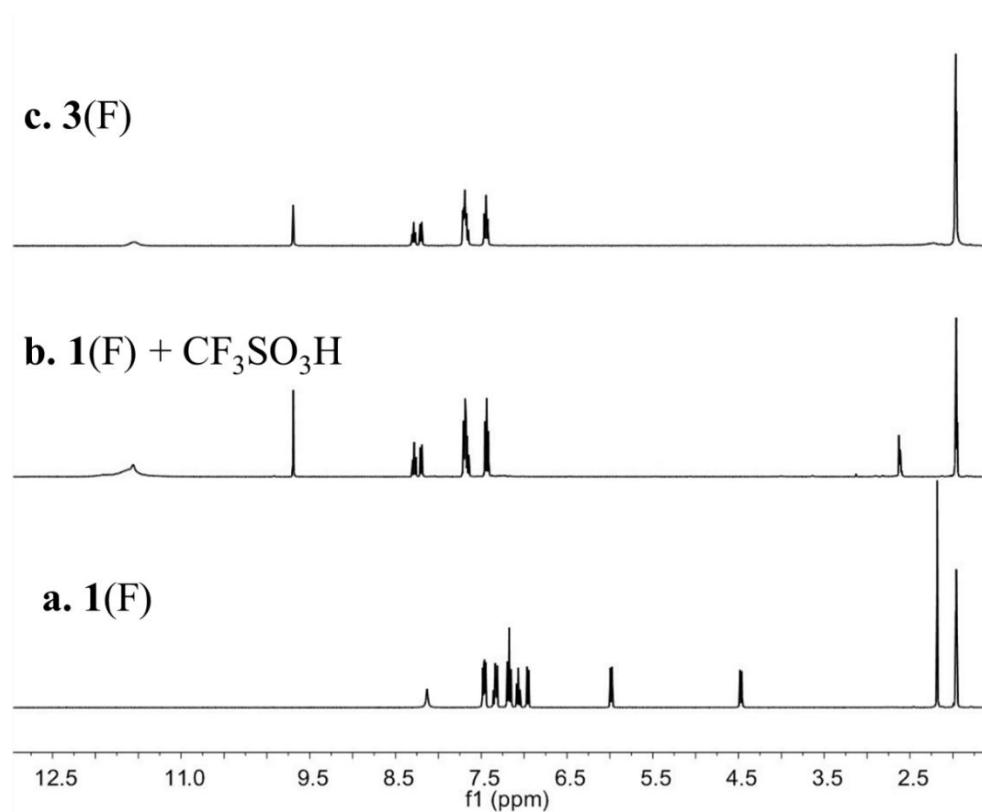


Figure S85. ^1H NMR spectra of **1(F)** (a), **3(F)** created from *in situ* reaction of **1(F)** and acid (b), and synthesized **3(F)** (c) in CD₃CN.

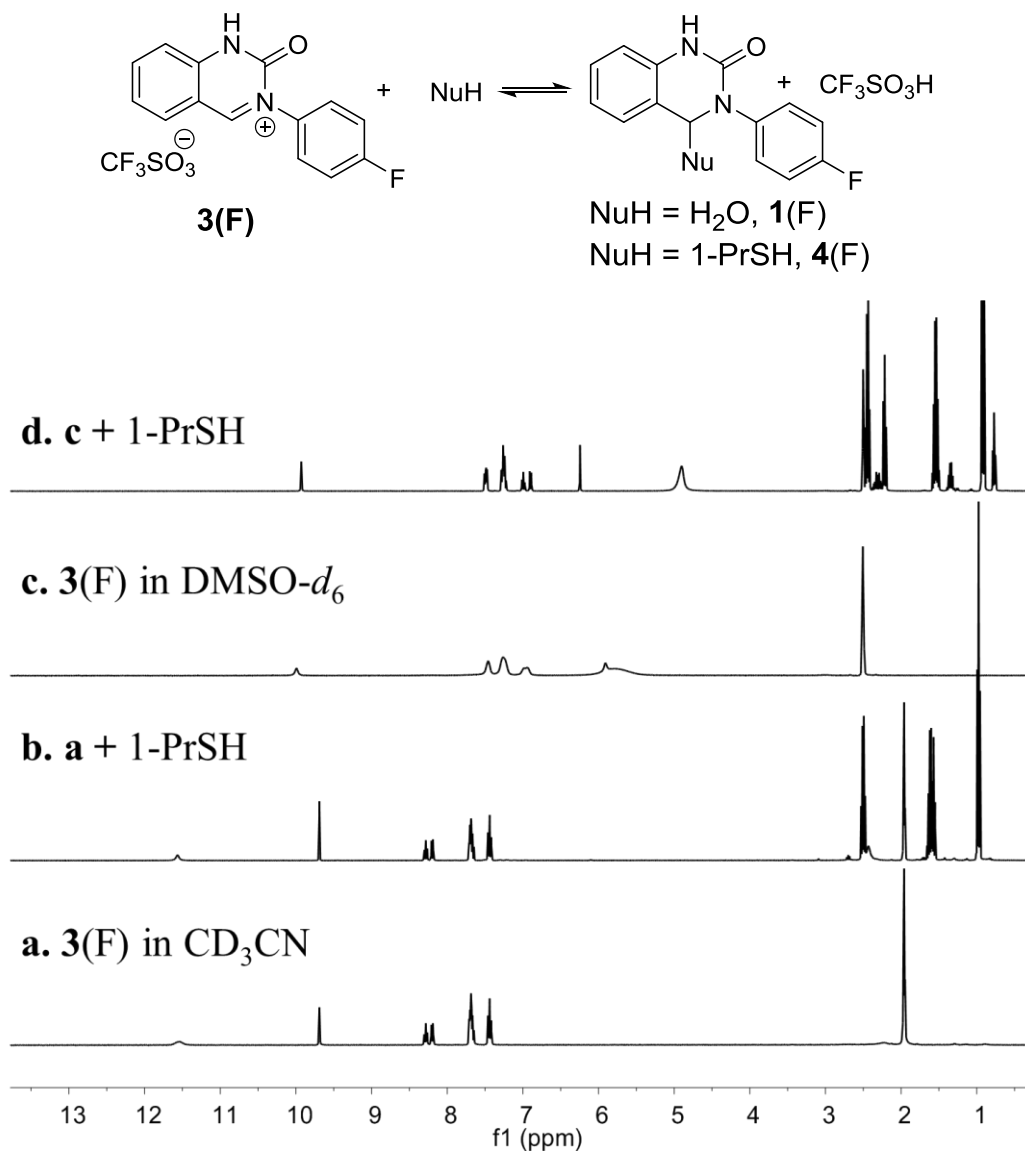


Figure S86. ¹H NMR spectra of the reaction of **3(F)** with 1-propanethiol in CD₃CN or DMSO-*d*₆. This figure shows full NMR spectra of Figure 5A in the main text.

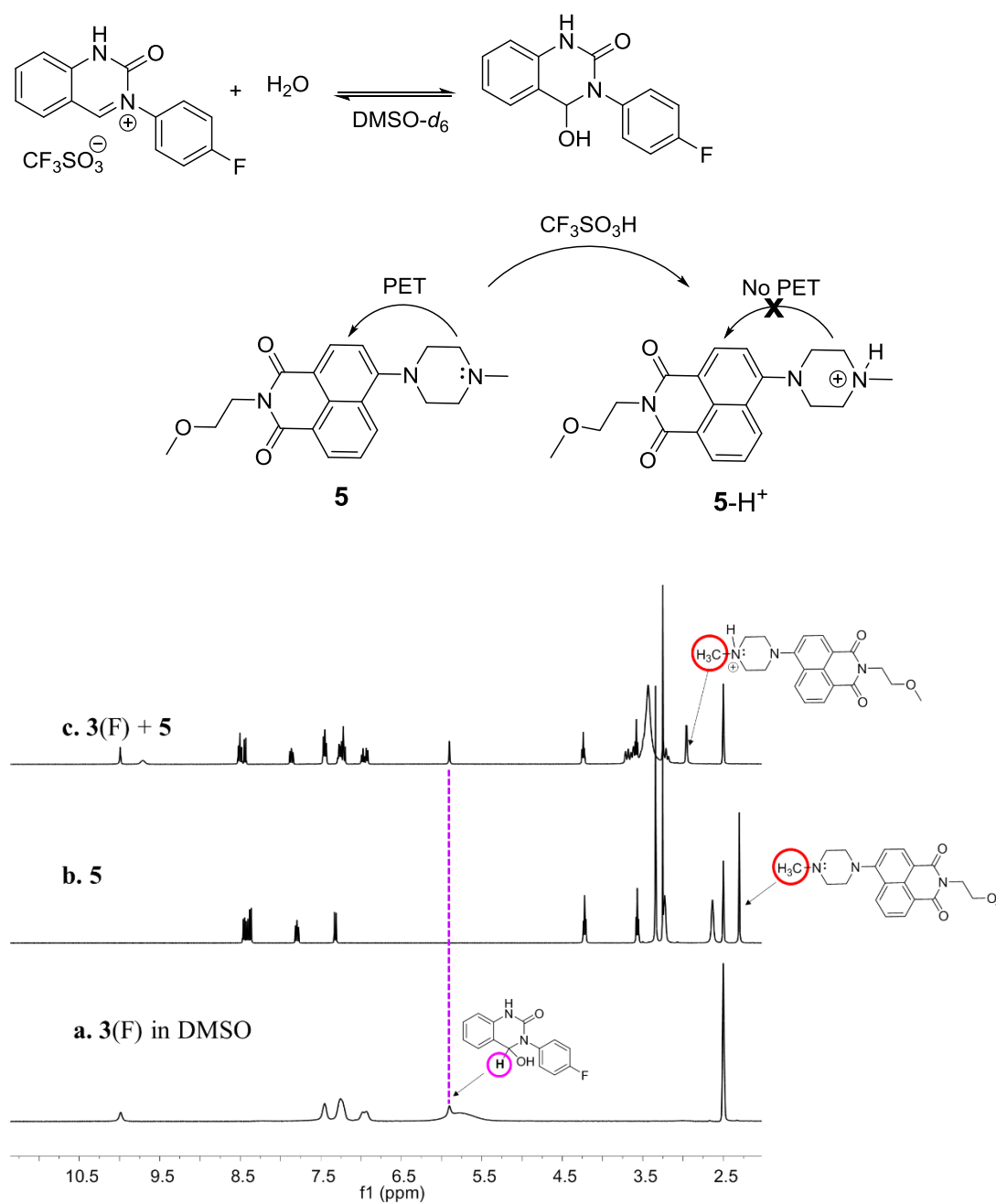


Figure S87. ^1H NMR spectra of the reaction of **3(F)** with water in $\text{DMSO-}d_6$, coupled with fluorescence switch **5**. This figure shows associated NMR spectra of Figure 5B in the main text.

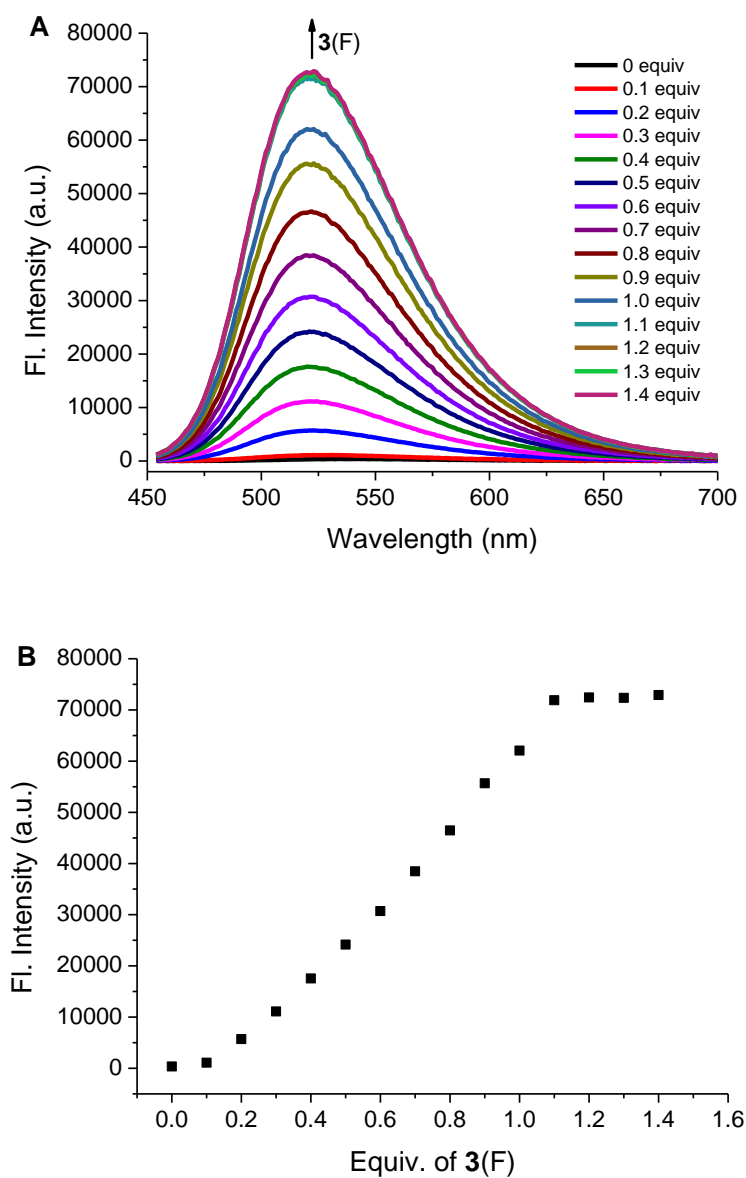


Figure S88. A: Fluorescence spectra of **5** in response to increasing concentration of **3F** (0–1.4 equiv) in DMSO ($\lambda_{\text{ex}} = 435 \text{ nm}$). B: The corresponding titration curve from part A ($\lambda_{\text{em}} = 523 \text{ nm}$).

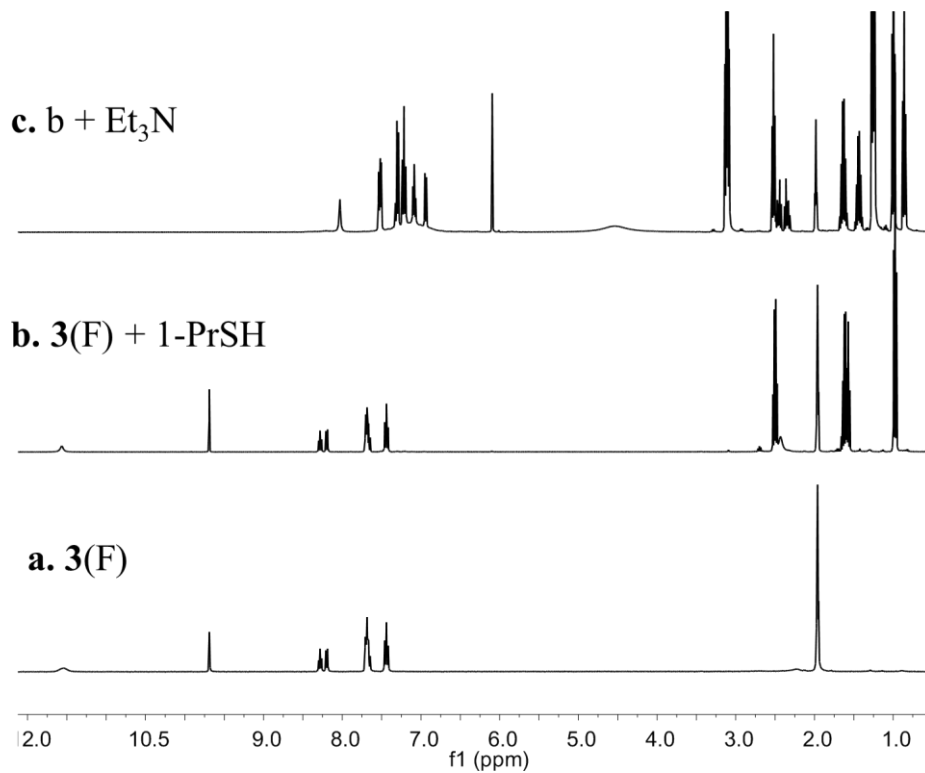
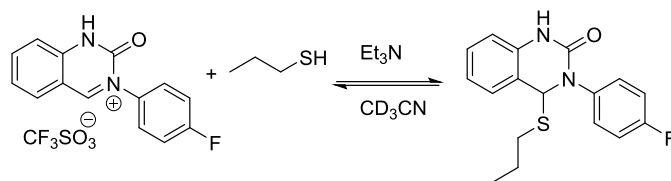


Figure S89. ^1H NMR spectra of the reactions of **3(F)** with 1-propanethiol in CD_3CN . (a) **3(F)**; (b) the addition of 1-propanethiol (3.0 equiv) into panel a; (c) the addition of Et_3N (3.0 equiv) into panel b.

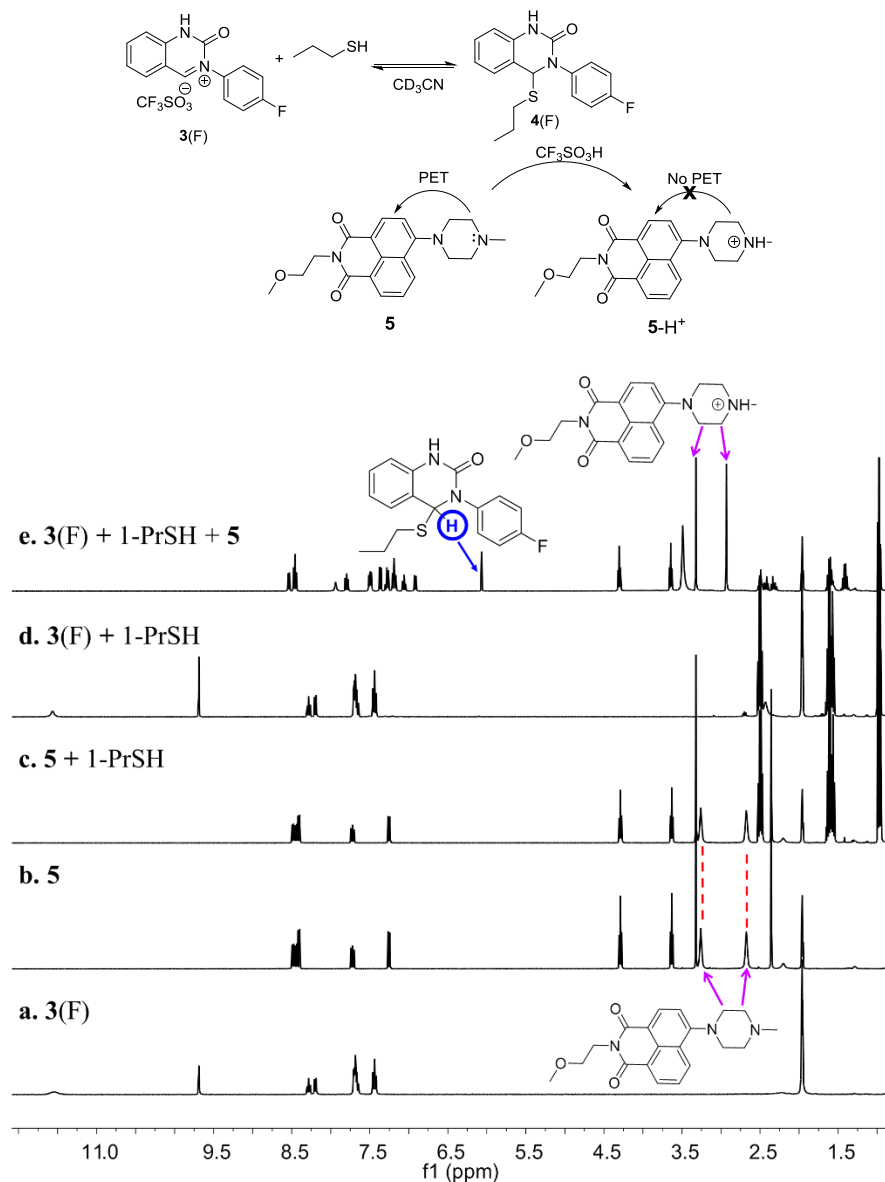


Figure S90. ^1H NMR spectra of coupling of dynamic covalent reaction and fluorescence switch **5** in CD_3CN . (a) **3(F)**; (b) **5**; (c) a mixture of 1-propanethiol (3.0 equiv) and **5**; (d) a mixture of **3(F)** and 1-propanethiol (3.0 equiv); (e) the addition of **5** into panel d.

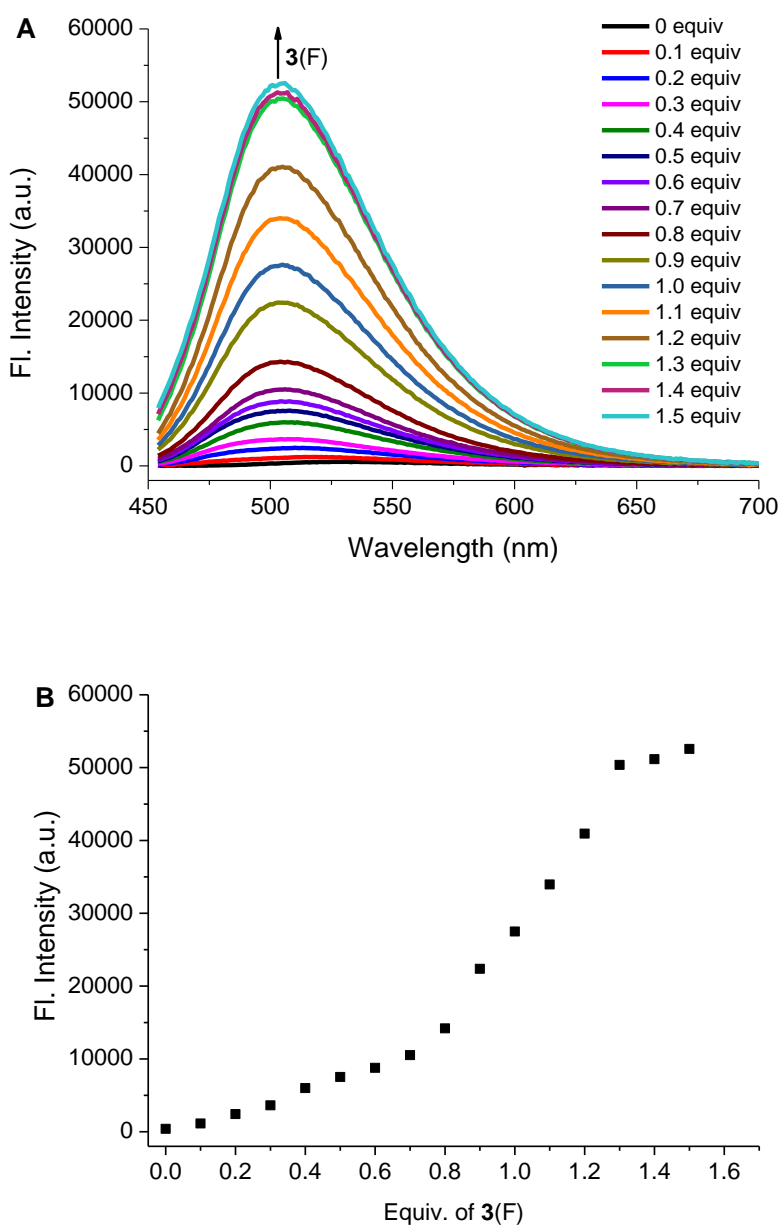


Figure S91. A: Fluorescence spectra of **5** (0.2 mM) in acetonitrile in the presence of a constant concentration of 1-propanethiol (3.0 equiv) and an increasing concentration of **3(F)** (0–1.5 equiv) ($\lambda_{\text{ex}} = 435$ nm). B: The corresponding titration curve from part A ($\lambda_{\text{em}} = 506$ nm).

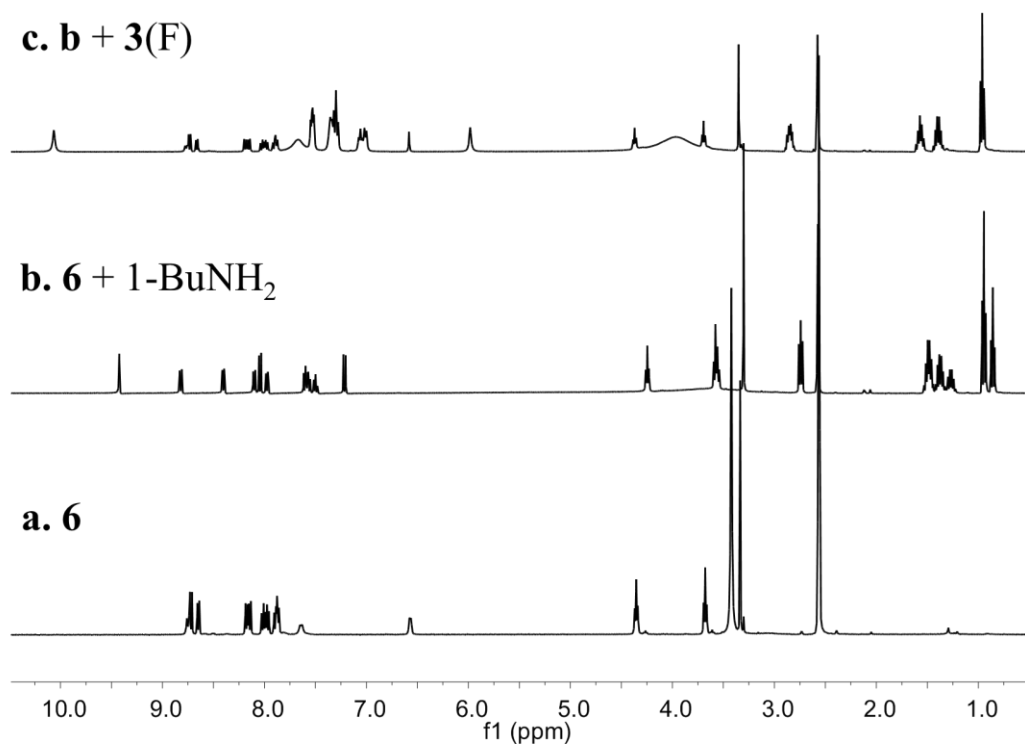
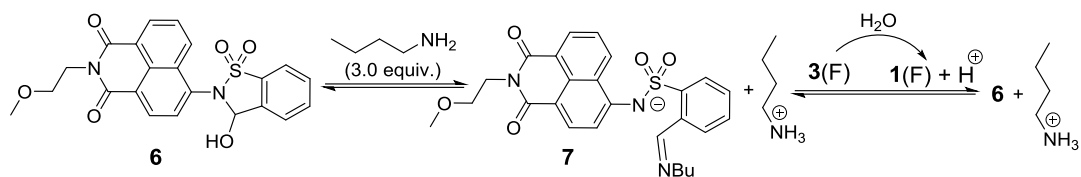


Figure S92. ^1H NMR spectra of fluorescent switch **6** (a), its reaction with 1-BuNH₂ (3.0 equiv) (b), followed by the addition of **3(F)** (3.3 equiv) to panel b in DMSO-*d*₆ (c). This figure shows full NMR spectra of Figure 5C in the main text.

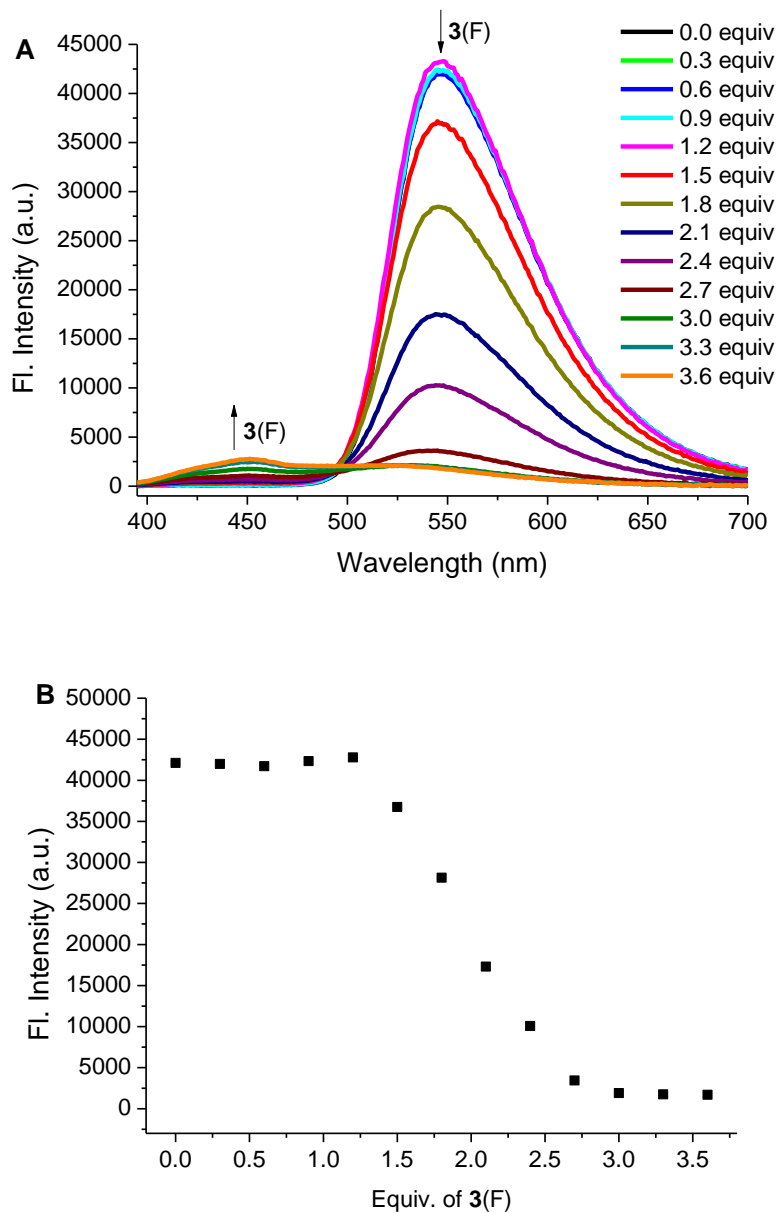


Figure S93. A: Fluorescence spectra of **7** created from *in situ* reaction of **6** (0.2 mM) and 1-BuNH₂ (3.0 equiv) in response to increasing concentration of **3(F)** (0–3.6 equiv) in DMSO ($\lambda_{\text{ex}} = 375$ nm). B: The corresponding titration curve from part A ($\lambda_{\text{em}} = 550$ nm).

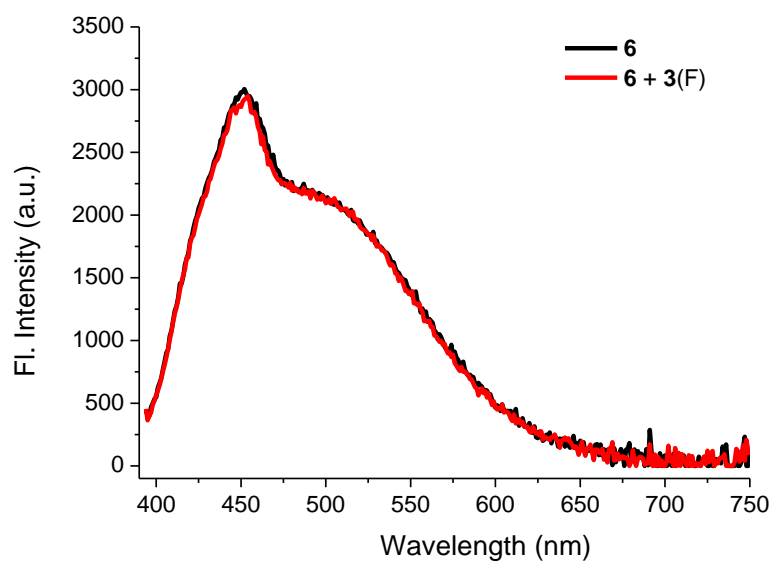


Figure S94. Fluorescence spectra of **6** (0.2 mM) with the addition of **3(F)** (1.0 equiv) in DMSO ($\lambda_{\text{ex}} = 375 \text{ nm}$)..

7. Solid State Luminescent Materials

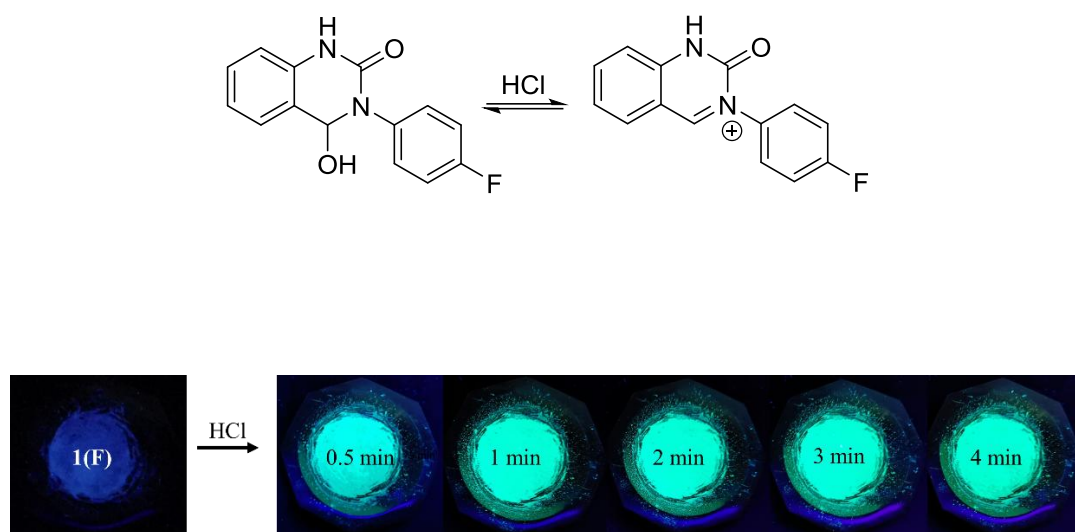


Figure S95. The photographs of color change of powder **1(F)** in response to HCl vapor at varied time.

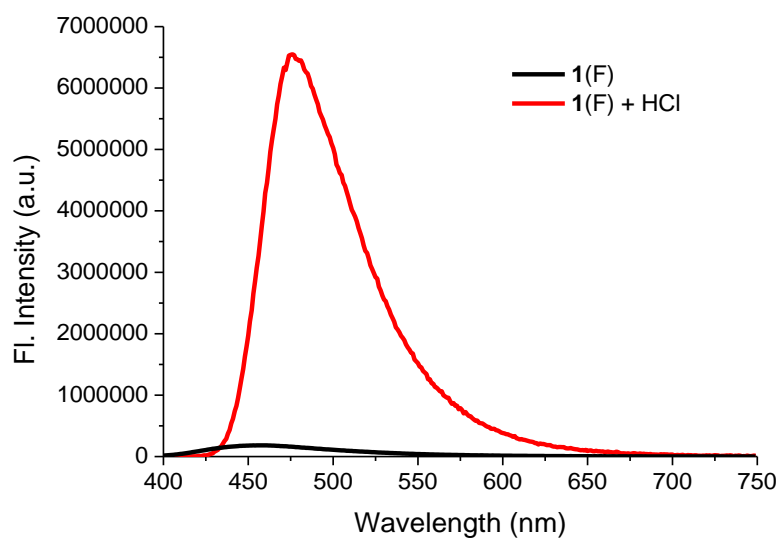


Figure S96. Solid state fluorescence spectra of **1(F)** upon activation with HCl vapor ($\lambda_{\text{ex}} = 365 \text{ nm}$).

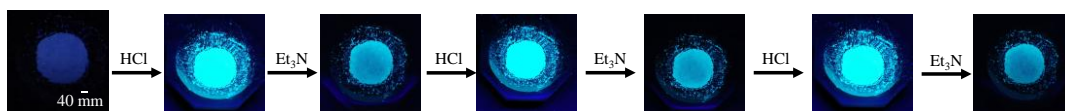
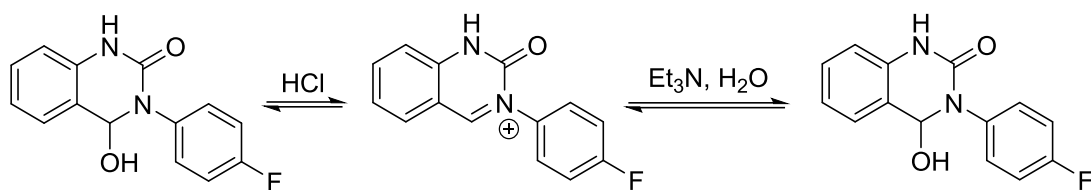


Figure S97. The photographs of color change of powder **1(F)** with consecutive exposure to HCl (1 min), followed by Et₃N vapor (15 min).

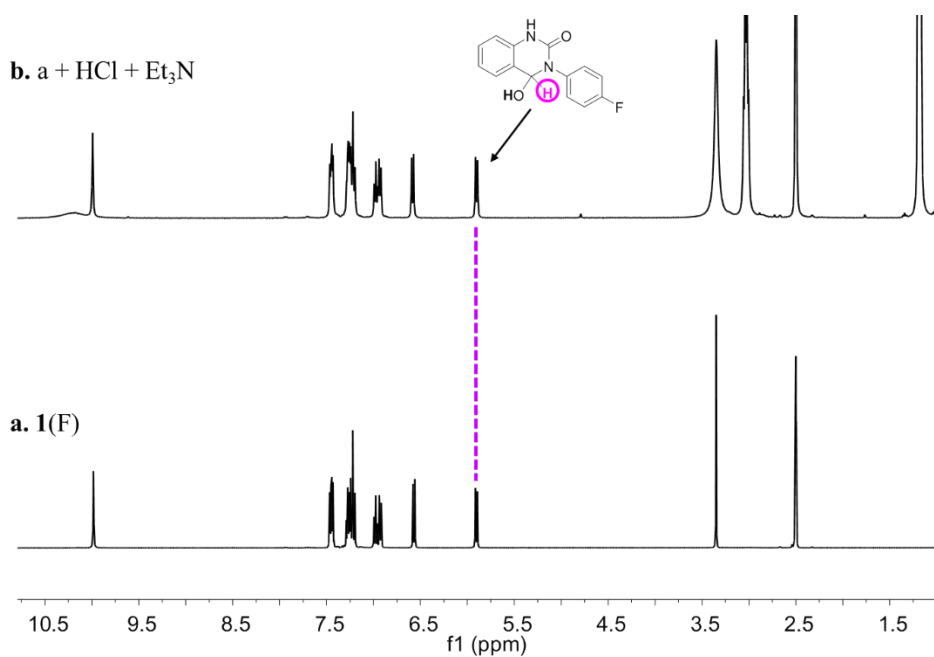


Figure S98. ¹H NMR spectra of **1(F)** (a) and the reaction of **1(F)** with HCl, followed by Et₃N vapor (b). This figure supports vapor induced reaction in Figure S84.

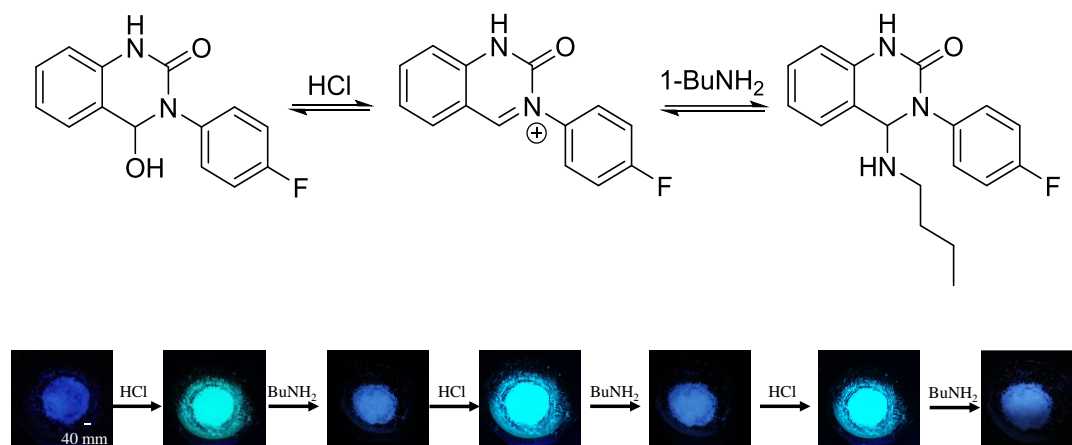


Figure S99. The photographs of color change of powder **1(F)** with consecutive exposure to HCl (1 min), followed by 1-BuNH₂ vapor (5 min).

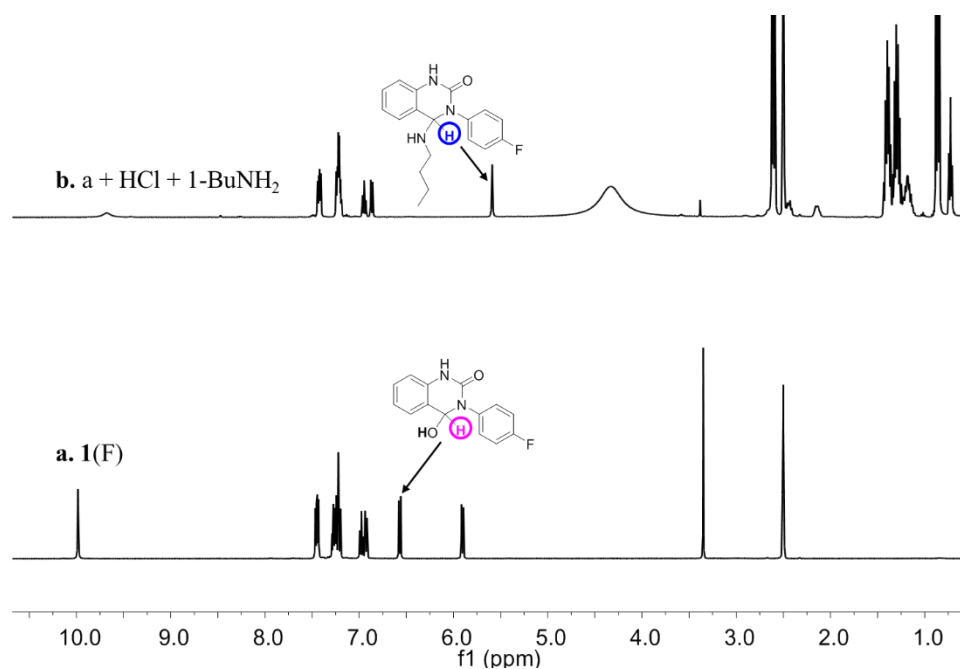


Figure S100. ¹H NMR spectra of **1(F)** (a) and the product created by the reaction of **1(F)** with 1-BuNH₂ vapor (b). This figure supports vapor induced reaction in Figure S86.

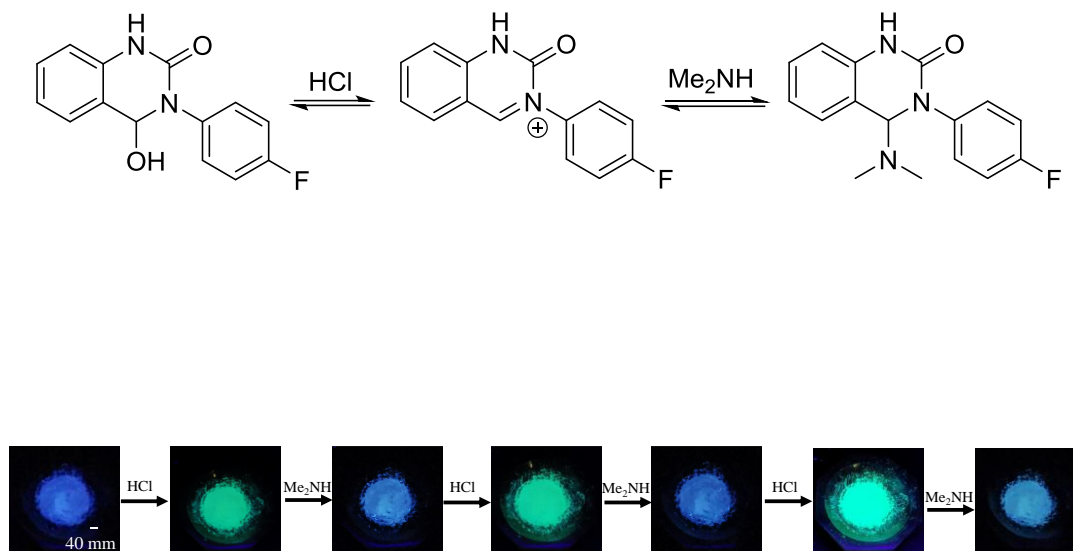


Figure S101. The photographs of color change of powder **1(F)** with consecutive exposure to HCl (1 min), followed by Me₂NH vapor (5 min).

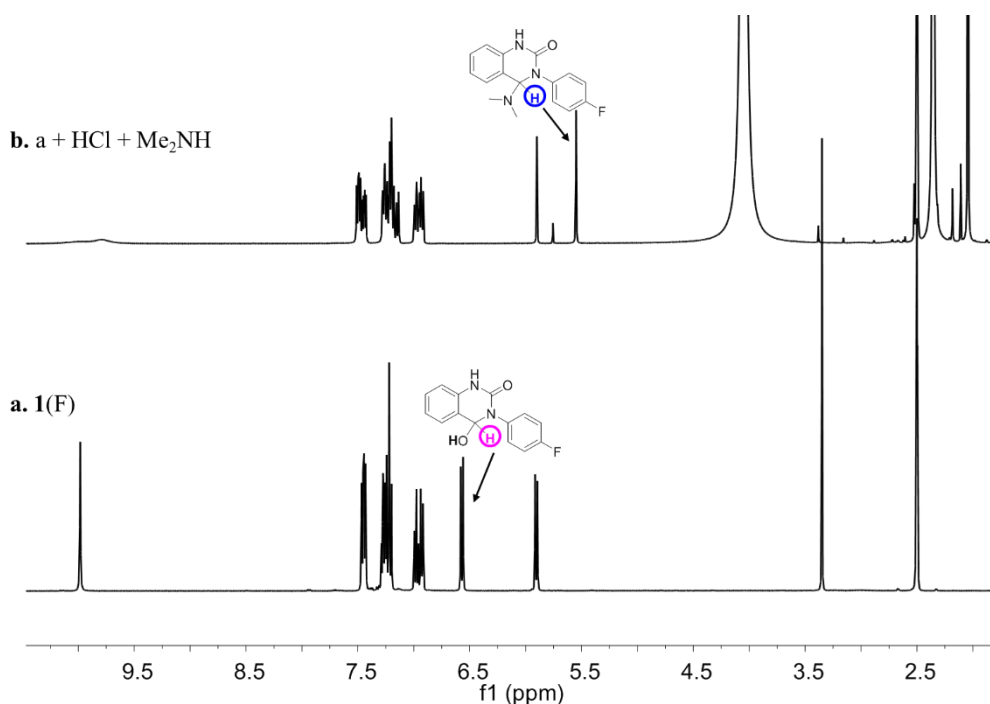


Figure S102. ¹H NMR spectra of **1(F)** (a) and the product created by the reaction of **1(F)** with 1-BuNH₂ vapor (b). This figure supports vapor induced reaction in Figure S88.

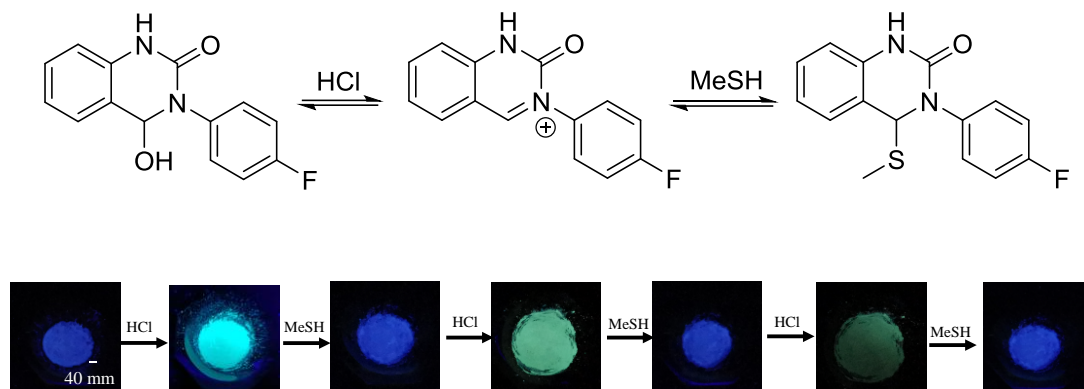


Figure S103. The photographs of color change of powder **1(F)** with consecutive exposure to HCl (1 min), followed by MeSH released from 5% solution in 1,3-propanediol (150 min).

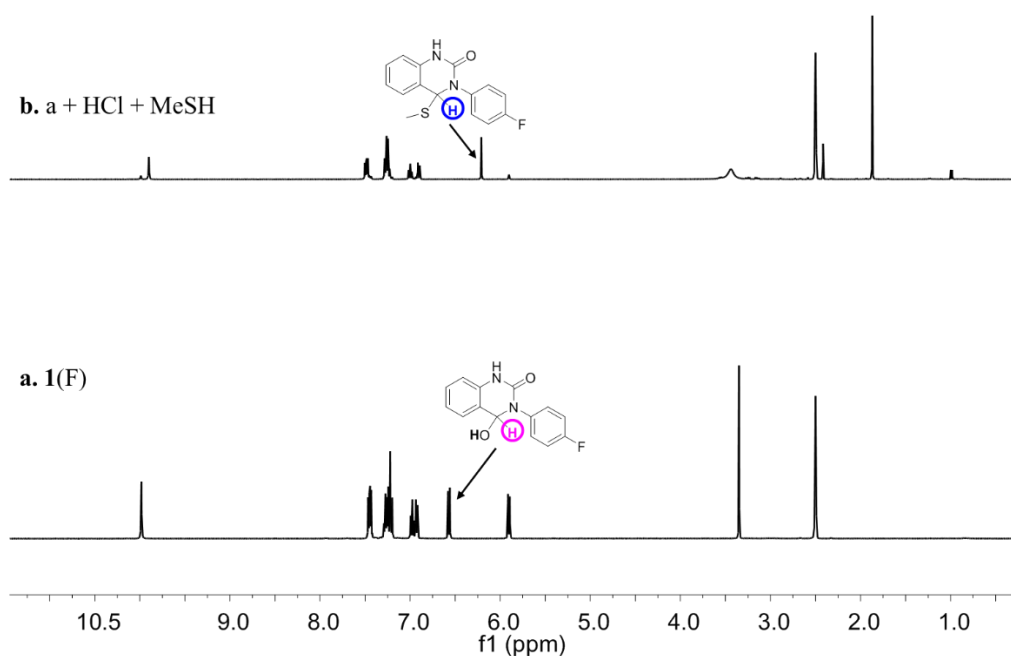


Figure S104. ^1H NMR spectra of **1(F)** (a) and the product created by the reaction of **1(F)** with MeSH vapor (b). This figure supports vapor induced reaction in Figure S90.

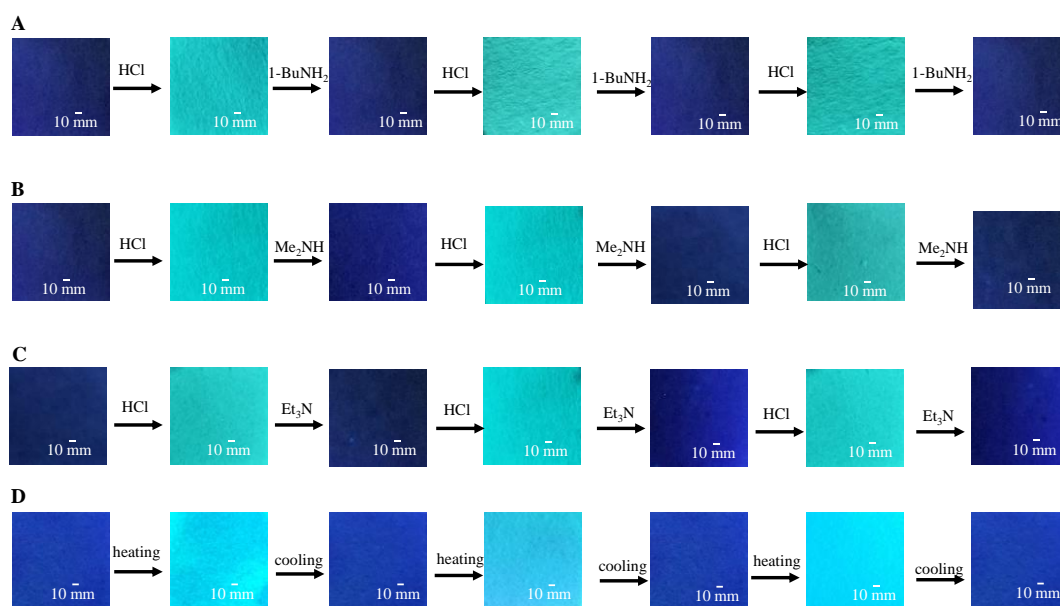


Figure S105. The photographs of color change of **1(F)** with exposure to HCl (1 minute), followed by (A) 1-BuNH₂ (1 minute); (B) Me₂NH (1 minute); and (C) Et₃N (1 minute) on filter papers. (D) The photographs of color change of **1(F)** during a heating and cooling process. The pictures were taken under a 365 nm UV lamp, and the images are a representative fragment (75%) of a 2 cm × 2 cm filter paper.

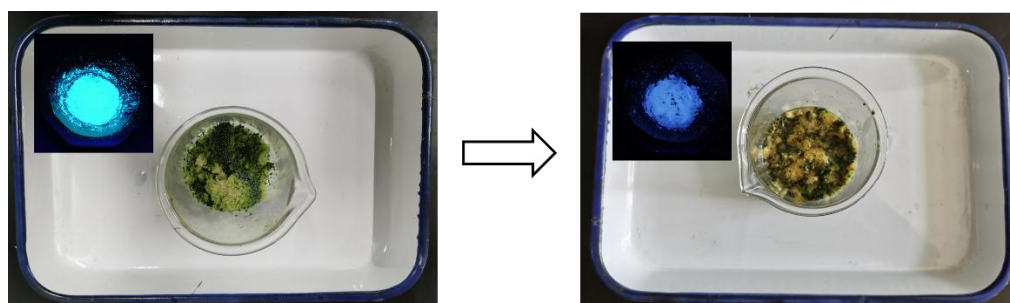


Figure S106. The photographs of color change of HCl vapor activated **1(F)** during a broccoli florets spoilage. (a) **1(F)** with fresh Broccoli Florets; (b) **1(F)** with broccoli florets after 12 h.

8. Computational Data

Gaussian 09 package^{S6} was used for geometry optimizations and the calculation of energies. The method and basis set of M06-2X/def2-TZVP were employed for the optimization and frequency analysis. The PCM solvent model was used for acetonitrile. All the DFT geometries were found to have zero imaginary frequencies.

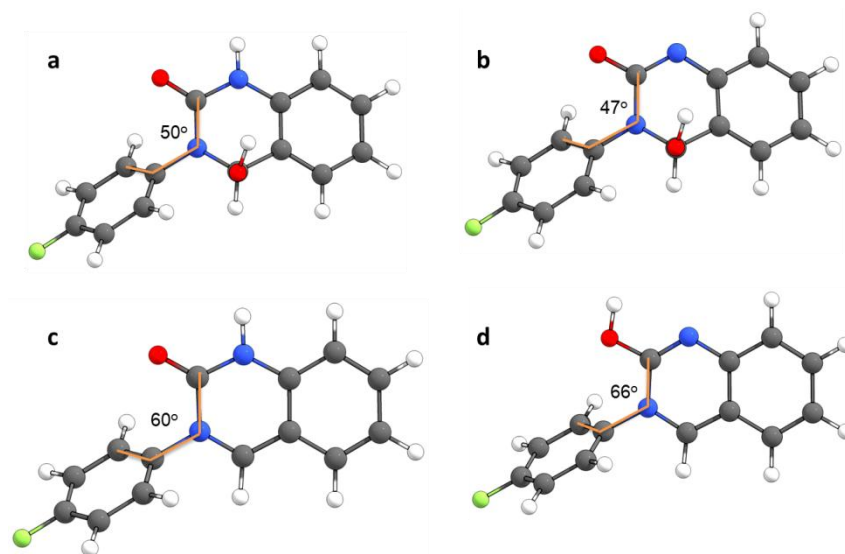
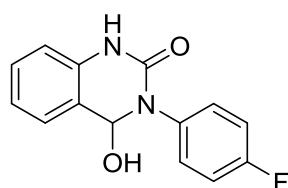


Figure S107. The calculated structures of **1(F)** (a), conjugate base of **1(F)** (b), keto form of **3(F)** (c), and enol form of **3(F)** (d), respectively. The dihedral angles of C-N bond are shown. The keto form is dominant for **3(F)** (distribution around 100%).



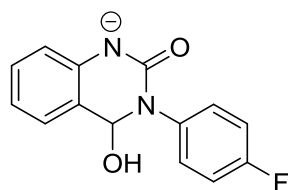
1(F) (acetonitrile)

Imaginary frequency: 0

G = -899.765298 hartree

| | | | |
|---|-------------|-------------|------------|
| C | -2.10394800 | -0.65362100 | 0.10850800 |
| C | -2.92465100 | -1.65584300 | 0.60796100 |

| | | | |
|---|-------------|-------------|-------------|
| C | -4.24157200 | -1.37964200 | 0.94049200 |
| C | -4.73724700 | -0.09009700 | 0.76805400 |
| C | -3.92580500 | 0.92139200 | 0.28243600 |
| C | -2.60243700 | 0.63489200 | -0.04243000 |
| H | -2.52613200 | -2.65654700 | 0.72496300 |
| H | -4.88013000 | -2.16147600 | 1.32792300 |
| H | -5.76536000 | 0.13204500 | 1.02215500 |
| H | -4.30561900 | 1.92772100 | 0.15993900 |
| N | -1.73873700 | 1.61584900 | -0.52214600 |
| C | -0.36974400 | 1.52064900 | -0.49569100 |
| H | -2.08699200 | 2.55147600 | -0.66925300 |
| O | 0.33324600 | 2.49431400 | -0.70499700 |
| N | 0.12173100 | 0.26388200 | -0.21092000 |
| C | -0.70632100 | -0.92624200 | -0.36046400 |
| C | 1.52495300 | 0.08702400 | -0.03465600 |
| C | 2.18788000 | -0.95187800 | -0.67899800 |
| C | 2.22630200 | 0.92260200 | 0.83187700 |
| C | 3.54297200 | -1.16249600 | -0.45712600 |
| H | 1.64925000 | -1.59425500 | -1.36139600 |
| C | 3.58028200 | 0.73071900 | 1.04531000 |
| H | 1.70793400 | 1.72333900 | 1.33918300 |
| C | 4.21308900 | -0.31282700 | 0.39588300 |
| H | 4.07365100 | -1.96715200 | -0.94707600 |
| H | 4.14082300 | 1.36912100 | 1.71429500 |
| F | 5.52833500 | -0.50551000 | 0.60836400 |
| H | -0.24470900 | -1.70836400 | 0.23981800 |
| O | -0.69470400 | -1.42427000 | -1.68637100 |
| H | -1.28955200 | -0.89259600 | -2.23036100 |



1(F)-conjugate base

Imaginary frequency: 0

G = -899.292380 hartree

| | | | |
|---|-------------|-------------|-------------|
| C | 2.11445900 | -0.62441600 | -0.09870200 |
| C | 2.95211900 | -1.63398800 | -0.55448100 |
| C | 4.26851600 | -1.36104200 | -0.89484300 |
| C | 4.73847300 | -0.05323400 | -0.76386900 |
| C | 3.90810000 | 0.95738200 | -0.31637900 |
| C | 2.56480300 | 0.70089300 | 0.02100300 |
| H | 2.56489900 | -2.64452400 | -0.63423700 |
| H | 4.91995900 | -2.14792300 | -1.25057800 |
| H | 5.76584100 | 0.17652100 | -1.02018900 |
| H | 4.27300500 | 1.97309000 | -0.22201900 |
| N | 1.76307600 | 1.72596600 | 0.45634400 |
| C | 0.44321200 | 1.55059000 | 0.50317300 |
| O | -0.35640500 | 2.45031100 | 0.80883400 |
| N | -0.09319700 | 0.26883000 | 0.16831500 |
| C | 0.72091200 | -0.90444500 | 0.36037900 |
| C | -1.48583400 | 0.08938000 | 0.02109600 |
| C | -2.13131200 | -1.01901200 | 0.56885300 |
| C | -2.23421200 | 0.99092100 | -0.74246800 |
| C | -3.48910800 | -1.23288100 | 0.35445400 |
| H | -1.57682600 | -1.71580100 | 1.18145400 |
| C | -3.58836900 | 0.79540300 | -0.94760700 |
| H | -1.74256300 | 1.84969700 | -1.17448700 |

| | | | |
|---|-------------|-------------|-------------|
| C | -4.19342100 | -0.31889500 | -0.39525300 |
| H | -3.99376300 | -2.09215200 | 0.77516500 |
| H | -4.17246300 | 1.48742800 | -1.53939500 |
| F | -5.51405900 | -0.51363100 | -0.60148500 |
| H | 0.27762500 | -1.72298200 | -0.20658800 |
| O | 0.70770700 | -1.36746100 | 1.71701400 |
| H | 1.28121400 | -0.78698900 | 2.23270100 |



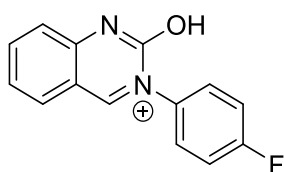
3(F)-keto form (acetonitrile)

Imaginary frequency: 0

G = -823.756984 hartree

| | | | |
|---|-------------|-------------|-------------|
| C | -2.13543300 | -0.70933700 | 0.14046100 |
| C | -2.99861800 | -1.81233300 | 0.32018500 |
| C | -4.35042000 | -1.61926000 | 0.26389500 |
| C | -4.86239600 | -0.32843500 | 0.02901400 |
| C | -4.04374300 | 0.76417900 | -0.14627100 |
| C | -2.66334400 | 0.57553400 | -0.08895800 |
| H | -2.57277100 | -2.79086600 | 0.49725800 |
| H | -5.02921700 | -2.44881500 | 0.39745700 |
| H | -5.93437200 | -0.18855300 | -0.01537500 |
| H | -4.45229500 | 1.74882600 | -0.32546600 |
| N | -1.78090000 | 1.60907000 | -0.24922200 |
| C | -0.42141100 | 1.52097100 | -0.22495100 |
| H | -2.13637600 | 2.54389000 | -0.41586700 |
| O | 0.32554600 | 2.44468000 | -0.38712900 |
| N | 0.06390900 | 0.19299100 | 0.01211600 |

| | | | |
|---|-------------|-------------|-------------|
| C | -0.74533800 | -0.83451100 | 0.18479900 |
| C | 1.49534400 | -0.00322100 | 0.01273600 |
| C | 2.04142400 | -0.88812200 | -0.90184900 |
| C | 2.27672500 | 0.67605600 | 0.93508500 |
| C | 3.40891100 | -1.11498100 | -0.88944400 |
| H | 1.40980000 | -1.38756600 | -1.62490600 |
| C | 3.64189200 | 0.45483700 | 0.94835400 |
| H | 1.82451300 | 1.36347200 | 1.63576400 |
| C | 4.17756800 | -0.43731600 | 0.03580200 |
| H | 3.87442500 | -1.79691800 | -1.58657200 |
| H | 4.28786800 | 0.95799500 | 1.65370800 |
| F | 5.49867200 | -0.64955000 | 0.05094400 |
| H | -0.27202000 | -1.79175600 | 0.36913300 |



3(F)-enol from (acetonitrile)

Imaginary frequency: 0

G = -823.743664 hartree

| | | | |
|---|------------|-------------|-------------|
| C | 2.14988700 | -0.72310400 | -0.11954700 |
| C | 3.04426700 | -1.81081600 | -0.28380900 |
| C | 4.38494900 | -1.57420700 | -0.24216600 |
| C | 4.87060800 | -0.25895800 | -0.03816100 |
| C | 4.02730800 | 0.80799400 | 0.12189800 |
| C | 2.63848500 | 0.59451500 | 0.08372500 |
| H | 2.64662700 | -2.80500800 | -0.43802500 |
| H | 5.08745000 | -2.38633400 | -0.36439300 |
| H | 5.94019100 | -0.09738200 | -0.00888800 |

| | | | |
|---|-------------|-------------|-------------|
| H | 4.39721300 | 1.81154400 | 0.27740700 |
| N | 1.78299200 | 1.63721200 | 0.24151300 |
| C | 0.51667100 | 1.41742900 | 0.20317200 |
| H | 0.08830000 | 3.21259300 | 0.50255900 |
| O | -0.37511600 | 2.37200000 | 0.36177400 |
| N | -0.03768700 | 0.16550100 | 0.00153400 |
| C | 0.77273800 | -0.87956000 | -0.15516700 |
| C | -1.47511600 | -0.02272900 | -0.01056300 |
| C | -2.04672500 | -0.78777900 | 0.99113300 |
| C | -2.22564500 | 0.54206800 | -1.02933900 |
| C | -3.41598600 | -1.00309700 | 0.97444700 |
| H | -1.43361900 | -1.20390200 | 1.77947000 |
| C | -3.59287500 | 0.33185600 | -1.04682800 |
| H | -1.75000400 | 1.13370400 | -1.79949500 |
| C | -4.15722300 | -0.43692900 | -0.04397200 |
| H | -3.90388200 | -1.59304900 | 1.73711600 |
| H | -4.21763900 | 0.74894500 | -1.82375500 |
| F | -5.47925700 | -0.63988700 | -0.06346900 |
| H | 0.29441700 | -1.83720600 | -0.31522600 |

9. References

- S1. Boyer, J. E.; Veggel, F. C. J. M. van. Absolute Quantum Yield Measurements of Colloidal NaYF₄: Er³⁺, Yb³⁺ Upconverting Nanoparticles. *Nanoscale* **2010**, 2, 1417–1419.
- S2. Ishida, H.; Tobita, S.; Hasegawa, Y.; Katoh, R.; Nozaki, K. Recent Advances in Instrumentation for Absolute Emission Quantum Yield Measurements. *Coord. Chem. Rev.* **2010**, 254, 2449–2458.
- S3 Tulio, A. Z.; Yamanaka, H.; Ueda, Y.; Imahori, Y. Formation of Methanethiol and Dimethyl Disulfide in Crushed Tissues of Broccoli Florets and Their Inhibition by Freeze–Thawing. *J. Agr. Food. Chem.* **2002**, 50, 1502–1507.
- S4 Clayden, J.; Pickworth, M.; Jones, L. H. Relaying Stereochemistry Through Aromatic Ureas: 1,9 and 1,15 Remote Stereocontrol. *Chem. Commun.* **2009**, 547–549.
- S5 Miyashita, M.; Matsumoto, T.; Matsukubo, H.; Iinuma, F.; Taga, F.; Sekiguchi, H.; Hamada, K.; Okamura, K.; Nishino, K., Synthesis and Antiulcer Activity of N-Substituted N'-[3-[3-(Piperidinomethyl)Phenoxy]Propyl]Ureas - Histamine-H₂-Receptor Antagonists with a Potent Mucosal Protective Activity. *J. Med. Chem.* **1992**, 35, 2446–2451.
- S6 Frisch, M. J.; Trucks, G. W.; Schlegel, H. B.; Scuseria, G. E.; Robb, M. A.; Cheeseman, J. R.; Scalmani, G.; Barone, V.; Mennucci, B.; Petersson, G. A.; Nakatsuji, H.; Caricato, M.; Li, X.; Hratchian, H. P.; Izmaylov, A. F.; Bloino, J.; Zheng, G.; Sonnenberg, J. L.; Hada, M.; Ehara, M.; Toyota, K.; Fukuda, R.; Hasegawa, J.; Ishida, M.; Nakajima, T.; Honda, Y.; Kitao, O.; Nakai, H.; Vreven, T.; Montgomery, J. A., Jr.; Peralta, J. E.; Ogliaro, F.; Bearpark, M.; Heyd, J. J.; Brothers, E.; Kudin, K. N.; Staroverov, V. N.; Kobayashi, R.; Normand, J.; Raghavachari, K.; Rendell, A.; Burant, J. C.; Iyengar, S. S.; Tomasi, J.; Cossi, M.; Rega, N.; Millam, J. M.; Klene, M.; Knox, J. E.; Cross, J. B.; Bakken, V.; Adamo, C.; Jaramillo, J.; Gomperts, R.; Stratmann, R. E.; Yazyev, O.; Austin, A. J.; Cammi, R.; Pomelli, C.; Ochterski, J. W.; Martin, R. L.; Morokuma, K.; Zakrzewski, V. G.; Voth, G. A.; Salvador, P.; Dannenberg, J. J.; Dapprich, S.; Daniels, A. D.; Farkas, Ö.; Foresman, J. B.; Ortiz, J. V.; Cioslowski, J.; Fox, D. J. *Gaussian 09*, revision E.01; Gaussian, Inc.: Wallingford, CT, **2010**.